ETH Zürich

Department of High Energy Physics

PSI Villigen

Group Accelerator Modelling & Advanced Simulations

Master Thesis

# A Relativistic Fluid Model for Particle Beams in Cyclotrons

*Author:*
Carina Stritt

*Supervisors:*
Dr. Andreas Andelmann
Prof. Klaus Kirch

August 31, 2013

**Abstract**

This work describes the derivation and implementation of a relativistic set of fluid equations for the simulation of the dynamics of a particle beam in an accelerator. Rotational invariance and hyperbolicity in time of the set of equations was proven and a condition for hyperbolicity in space was derived. The general set of relativistic equations was implemented in a reduced two-dimensional version with a static homogeneous external magnetic field. The aim of the simulation was to see the effects of beam spiralling already discovered in particle-in-cell cyclotron simulations. For the simulation, the fluid dynamical approach of using conservation schemes with source terms was used. The beam spiralling effect could be observed and compared to [4], despite some remaining energy problems in the code.

**Acknowledgements**

This Master Thesis would not have been possible without the support of many people. I wish to express my gratitude to my supervisor, Dr. Andreas Adelmann for the helpful discussions and infinite coffee supply. I would like to show my greatest appreciation to Dr. Tulin Kaman. I can't say thank you enough for her support and help. Special thanks also to A.J. Cerfon, who kindly shared his Matlab code with us. Finally, I wish to express my love and gratitude to my beloved family, my boyfriend Benjamin and all of my friends for their endless patience, understanding and encouragement during my studies.

# Contents

# 1 Introduction

The purpose of a normal particle accelerator like a cyclotron for example is to produce a particle beam with certain characteristics. The accelerator itself consists of many different parts. To make sure that the accelerator works perfectly, it has to be tested. The test in the machine itself can be difficult and some times even impossible. At this point simulations can help testing the dynamics of the particle beam in the accelerator.

The current simulation tool for modelling beam dynamics is the Particle-in-cell (PIC) method [2]. This method discretizes the problem to calculate all relevant quantities like densities and fields on the mesh points. Then each individual element, that means each particle, is tracked in phase space. This method has an intuitive implementation and leads naturally to parallel solvers. Moreover, exact magnetic and geometric inputs are possible. To sum it up, the PIC method is self-consistent and accurate, but the tracking of the elements does lead to long calculation times.

Another possible way of simulating the dynamics of the particle beam would be a continuum description rather than the description of all individual elements. This can be done in the form of a fluid model. A model like this could lead to new insights into the physical mechanisms at work and it could be computationally more efficient. However, the main reason for the implementation of a fluid model is that it could complement PIC simulations.

In the paper 'Analytic fluid theory of beam spiraling in high intensity cyclotrons' [4] the idea of a fluid model was implemented. The 2D radial-longitudinal motion in high intensity cyclotrons was investigated with the aim of understanding the effect of beam spiralling, that has already been seen in PIC simulations. Further approximations had been done to make the analysis more tractable, these included considering nonrelativistic motion, a coasting beam and a homogeneous magnetic field along the beam line. As it is also done in PIC simulations, in the fluid model the two timescales of a rapidly oscillating betatron oscillation and a slow space charge evolution were distinguished. The problem of closure of the fluid equations could in this case be adressed by approximating the pressure to be gyrotropic on the space charge time scale. In the end the beam spiralling could be explained to be the result of the radial-longitudinal vortex motion, which is proportional to $\mathbf{E} \times \mathbf{B}$. This vortex motions leads to distortions in elongated beams, which are larger farther away from the beam center. The distortion then gives rise to the spiral arms.

The aim of this work is to pursue the idea of the fluid model for the description of particle beams further. A relativistic extension to the fluid model will be made that allows the use of acceleration and non uniform magnetic fields.

# 2 Description of non-neutral plasma

Usually, plasma is defined to be a medium consisting of positively and negatively charged elements, where the overall charge averages out to be roughly zero. This form of plasma naturally arises, when for example a gas has been completely ionized. As opposed to this, in a non-neutral plasma the total charge is either positive or negative. From now on we will consider the so-called single species non-neutral plasma. This plasma consists of only one type of ion. As Davidson, in his book [7] about the physics of non-neutral plasmas already pointed out, the non-neutral plasma can be characterized in two different ways. The Fluid can be described using a kinetic description of single particle distribution functions, which will be done in the following section 2.1. The other description used the macroscopic point of view, we will look at it in section 2.2.

## 2.1 Kinetic description of the plasma

In the kinetic description of the plasma, single particle distribution functions $f(x, p, t)$ are used to describe the plasma. The evolution of these distribution functions is given by the Vlasov-Maxwell equation.

$$(\partial_t + v\nabla_x + q(E + \frac{1}{c}v \times B)\nabla_p)f(x, p, t) = 0$$

The velocity $v$ in this equation can be related to the momentum using $v = \frac{p}{\gamma m}$. This equation holds as long as Liouvilles theorem is satisfied, that means the flow in phase-space is incompressible. The system now can be viewed at two different intrinsic time scales, which correspond to the cyclotron frequency

$$\omega_c = |eB/\gamma mc| \tag{1}$$

and the plasma frequency

$$\omega_p = (4\pi ne^2/\gamma m)^{1/2}. \tag{2}$$

## 2.2 Macroscopic description of the plasma

Fluid Dynamics is a part of continuum mechanis, that means the fluid is described by its macroscopic behaviour and the physical quantities of the fluid are varying continuously. Hence, rather than examining the plasma with one particle distribution functions, the evolution of the averaged, mean parameters given by those functions can be observed. Averaging is only meaningful on a specific scale. In this case it is useful as long as the total region to be averaged over is large enough to contain sufficiently many particles. On the other hand, it has to be small enough compared to the length scale of all macroscopic phenomena that are of interest. It certainly has to be larger than the average spacing between the fluid molecules. If microscopic properties of the fluid are of interest, this description can't be used. In that case the kinetic description of the single particle distribution functions has to be considered.

The most important averaged quantities in this case are the number density $n(x, t)$, the flow velocity $V(x, t)$ and the pressure tensor $P(x, t)$. All of the are computed by averaging the distribution function over the velocity:

$$n(x,t) = \int d^3v f(x,p,t),$$

$$n(x,t)V(x,t) = \int d^3v \mathbf{v} f(x,p,t),$$

$$n(x,t)P(x,t) = \int d^3p f(x,p,t),$$

$$P(x,t) = \int d^3v m(v - V(x,t))^2 f(x,p,t).$$

Starting from the already mentioned collisionless Vlasov equation, these averaged quantities can be used to define the so-called moments of the Vlasov equation, which will become our main equations to describe the fluid system. The first moment of the Vlasov equation can be obtained by averaging the Vlasov equation over the velocity.

$$\int d^3v \frac{Df}{Dt} = \int d^3v \left[\partial_t + v\nabla_x + q\left(E + \frac{1}{c}v \times B\right)\nabla_p\right] f(x,p,t) = 0$$

Using the above definitions of number density and flow velocity we get the **continuity equation**, which describes the particle number density conservation.

$$\partial_t n + \nabla_x(nV) \quad = \quad 0$$

The second moment of the Vlasov equation can be derived by multiplying the equation by $mv$ and integrating it like before.

$$\int d^3v\, mv \left[\partial_t + v\nabla_x + q\left(E + \frac{1}{c}v \times B\right)\nabla_p\right] f(x,p,t) = 0$$

With the definition of the pressure tensor this can be rewritten to get the **momentum equation**, which describes the conservation of momentum.

$$nm\left(\partial_t + V\nabla_x\right)V + \nabla_x P \quad = \quad nq\left(E + \frac{1}{c}(V \times B)\right)$$

Additionally, the approximation $\partial_x P \sim 0$ can be made, as long as no finite temperature effects are included.

## 2.3 Validity of the fluid description for plasmas

The aim of this work is to apply the fluid dynamical approach to the description of a particle beam in an accelerator, specifically in a cyclotron. But before we can do this, it has to be proven, that a hydrodynamical description of a system like the particle beam is valid. At first, it might seem like this is not the case, since a simple comparison between the classical hydrodynamical description and the description of a particle beam shows big differences. First of all a

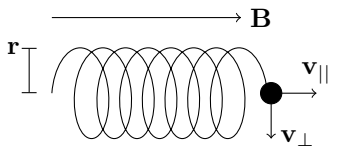


Figure 1: A charged particle moving in a magnetic field. The particle is forced on a helical orbit.

fluid in the hydrodynamical model has no net charge as opposed to the Particle beam, which can be described by a single ion species and thus has a nonzero net charge. Furtheremore, a normal fluid description arises from a velocity distribution that is the result of collisions (Maxwellian distribution). In the case of a particle beam, collisions don't play an important role and in most cases they can even be neglected and the beam can be described collisionless.

Nevertheless, a fluid approach can be used to describe the non-neutral plasma. Francis F. Chen gives 3 reasons for that in his book about Plasma Physics [5]. First of all, the fluid description allows deviations from the Maxwellian velocity distribution as long as the averaged square value remains the same. Secondly, we have to consider that already Irving Langmuir discovered in his famous Langmuir paradox, electrons with an distribution function more Maxwellian than their collisions would allow. However, since a moving plasma will be the focus of interest here, a Maxwellian distribution can not be assumed a priori in this case.

A fluid description can be done nevertheless. The reason for this lies in the limiting nature of the magnetic field. Charged particles in a magnetic field will be forced to move on a finite Larmor radius ($v_E = \frac{\mathbf{E}\times\mathbf{B}}{B^2}$) and this way they will be limited in their free stream. This behavior can be seen in Fig 1. The same feature can be seen for ions in E fields, where the acceleration is limited by the so-called mobility factor ($v = \mu E$).

This approach has been closely examined by Chew, Goldberger and Low [6]. They replaced the collision term in the Vlasov equation with the Lorentz force and showed that the Fluid equations can still be derived in their known form. Still, this last argument still has to be handled carefully. The stream along the magnetic field lines is excluded from this effect.

Nevertheless, the fluid theory can be used as approximation for motions perpendicular and parallel to the B field as long as some conditions in the parallel direction are fulfilled. When pressure-transport terms along the magnetic field lines are small the fluid description works perfectly well, this is also shown in Chew, Goldberger and Lows paper [6].

So to conclude we can say that a collisionless plasma can be treated like a collisional fluid under certain circumstances and the hydrodynamical description of the particle beam is possible as long as the variations along the magnetic field lines are small. For the description of a cyclotron this means, that perturbations

in radial and longitudinal direction can be described. Pertubations in direction of the magnetic field will not be the subject of this thesis, because a model exceeding the fluid approach has to be found for that.

# 3 Relativistic Fluid equations for the particle beam

In the following section the macroscopic description of the particle beam as a non-neutral plasma in an electromagnetic field will be derived. First we will look at the energy-momentum tensor of such a fluid and after that the equations of motions in an electromagnetic field will be discussed. Finally we derive the nonrelativistic limit and the limit $\gamma \gg 1$.

## 3.1 The Energy-Momentum Tensor

A general fluid is represented by its macroscopic quantities pressure and viscosity. It can be defined through its energy-momentum tensor $\mathbf{T}$. The first element of this tensor, $T^{00}$, describes the energy density. The elements $T^{0i}$ are the flux of energy, here we can also speak of heat conduction. The elements $T^{i0}$ are the flux of momentum. Both the flux of energy and momentum are measured across a surface of constant time. The remaining elements $T^{ij}$ describe the j flux of the i-th part of the momentum, that means it represents the stress forces between the elements of the fluid. To sum up, the stress energy tensor $\mathbf{T}$ is given as [11]

$$\mathbf{T} = \begin{pmatrix} T^{00} & T^{0i} \\ T^{i0} & T^{ij} \end{pmatrix} = \begin{pmatrix} \text{energy density} & \text{energy flux} \\ \text{momentum flux} & \text{stresses} \end{pmatrix}. \tag{3}$$

A perfect fluid is defined to have zero heat conduction in its co-moving frame of reference. That means in its rest frame the tensor of a perfect fluid has the simple form [i]

$$T^{\alpha\beta} = \begin{pmatrix} \tilde{\epsilon} & 0 \\ 0 & \tilde{p}\delta^{\alpha}_{\beta} \end{pmatrix}$$

with the energy density $\tilde{\epsilon} = \rho(1+e_{int})$ and the internal energy per unit mass $e_{int}$ [ii]. Let the total energy density be $\tilde{\rho} = \rho(1 + \frac{e_{int}}{c^2})$ with $\rho = mn$ (individual mass $m$ and number density $n$). The final energy momentum tensor can now be computed and a Lorentz transformation from the co-moving frame of reference to the lab frame can be made. [iii]

[i] Kronecker-Delta: $\delta^{\alpha}_{\beta} = \begin{cases} 1, & \alpha = \beta \\ 0, & \alpha \neq \beta \end{cases}$

[ii] Quantities marked with $\tilde{}$ are defined in the proper frame of the moving plasma.

[iii] The notation here contains upper and lower indices. Vectors are written with upper indices and called contravariant, while dual vectors are written with lower indices and called covariant. A tensor has mixed variance, that means it has both covariant and contravariant elements. An index that appears twice in a term indicates that the term will be summed over this index, this is the so-called Einstein notation. For example $a_i b^i = \sum_{i=1}^{3} a_i b^i$ for vectors $\mathbf{a}$ and $\mathbf{b}$ in three dimensional space. A classic example for this notation used in the context of tensors is the matrix multiplication. The product of two matrices is normally written as $C_{ik} = (AB)_{ik} = \sum_{j=1}^{N} A_{ij}B_{jk}$, but using the Einstein notation this can shortly be written as $C^i_k = A^i_j B^j_k$. Here the index $j$ appears as lower index on $A$ and as upper index on $B$ that means the sum will go over the range of $j$.

$$
\begin{aligned}
T^{\alpha\beta} &= (\Lambda^{-1})^{\alpha}_{\alpha'}(\Lambda^{-1})^{\beta}_{\beta'}T^{\alpha'\beta'} \\
&= (\rho c^2 + \rho e_{int} + \tilde{P})\frac{u^\alpha u^\beta}{c^2} + \tilde{P}g^{\alpha\beta} \\
&= \frac{\tilde{P} + \tilde{\rho}c^2}{c^2}u^\alpha u^\beta + \tilde{P}g^{\alpha\beta} \qquad (4)
\end{aligned}
$$

$\Lambda$ describes the relativistic transformation matrix.

$$
\Lambda = \begin{pmatrix} 1 & \gamma\beta_x & \gamma\beta_y & \gamma\beta_z \\ \gamma\beta_x & 1 & 0 & 0 \\ \gamma\beta_y & 0 & 1 & 0 \\ \gamma\beta_z & 0 & 0 & 1 \end{pmatrix}
$$

The variable $g^{\alpha\beta}$ describes the metric of the system. Here the so-called Minkowski metric is used, that means $g^{\alpha\beta} = \mathrm{diag}(+1, -1, -1, -1)$.

## 3.2 The Pressure Tensor

We can assume, that the pressure tensor or shear stress tensor $P$ included in the energy momentum tensor has the following properties:

$$
\begin{aligned}
P = P(\rho) > 0 \\
P(0) = 0
\end{aligned}
$$

Here the pressure is supposed only to depend on the density $\rho$. The specific form of the pressure tensor $P_{\alpha\beta} = mn\langle v_\alpha v_\beta \rangle$ [iv] depends on the problem:

- **isotropic Maxwellian distribution function**: $P = \begin{pmatrix} p & 0 & 0 \\ 0 & p & 0 \\ 0 & 0 & p \end{pmatrix}$
- **gyroscopic non-viscous pressure**:
  The term gyroscopic means that the pressure can be defined by a parallel and perpendicular contribution with respect to the magnetic field. In the plane perpendicular to the magnetic field the gyromotion of the plasma leads to an isotropization of the pressure. A gyrotropic pressure has the advantage that its divergence is zero.

  $$P = P_\perp \mathbb{I} + (P_{||} - P_\perp)\mathbf{bb},\ \mathbf{b} = \frac{\mathbf{B}}{|B|}$$

  If the B field is in z direction this tensor, which is also called the CGL tensor, after the paper of Chew, Goldberger and Low [6] can be written in the form of a matrix

  $$P = \begin{pmatrix} p_\perp & 0 & 0 \\ 0 & p_\perp & 0 \\ 0 & 0 & p_{||} \end{pmatrix}$$

[iv] The notation $\langle a \cdot b \rangle$ describes the average over the product of $a$ and $b$.

- **ordinary fluid**: the off diagonal terms of the pressure are non zero and correspond to the viscosity
  The viscosity can be interpreted as a resistance to shear flow, like particles that come off due to collisions. In the case of a collisionless viscosity, the Larmor gyration leads to an equalization of fluid velocities and the finite Larmor radius effect is related to the $v_E$ drift in nonuniform E fields, like it was already discussed in section 2.3.

If the fluid can approximatively assumed to be an ideal fluid the so-called polytropic equation of state can be used. An ideal or perfect fluid can be described only by its mass density and pressure in contrast to real fluids that also contain heat transfer and viscosity. The polytropic equation of state can be also given in relativistic form,

$$\begin{aligned} P &= \frac{K\rho^{\Gamma}}{\gamma},\ K = const \\ \frac{D}{Dt}\left(\gamma P \rho^{-\Gamma}\right) &= 0 \\ \text{with } \frac{D}{Dt} &= c\partial_t + \mathbf{v}\nabla. \end{aligned}$$

The exponent $\Gamma$ can be written as $\Gamma = 1 + \frac{1}{n}$ with $n$ being the so-called polytropic index. For a monoatomic ideal gas $\Gamma = \frac{5}{3}$.

## 3.3 The Continuity equation

The first equation that describes the particle beam is the so-called continuity equation. It addresses the fact, that the particle number in the beam does not change in time. The derivation of the continuity equation from the Vlasov-Maxwell equation has already been made in section 2.3.

$$\partial_t \rho + \nabla(\rho \mathbf{v}) = 0$$

This continuity equation can be rewritten, such that it contains the so-called Material or Convective Time Derivative.

$$\begin{aligned} \partial_t \rho + \mathbf{v}\nabla\rho + \rho\nabla\mathbf{v}) &= 0 \\ (\partial_t + \mathbf{v}\nabla)\rho + \rho\nabla\mathbf{v} &= 0 \\ \frac{D}{Dt}\rho + \rho\nabla\mathbf{v} &= 0 \end{aligned}$$

The relativistic version of the continuity equation can be easily found by replacing $\rho$ with $\gamma\rho$, to account for the relativistic relation $m_{relativistic} = \gamma m$, keeping in mind that the density $\rho$ is the product of number density $n$ and mass $m$.

$$\frac{D}{Dt}(\gamma\rho) + (\gamma\rho)\nabla\mathbf{v} = 0$$

### 3.3.1 The Convective Time derivative

The term $\partial_t X$ of a quantity $X$ is the partial time derivative of that quantity at a given fixed point in space [13]. It can also be called the local time derivative. For a moving fluid it can be useful to define another quantity called the Convective Time Derivative, which is a combination of the partial time derivative and the derivative $(\vec{v}\ \nabla)$ in direction of the velocity.

$$\begin{aligned}\frac{D}{Dt}X &= \lim_{\Delta T\to 0}\frac{X(\vec{x}+\Delta T\cdot\vec{v},t+\Delta T)}{\Delta T}\\ &= \partial_t X+(\vec{v}\ \nabla)X\end{aligned}$$

This Convective Time derivative corresponds to the time derivative as seen from the local rest frame, that means it is seen from the frame co-moving with the quantity $X$.

## 3.4 The Equations of Motion

For a fluid in a electromagnetic field the energy stress tensor is a combination of the energy momentum tensor of a fluid and the electromagnetic energy momentum tensor [v].

$$\begin{aligned}T^{ij} &= T^{ij}_{fluid}+T^{ij}_{em}\\ T_{ij} &= \frac{\tilde{P}+\tilde{\rho}c^2}{c^2}u^\alpha u^\beta+\tilde{P}g^{\alpha\beta}+\frac{1}{4\pi}(F^k_i F_{jk}-\frac{1}{2}g_{ij}F^{kl}F_{kl})\end{aligned}$$

Assuming energy conservation the equations of motion can be derived.

$$\begin{aligned}\nabla T^{ij} &= 0\\ \nabla_j T^{ij}_{fluid} &= -\nabla_j T^{ij}_{em}=\mathbf{J}_j F^{ij}\end{aligned}$$

The general relativistic equations of motion in an electromagnetic field can be derived just as it is done in relativistic magnetohydrodynamics [9].

$$\begin{aligned}\partial_j T^{ij} &= \mathbf{J}_j F^{ij}\\ \partial_j T^{ij} &= q\Gamma_j F^{ij}\\ \partial_j T^{ij} &= q\tilde{n}u_j F^{ij}\end{aligned}\tag{5}$$

Here the four-vector current $\mathbf{J}_j$ was replaced by the product of the charge and the flow vector $\Gamma_j$. The electromagnetic four-tensor $F_{ij}=\partial_i A_j-\partial_j A_i$ is given by the vector field $A^i=(\phi,\mathbf{A})$, which satisfies the Lorentz gauge $\partial_i A^i=0$. This tensor can be written in matrix form using the electric and magnetic field:

$$F^{ij}=\begin{pmatrix}0 & -\frac{E_x}{c} & -\frac{E_y}{c} & -\frac{E_z}{c}\\ \frac{E_x}{c} & 0 & -B_z & B_y\\ \frac{E_y}{c} & B_z & 0 & -B_x\\ \frac{E_z}{c} & -B_y & B_x & 0\end{pmatrix},\ F_{ij}=\begin{pmatrix}0 & \frac{E_x}{c} & \frac{E_y}{c} & \frac{E_z}{c}\\ -\frac{E_x}{c} & 0 & -B_z & B_y\\ -\frac{E_y}{c} & B_z & 0 & -B_x\\ -\frac{E_z}{c} & -B_y & B_x & 0\end{pmatrix}.$$

[v] Quantities marked with ˜ are defined in the proper frame of the moving plasma.

The equation of motion (5) can now be divided in its time and spatial components as done in [10]. The time component of (5) can be found by setting $i = 0$ [vi].

$$\begin{aligned}
\partial_j T^{0j} &= q\tilde{n}u_j F^{0j} \\
\partial_j \left( \frac{\tilde{P}+\rho c^2}{c^2} u^0 u^j - \tilde{P} g^{0j} \right) &= q\tilde{n}u_j F^{0j} \\
\partial_0 \left( \frac{\tilde{P}+\rho c^2}{c^2} u^0 u^0 - \tilde{P} g^{00} \right) + \partial_\alpha \left( \frac{\tilde{P}+\rho c^2}{c^2} u^0 u^\alpha - \tilde{P} g^{0\alpha} \right) &= q\tilde{n}u_j F^{0j} \\
\partial_t \left( \frac{\tilde{P}+\rho c^2}{c^2} \gamma^2 c^2 - \tilde{P} \right) + \nabla \left( \frac{\tilde{P}+\rho c^2}{c^2} \gamma c \gamma \mathbf{v} \right) &= q\tilde{n}\gamma \mathbf{v} \left( -\frac{\mathbf{E}}{c} \right) \\
\partial_t \left( (\tilde{P}+\rho c^2)\gamma^2 - \tilde{P} \right) + \nabla \left( (\tilde{P}+\rho c^2)\gamma^2 \frac{\mathbf{v}}{c} \right) &= -\frac{q}{c}\tilde{n}\gamma \mathbf{v}\mathbf{E} \quad (6)
\end{aligned}$$

The spatial component of the equation is given by the indices $\alpha = 1, 2, 3$.

$$\begin{aligned}
\partial_j T^{\alpha j} &= q\tilde{n}u_j F^{\alpha j} \\
\partial_j \left( \frac{\tilde{P}+\rho c^2}{c^2} u^\alpha u^j - \tilde{P} g^{\alpha j} \right) &= q\tilde{n}u_j F^{\alpha j} \\
\partial_t \left( (\tilde{P}+\rho c^2)\gamma^2 \frac{\mathbf{v}}{c} \right) + \nabla \left( (\tilde{P}+\rho c^2)\gamma^2 \frac{\mathbf{v}\mathbf{v}}{c^2} \right) + \nabla \tilde{P} &= q\tilde{n}\gamma \left( \mathbf{E} + \frac{1}{c}\mathbf{v} \times \mathbf{B} \right) \quad (7)
\end{aligned}$$

see $u_j F^{\alpha j} = \gamma(\mathbf{E} + \mathbf{u} \times \mathbf{B})$ in the Appendix.

The equation of continuity completes the set of equations for the fluid description of the particle beam.

$$\partial_t(\gamma\tilde{n}) + \nabla(\tilde{n}\gamma\mathbf{v}) = 0 \quad (8)$$

Restricting us to the case with no external charges and no external current sources the corresponding Maxwell equations can be reduced to an easier form.

$$\nabla \times \mathbf{B} = -\frac{1}{c}\partial_t \mathbf{E} + \frac{4\pi}{c}\mathbf{j} \quad (9)$$

$$\nabla \times \mathbf{E} = -\frac{1}{c}\partial_t \mathbf{B} \quad (10)$$

$$\nabla \mathbf{E} = 4\pi(\gamma q \tilde{n}) \quad (11)$$

$$\nabla \mathbf{B} = 0 \quad (12)$$

with the current $\mathbf{j} = \gamma q \tilde{n} \mathbf{v}$.

[vi] Latin indices go from 0 to 3, while greek indices go from 1 to 3.

## 3.5 Nonrelativistic limit

In the nonrelativistic limit we can assume that the velocity is negligible compared to the speed of light.

$$v \ll c \Rightarrow \gamma = \frac{1}{\sqrt{1 - v^2/c^2}} \sim 1$$

With this value of $\gamma$ the above equations (6),(7) and (8) can be written in their nonrelativistic form. First equation (6) will be rewritten in the nonrelativistic limit.

$$\partial_t(\rho c^2) + \frac{1}{c}\nabla((\tilde{P} + \rho c^2)\mathbf{v}) = -\frac{q}{c}\tilde{n}\mathbf{v}\mathbf{E} \tag{13}$$

The continuity equation (8) in the nonrelativistic limit becomes

$$\partial_t \tilde{n} + \nabla(\tilde{n}\mathbf{v}) = 0$$

which can be rewritten using $\rho = mn$

$$\partial_t \tilde{\rho} + \nabla(\tilde{\rho}\mathbf{v}) = 0 \tag{14}$$

Equation (7) becomes

$$\begin{aligned}
\partial_t((\tilde{P} + \rho c^2)\frac{\mathbf{v}}{c}) + \nabla((\tilde{P} + \rho c^2)\frac{\mathbf{v}\mathbf{v}}{c^2}) + \nabla\tilde{P} &= q\tilde{n}(\mathbf{E} + \frac{1}{c}\mathbf{v} \times \mathbf{B}) \\
\partial_t(\tilde{P}\frac{\mathbf{v}}{c}) + \nabla(\tilde{P}\frac{\mathbf{v}\mathbf{v}}{c^2}) + c\partial_t(\rho c^2\mathbf{v}) + \nabla(\rho\mathbf{v}\mathbf{v}) + \nabla\tilde{P} &= q\tilde{n}(\mathbf{E} + \frac{1}{c}\mathbf{v} \times \mathbf{B}) \\
\partial_t(\tilde{P}\frac{\mathbf{v}}{c}) + \nabla(\tilde{P}\frac{\mathbf{v}\mathbf{v}}{c^2}) + \mathbf{v}(c\partial_t\rho + \nabla(\rho\mathbf{v})) + \rho(c\partial_t + \mathbf{v}\nabla)\mathbf{v} + \nabla\tilde{P} &= q\tilde{n}(\mathbf{E} + \frac{1}{c}\mathbf{v} \times \mathbf{B})
\end{aligned}$$

The third term corresponds to the continuity equation.

$$\partial_t(\tilde{P}\frac{\mathbf{v}}{c}) + \nabla(\tilde{P}\frac{\mathbf{v}\mathbf{v}}{c^2}) + \rho(c\partial_t + \mathbf{v}\nabla)\mathbf{v} + \nabla\tilde{P} = q\tilde{n}(\mathbf{E} + \frac{1}{c}\mathbf{v} \times \mathbf{B})$$

If we assume that the pressure doesnot explicitly depend on time, we can neglect the term $\frac{\mathbf{v}}{c}\partial_t\tilde{P}$. The term $\nabla\frac{\tilde{P}\mathbf{v}^2}{c^2}$ will go to zero for $v \ll 1$.

$$\rho(\partial_t + \mathbf{v}\nabla)\mathbf{v} + \nabla\tilde{P} = q\tilde{n}(\mathbf{E} + \frac{1}{c}\mathbf{v} \times \mathbf{B}) \tag{15}$$

These nonrelativistic formulas can now be compared to the formulas in [4].

| Formulas derived here | Formulas from [4] |
|---|---|
| $\partial_t\tilde{n} + \nabla(\tilde{n}\mathbf{v}) = 0$ | $\partial_t n + \nabla(n\mathbf{v}) = 0$ |
| $\rho(\partial_t\mathbf{v} + \mathbf{v}\nabla\mathbf{v}) + \nabla\tilde{P} = q\tilde{n}(\mathbf{E} + \frac{1}{c}\mathbf{v} \times \mathbf{B})$ | $mn(\partial_t\mathbf{v} + \mathbf{v}\nabla\mathbf{v}) + \nabla P = en(E + \mathbf{v} \times B)$ |

## 3.6 Regime $\gamma \gg 1$, coasting

Now, we consider $\gamma$ to be much bigger than 1, that means the motion is highly relativistic. At the same time the beam should be coasting for this case, this means there will be no acceleration. Then the above equations (6),(7) and (8) can be rewritten.

Equation (6) becomes

$$\gamma^2 \partial_t(\rho c^2) + (\gamma^2 - 1)\partial_t \tilde{P} + \gamma^2 \nabla \left( (\tilde{P} + \rho c^2) \frac{\mathbf{v}}{c} \right) = -\frac{q}{c} \tilde{n} \gamma \mathbf{v} \mathbf{E} \tag{16}$$

Equation (7) becomes

$$\gamma^2 \partial_t \left( (\tilde{P} + \rho c^2) \frac{\mathbf{v}}{c} \right) + \gamma^2 \nabla \left( (\tilde{P} + \rho c^2) \frac{\mathbf{v}\mathbf{v}}{c^2} \right) + \nabla \tilde{P} = q \tilde{n} \gamma (\mathbf{E} + \frac{1}{c} \mathbf{v} \times \mathbf{B}) \tag{17}$$

Equation (8) becomes

$$\partial_t \tilde{n} + \nabla(\tilde{n}\mathbf{v}) = 0 \tag{18}$$

## 3.7 Acceleration $\gamma(t_2) > \gamma(t_1)$ and its effects

Especially in a rotating frame of reference the acceleration of the plasma can't be neglected. Moreover, in a cyclotron additional acceleration in the direction of the velocity takes place. This means we have to deal with the fact that we're not in an inertial frame of reference any more. The purpose of this section is to show, that a Lorentz transformation is still valid as long as infinitesimal changes along the trajectory are considered. To show this, in a first step the example of the movement on a circle will be discussed by introducing the concept of co-moving inertial frames. In a second step the general effect of an acceleration will be investigated. The following derivations require a basic knowledge in special and general relativity.

### 3.7.1 Example of a cylindrical coordinate system

Let us consider the following situation, where the primed coordinate system is rotating with respect to the cylindrical coordinate system $(t, r, \phi, z)$. Additionally to the nonrotating lab frame C and the rotating frame C', infinitesimal co-moving inertial frames C" are defined at each point along the circumference of the path that is described by the rotating frame as it is done in [15]. Two events 1 and 2 are defined two be simultaneous in one of the co-moving inertial frames (that means in the lab frame they are not simultaneous). Here we want to consider the simultaneity of the events A and B by sending light signals and reflecting them from A and B. It is now interesting to look if time and lengths measured in the co-moving inertial frames are the same as the ones measured in the rotating frame.

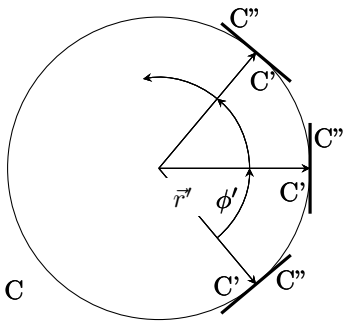


The line element in the rotating frame can be found by making this coordinate transformation:

$$\begin{aligned} t' &= t \\ r' &= r \\ \phi' &= \phi - \omega t \\ z' &= z \end{aligned}$$

$$\Rightarrow ds^2 = (c^2 - r'^2\omega^2)dt'^2 - dr'^2 - r'^2 d\phi'^2 - dz'^2 - 2\omega r'^2 d\phi' dt' \tag{19}$$

The proper time for a particle at rest in the rotating frame directly follows from this formula:

$$c^2 dt^2 = (c^2 - \omega^2 r'^2)dt'^2 \;\Rightarrow\; dt' = \sqrt{\frac{c^2}{c^2 - \omega^2 r'^2}}dt \tag{20}$$

Light now fulfills by definition $ds^2 = 0$. This lets us solve the equation (19) for $dt'$:

$$(c^2 - r'^2\omega^2)dt'^2 - 2\omega r'^2 d\phi' dt' - dr'^2 - r'^2 d\phi'^2 - dz'^2 = 0$$

$$\begin{aligned} dt'_{1/2} &= \frac{2\omega r'^2 d\phi' \pm \sqrt{(-2\omega r'^2 d\phi')^2 - 4(c^2 - r'^2\omega^2)(-dr'^2 - r'^2 d\phi'^2 - dz'^2)}}{2(c^2 - r'^2\omega^2)} \\ &= \frac{\omega r'^2 d\phi'}{c^2 - r'^2\omega^2} \pm \frac{\sqrt{c^2 dr'^2 - r'^2\omega^2 dr'^2 + c^2 r'^2 d\phi'^2 + c^2 dz'^2 - r'^2\omega^2 dz'^2}}{c^2 - r'^2\omega^2} \\ &= \frac{\omega r'^2 d\phi'}{c^2 - r'^2\omega^2} \pm \frac{\sqrt{(c^2 - \omega^2 r'^2)(dz'^2 + dr'^2) + c^2 r'^2 d\phi'^2}}{c^2 - r'^2\omega^2} \end{aligned} \tag{21}$$

It can be easily seen, that there are two solutions to the null geodesic equation for light. Considering just for the moment that $dr' = 0$ and $dz' = 0$ it can be seen, that the two solutions probably corresponds to the two directions the light can travel, either in direction of rotation or against it.

$$dt'_{1/2} = \frac{\omega r'^2 d\phi'}{c^2 - r'^2\omega^2} \pm \frac{cr' d\phi'}{c^2 - r'^2\omega^2} \tag{22}$$

That means measuring the time it takes for a light signal from 1 and 2 to meet a point in the middle, from a viewpoint of one of the co-moving inertial frames of references, is given by

$$dt' = \frac{1}{2}(dt_1 + dt_2) = \frac{\omega r'^2 d\phi'}{c^2 - r'^2\omega^2}$$

If we plug this value for $dt'$ into equation (19) we get the spatial line element

$$\begin{aligned}
-dl^2 &= (c^2 - r'^2\omega^2)(\frac{\omega r'^2 d\phi'}{c^2 - r'^2\omega^2})^2 - dr'^2 - r'^2 d\phi'^2 - dz'^2 - 2\omega r'^2 d\phi' \frac{\omega r'^2 d\phi'}{c^2 - r'^2\omega^2} \\
&= \frac{\omega^2 r'^4 d\phi'^2}{c^2 - r'^2\omega^2} - dr'^2 - r'^2 d\phi'^2 - dz'^2 - \frac{2\omega^2 r'^4 d\phi'^2}{c^2 - r'^2\omega^2} \\
&= -dr'^2 - r'^2 d\phi'^2 - dz'^2 - \frac{\omega^2 r'^4 d\phi'^2}{c^2 - r'^2\omega^2} \\
&= -dr'^2 - dz'^2 - \frac{c^2 r'^2 d\phi'^2 - \omega^2 r'^4 d\phi'^2 + \omega^2 r'^4 d\phi'^2}{c^2 - r'^2\omega^2} \\
&= -dr'^2 - dz'^2 - \frac{c^2 r'^2 d\phi'^2}{c^2 - r'^2\omega^2} \\
&\Rightarrow dl^2 = dr'^2 + dz'^2 + \frac{c^2 r'^2 d\phi'^2}{c^2 - r'^2\omega^2}
\end{aligned} \tag{23}$$

[8] now suggests to compare this measurement to the one which takes place in the rotating frame of reference.

$$dt' = \frac{1}{2}(dt_1 - dt_2) = \frac{\sqrt{(c^2 - \omega^2 r'^2)(dz'^2 + dr'^2) + c^2 r'^2 d\phi'^2}}{c^2 - r'^2\omega^2}$$

using the time coordinate $t$ of the lab frame, we end up with this value for the line element:

$$\begin{aligned}
dl^2 = (cdt)^2 &= c^2 \frac{(c^2 - \omega^2 r'^2)(dz'^2 + dr'^2) + c^2 r'^2 d\phi'^2}{(c^2 - r'^2\omega^2)^2} \\
&= c^2 \frac{dz'^2 + dr'^2}{c^2 - r'^2\omega^2} + c^2 \frac{c^2 r'^2 d\phi'^2}{(c^2 - r'^2\omega^2)^2}
\end{aligned} \tag{24}$$

From the definition of the proper time (20) we know that the time scales differ by a factor of $\sqrt{\frac{c^2}{c^2 - \omega^2 r'^2}}$, which means taking this line element from the rotating into the co-moving frame one has to multiply by $\frac{c^2 - \omega^2 r'^2}{c^2}$:

$$\begin{aligned}
dl^2 &= c^2 \frac{(c^2 - \omega^2 r'^2)(dz'^2 + dr'^2) + c^2 r'^2 d\phi'^2}{(c^2 - r'^2\omega^2)^2} \frac{c^2 - \omega^2 r'^2}{c^2} \\
&= dz'^2 + dr'^2 + \frac{c^2 r'^2 d\phi'^2}{c^2 - r'^2\omega^2}
\end{aligned}$$

which is the same result as we had before.

### 3.7.2 General effect of acceleration

Lets think of the famous problem of the light clock. The light in the clock in an inertial frame at rest will need the time

$$t = L/c$$

to travel from one mirror to the other, while the same light in a clock travelling with velocity $\mathbf{v}$ will need

$$t/\sqrt{1 - v^2/c^2}$$

due to time dilation. This is easy shown applying Pythagoras' theorem to the problem. The same can now be done with an accelerated clock. We can say that the accelerated clock travelled a distance

$$s \sim \mathbf{v}t' + \frac{1}{2}at'^2$$

until the light reaches the first mirror again. That means Pythagoras' theorem leads to

$$c^2t'^2 = L^2 + s^2 = L^2 + v^2t'^2 + a\mathbf{v}t'^3 + \frac{1}{4}a^2t'^4$$

There is obviously a dependency on the acceleration, but it depends on the size L of the clock and thus can be reduced to an infinitesimal contribution. That means the idea of looking at the problem at infintesimal timesteps solves the problem of not being in an inertial frame.

This result means, that for the problem of the movement on a circular trajectory, we can use a Lorentz transformation without having to consider general relativity. This is of particular interest here, since in the end we want to simulate the motion in a cyclotron, which describes outward going spirals. Of course other effects coming from the circular accelerated motion, especially the fictitious forces, can't be neglected. This effects will be discussed in the section about the rotating frame of reference, section 6.

# 4 Dimensional Analysis

To check the formulas of the Fluid Model for the particle beam derived so far, it is useful to do a dimensional analysis. That means the dimensions of the equations are checked to see if the equations are consistent. This dimensional analysis will be done in SI units. First of all the basic physical dimensions of the quantities in the equations should be figured out.

We defined density $\rho$ to be equal to the product of number density and individual mass that means the dimension of this quantity has to be mass over volume.

$$[\rho] = \frac{kg}{m^3}$$

Pressure is usually measured in the unit Pascal, which can be expressed in basic SI units as well.

$$[P] = \text{Pa} = \frac{N}{m^2} = \frac{kg}{ms^2}$$

The electric, the magnetic field and the charge on the right hand side of the equations are measured in $\frac{V}{m}$, Tesla and Coulomb, which can also be further disassembled to

$$\begin{aligned} [E] &= \frac{kgm}{As^3} \\ [B] &= \frac{kg}{As} \\ [q] &= As \end{aligned}$$

That means with the velocity having the units $\frac{m}{s}$, at least both terms of the Lorentz force have the same units.

$$[\mathbf{v} \times B] = \frac{kgm}{As^3} = [E]$$

Now we can start checking the equations, first of all the continuity equation.

$$\begin{aligned} \partial_t(\gamma\rho) + \nabla(\rho\gamma\mathbf{v}) &= 0 \\ [\partial_t(\gamma\rho)] &= [-\nabla(\rho\gamma\mathbf{v})] \\ \frac{1}{s}\left(\frac{kg}{m^3}\right) &= \frac{1}{m}\left(\frac{kg}{m^3}\frac{m}{s}\right) \\ \frac{kg}{sm^3} &= \frac{kg}{m^3 s} \end{aligned}$$

The momentum equation will be checked in two steps. First the left hand side of the equations will be evaluated and after that the dimension of the right hand side will be checked.

$$
\begin{aligned}
\text{LHS} &= \partial_t \left( (P + \rho c^2)\gamma^2 \frac{\mathbf{v}}{c^2} \right) + \nabla \left( (P + \rho c^2)\gamma^2 \frac{\mathbf{vv}}{c^2} \right) + \nabla P \\
[\text{LHS}] &= \frac{1}{s} \left( \left( \frac{kg}{ms^2} + \frac{kg}{m^3} \frac{m^2}{s^2} \right) \frac{s}{m} \right) + \frac{1}{m} \left( \left( \frac{kg}{ms^2} + \frac{kg}{m^3} \frac{m^2}{s^2} \right) \right) + \frac{1}{m} \frac{kg}{ms^2} \\
&= \frac{kg}{m^2 s^2}
\end{aligned}
$$

$$
\begin{aligned}
\text{RHS} &= \frac{q}{m} \rho\gamma \left( \mathbf{E} + \frac{1}{c} \mathbf{v} \times \mathbf{B} \right) \\
[\text{RHS}] &= \left[ \frac{q}{m} \rho (\mathbf{E} + \mathbf{v} \times \mathbf{B}) \right] \\
&= \frac{As}{kg} \frac{kg}{m^3} \frac{kgm}{As^3} \\
&= \frac{kg}{m^2 s^2}
\end{aligned}
\tag{25}
$$

$$
\Rightarrow [\text{LHS}] = [\text{RHS}]
$$

Now there is only the energy equation left to be checked.

$$
\begin{aligned}
\left[ \frac{1}{c} \partial_t \left( (P + \rho c^2)\gamma^2 - P \right) + \nabla \left( (P + \rho c^2)\gamma^2 \frac{\mathbf{v}}{c} \right) \right] &= \left[ -\frac{q\rho}{mc} \gamma \mathbf{vE} \right] \\
\frac{1}{m} \left( \left( \frac{kg}{ms^2} + \frac{kg}{m^3} \frac{m^2}{s^2} \right) - \frac{kg}{ms^2} \right) + \frac{1}{m} \left( \frac{kg}{ms^2} + \frac{kg}{m^3} \frac{m^2}{s^2} \right) &= \frac{Askg}{kgm^3} \frac{kgm}{As^3} \\
\frac{kg}{m^2 s^2} &= \frac{kg}{m^2 s^2}
\end{aligned}
$$

That means all three equations make sense, when we look at there dimensions.

# 5 Properties of the two dimensional set of equations

For simplicity, the discussion of the different properties of the set of Fluid equations will be done using the two-dimensional form of the equations. For our purposes, this will be sufficient, since the simulations of the equations will be done only in two dimensions. This two-dimensional set of equations can be written in a simple form by introducing two flux functions **F** and **G**.

$$\begin{aligned}
\mathbf{F(U)} &= \begin{pmatrix} \rho\gamma u \\ (P+\rho c^2)\gamma^2 \frac{u^2}{c^2} + P \\ (P+\rho c^2)\gamma^2 \frac{uv}{c^2} \\ \left(P+\rho c^2\right)\gamma^2 \frac{u}{c} \end{pmatrix} \\
\mathbf{G(U)} &= \begin{pmatrix} \rho\gamma v \\ (P+\rho c^2)\gamma^2 \frac{uv}{c^2} \\ (P+\rho c^2)\gamma^2 \frac{v^2}{c^2} + P \\ \left(P+\rho c^2\right)\gamma^2 \frac{v}{c} \end{pmatrix} \\
\text{with} \qquad \mathbf{U} &= \begin{pmatrix} \rho\gamma \\ (P+\rho c^2)\gamma^2 \frac{u}{c^2} \\ (P+\rho c^2)\gamma^2 \frac{v}{c^2} \\ \left(P+\rho c^2\right)\gamma^2 - P \end{pmatrix}
\end{aligned}$$

Then the equation can be written in the following way:

$$\partial_t \mathbf{U} + \partial_x \mathbf{F(U)} + \partial_x \mathbf{G(U)} = \mathbf{RHS} = \frac{q\gamma\rho}{n}[\mathbf{E} + \frac{v}{c} \times \mathbf{B}].$$

This equation looks similar to the two-dimensional set of Euler equations. Toro approached the Euler equations in his book about Numerical Methods for Fluid Dynamics [17], by proofing their rotational invariance and hyperbolicity. Due to the similarity between the equation, the same approached will be used for these equations.

## 5.1 Rotational Invariance

To prove the rotational invariance of the equations above, the rotational transformation in the two dimensional plane has to be defined first. A rotation through an angle $\theta$ in the two-dimensional plane affects only the $x$ and $y$ coordinate. The new coordinates $\tilde{x}$ and $\tilde{y}$ after the rotation are a combination of the old coordinates and the rotation angle $\theta$.

$$\begin{aligned}
\tilde{x} &= x\cos\theta + y\sin\theta \\
\tilde{y} &= -x\sin\theta + y\cos\theta
\end{aligned}$$

The resulting rotation matrix that can be applied to the vectors of the equation above will be called $\mathbf{T}(\theta)$.

$$
\begin{aligned}
\mathbf{T}(\theta) &= \begin{pmatrix} 1 & 0 & 0 & 0 \\ 0 & \cos\theta & \sin\theta & 0 \\ 0 & -\sin\theta & \cos\theta & 0 \\ 0 & 0 & 0 & 1 \end{pmatrix} \\
\mathbf{T}^{-1}(\theta) &= \begin{pmatrix} 1 & 0 & 0 & 0 \\ 0 & \cos\theta & -\sin\theta & 0 \\ 0 & \sin\theta & \cos\theta & 0 \\ 0 & 0 & 0 & 1 \end{pmatrix}
\end{aligned}
$$

Here it can be seen that the first index corresponding to the continuity equation and the last one corresponding to the energy equation aren't affected by this transformation. Using these transformation matrices, the rotational invariance can be proven.

The two fluxes $\mathbf{F}$ and $\mathbf{G}$ are rotationally invariant iff

$$\mathbf{T}^{-1}\mathbf{F}(\mathbf{TU}) = \mathbf{F}(\mathbf{U})\cos\theta + \mathbf{G}(\mathbf{U})\sin\theta.$$

To proof that this equation holds, let us first compute the argument of the function $\mathbf{F}(\mathbf{TU})$.

$$
\begin{aligned}
\mathbf{TU} = \tilde{\mathbf{U}} &= \begin{pmatrix} 1 & 0 & 0 & 0 \\ 0 & \cos\theta & \sin\theta & 0 \\ 0 & -\sin\theta & \cos\theta & 0 \\ 0 & 0 & 0 & 1 \end{pmatrix} \cdot \begin{pmatrix} \rho\gamma \\ (P+\rho c^2)\gamma^2 \frac{u}{c} \\ (P+\rho c^2)\gamma^2 \frac{v}{c} \\ \left(P+\rho c^2\right)\gamma^2 - P \end{pmatrix} \\
&= \begin{pmatrix} \rho\gamma \\ (P+\rho c^2)\frac{\gamma^2}{c^2}(u\cos\theta + v\sin\theta) \\ (P+\rho c^2)\frac{\gamma^2}{c^2}(v\cos\theta - u\sin\theta) \\ \left(P+\rho c^2\right)\gamma^2 - P \end{pmatrix} \\
&= \begin{pmatrix} \rho\gamma \\ (P+\rho c^2)\frac{\gamma^2}{c^2}\tilde{u} \\ (P+\rho c^2)\frac{\gamma^2}{c^2}\tilde{v} \\ \left(P+\rho c^2\right)\gamma^2 - P \end{pmatrix}
\end{aligned}
$$

Here, $\tilde{u} = u\cos\theta + v\sin\theta$ and $\tilde{v} = v\cos\theta - u\sin\theta$. Then the term on the left hand side of the equation can be computed.

$$
\begin{aligned}
\mathbf{T}^{-1}\mathbf{F}(\tilde{\mathbf{U}}) &= \begin{pmatrix} 1 & 0 & 0 & 0 \\ 0 & \cos\theta & -\sin\theta & 0 \\ 0 & \sin\theta & \cos\theta & 0 \\ 0 & 0 & 0 & 1 \end{pmatrix} \cdot \begin{pmatrix} \rho\gamma\tilde{u} \\ (P+\rho c^2)\frac{\gamma^2}{c^2}\tilde{u}^2 + P \\ (P+\rho c^2)\frac{\gamma^2}{c^2}\tilde{u}\tilde{v} \\ \left(P+\rho c^2\right)\frac{\gamma^2}{c}\tilde{u} \end{pmatrix} \\
&= \begin{pmatrix} \rho\gamma\tilde{u} \\ ((P+\rho c^2)\frac{\gamma^2}{c^2}\tilde{u}^2 + P)\cos\theta - (P+\rho c^2)\frac{\gamma^2}{c^2}\tilde{u}\tilde{v}\sin\theta \\ ((P+\rho c^2)\frac{\gamma^2}{c^2}\tilde{u}^2 + P)\sin\theta + (P+\rho c^2)\frac{\gamma^2}{c^2}\tilde{u}\tilde{v}\cos\theta \\ \left(P+\rho c^2\right)\frac{\gamma^2}{c}\tilde{u} \end{pmatrix} \\
&= \begin{pmatrix} \rho\gamma\tilde{u} \\ P\cos\theta + (P+\rho c^2)\frac{\gamma^2}{c^2}(\tilde{u}^2\cos\theta - \tilde{u}\tilde{v}\sin\theta) \\ P\sin\theta + (P+\rho c^2)\frac{\gamma^2}{c^2}(\tilde{u}^2\sin\theta + \tilde{u}\tilde{v}\cos\theta) \\ \left(P+\rho c^2\right)\frac{\gamma^2}{c}\tilde{u} \end{pmatrix}
\end{aligned}
$$

$$
\begin{aligned}
\tilde{u}^2 &= u^2\cos^2\theta + 2uv\cos\theta\sin\theta + v^2\sin^2\theta \\
\tilde{u}\tilde{v} &= uv\cos^2\theta - u^2\cos\theta\sin\theta + v^2\cos\theta\sin\theta - uv\sin^2\theta
\end{aligned}
$$

$$
\begin{aligned}
\tilde{u}^2\cos\theta - \tilde{u}\tilde{v}\sin\theta &= u^2\cos^3\theta + 2uv\cos^2\theta\sin\theta + v^2\cos\theta\sin^2\theta \\
&\quad -uv\sin\theta\cos^2\theta + u^2\cos\theta\sin^2\theta - v^2\cos\theta\sin^2\theta + uv\sin^3\theta \\
&= \cos\theta(u^2\cos^2\theta + u^2\sin^2\theta) + \sin\theta(2uv\cos^2\theta - uv\cos^2\theta + uv\sin^2\theta) \\
&= u^2\cos\theta + uv\sin\theta \\
\tilde{u}^2\sin\theta + \tilde{u}\tilde{v}\cos\theta &= u^2\sin\theta\cos^2\theta + 2uv\cos\theta\sin^2\theta + v^2\sin^3\theta \\
&\quad +uv\cos^3\theta - u^2\cos^2\theta\sin\theta + v^2\cos^2\theta\sin\theta - uv\cos\theta\sin^2\theta \\
&= \cos\theta(2uv\sin^2\theta + uv\cos^2\theta - uv\sin^2\theta) + \sin\theta(v^2\sin^2\theta + v^2\cos^2\theta) \\
&= uv\cos\theta + v^2\sin\theta
\end{aligned}
$$

$$
\begin{aligned}
\mathbf{T}^{-1}\mathbf{F}(\tilde{\mathbf{U}}) &= \begin{pmatrix} \rho\gamma(u\cos\theta + v\sin\theta) \\ P\cos\theta + (P+\rho c^2)\frac{\gamma^2}{c^2}(u^2\cos\theta + uv\sin\theta) \\ P\sin\theta + (P+\rho c^2)\frac{\gamma^2}{c^2}(uv\cos\theta + v^2\sin\theta) \\ \left(P+\rho c^2\right)\frac{\gamma^2}{c}(u\cos\theta + v\sin\theta) \end{pmatrix} \\
&= \cos\theta \begin{pmatrix} \rho\gamma u \\ P + (P+\rho c^2)\frac{\gamma^2}{c^2}u^2 \\ (P+\rho c^2)\frac{\gamma^2}{c^2}uv \\ \left(P+\rho c^2\right)\frac{\gamma^2}{c}u \end{pmatrix} + \sin\theta \begin{pmatrix} \rho\gamma v \\ (P+\rho c^2)\frac{\gamma^2}{c^2}uv \\ P + (P+\rho c^2)\frac{\gamma^2}{c^2}v^2 \\ \left(P+\rho c^2\right)\frac{\gamma^2}{c}v \end{pmatrix} \\
&= \mathbf{F}(\mathbf{U})\cos\theta + \mathbf{G}(\mathbf{U})\sin\theta
\end{aligned}
$$

Which proofs the rotational invariance.

## 5.2 Hyperbolicity

Hyperbolicity is a key feature for our set of equations, because it confirms that the initial value problem corresponding to the equations can be locally solved.

In order to prove that the system of equations is hyperbolic, it first has to be rewritten.

$$\begin{aligned} \partial_t \mathbf{U} + \partial_x \mathbf{F}(\mathbf{U}) + \partial_x \mathbf{G}(\mathbf{U}) &= \mathbf{RHS} \\ \partial_t \mathbf{U} + \frac{\partial \mathbf{F}(\mathbf{U})}{\partial \mathbf{U}} \frac{\partial \mathbf{U}}{\partial x} + \frac{\partial \mathbf{G}(\mathbf{U})}{\partial \mathbf{U}} \frac{\partial \mathbf{U}}{\partial y} &= \mathbf{RHS} \\ \partial_t \mathbf{U} + \mathbf{J}_F \frac{\partial \mathbf{U}}{\partial x} + \mathbf{J}_G \frac{\partial \mathbf{U}}{\partial y} &= \mathbf{RHS} \end{aligned}$$

The terms $\mathbf{J}_F = \frac{\partial \mathbf{F}(\mathbf{U})}{\partial U}$ and $\mathbf{J}_G = \frac{\partial \mathbf{G}(\mathbf{U})}{\partial U}$ are called the Jacobians of the functions $\mathbf{F}(\mathbf{U})$ and $\mathbf{G}(\mathbf{U})$. Here you can see the Jacobian $\mathbf{J}_F$ in detail.

$$\mathbf{J}_F = \begin{pmatrix} \frac{\partial \mathbf{F}_1}{\partial \mathbf{U}_1} & \frac{\partial \mathbf{F}_1}{\partial \mathbf{U}_2} & \frac{\partial \mathbf{F}_1}{\partial \mathbf{U}_3} & \frac{\partial \mathbf{F}_1}{\partial \mathbf{U}_4} \\ \frac{\partial \mathbf{F}_2}{\partial \mathbf{U}_1} & \frac{\partial \mathbf{F}_2}{\partial \mathbf{U}_2} & \frac{\partial \mathbf{F}_2}{\partial \mathbf{U}_3} & \frac{\partial \mathbf{F}_2}{\partial \mathbf{U}_4} \\ \frac{\partial \mathbf{F}_3}{\partial \mathbf{U}_1} & \frac{\partial \mathbf{F}_3}{\partial \mathbf{U}_2} & \frac{\partial \mathbf{F}_3}{\partial \mathbf{U}_3} & \frac{\partial \mathbf{F}_3}{\partial \mathbf{U}_4} \\ \frac{\partial \mathbf{F}_4}{\partial \mathbf{U}_1} & \frac{\partial \mathbf{F}_4}{\partial \mathbf{U}_2} & \frac{\partial \mathbf{F}_4}{\partial \mathbf{U}_3} & \frac{\partial \mathbf{F}_4}{\partial \mathbf{U}_4} \end{pmatrix}$$

The Jacobian $\mathbf{J}_G$ can be computed accordingly.

If the Jacobians of a system of equations have real eigenvalues and if they are diagonalizable the system is called **hyperbolic**.

The first step will now be to compute the both Jacobians, that means the functions $\mathbf{F}(\mathbf{U})$ and $\mathbf{G}(\mathbf{U})$ have to be written in the variables $U_1$, $U_2$, $U_3$ and $U_4$. For simplicity we will set $c = 1$ in these computations.

$$\begin{aligned} \mathbf{U} &= \begin{pmatrix} \rho\gamma \\ (P+\rho)\gamma^2 u \\ (P+\rho)\gamma^2 v \\ E \end{pmatrix} = \begin{pmatrix} U_1 \\ U_2 \\ U_3 \\ U_4 \end{pmatrix} \\ \mathbf{F}(\mathbf{U}) &= \begin{pmatrix} \rho\gamma u \\ (P+\rho)\gamma^2 u^2 + P \\ (P+\rho)\gamma^2 uv \\ u \cdot (E+P) \end{pmatrix} \\ \mathbf{G}(\mathbf{U}) &= \begin{pmatrix} \rho\gamma v \\ (P+\rho)\gamma^2 uv \\ (P+\rho)\gamma^2 v^2 + P \\ v \cdot (E+P) \end{pmatrix} \end{aligned}$$

With $E = (P+\rho)\,\gamma^2 - P$, $E + P = (P+\rho)\gamma^2 = \frac{U_2}{u} = \frac{U_3}{v}$

At this point the variables in vector $\mathbf{U}$ are solved for $P$, $\rho$, $u$ and $v$ and to rewrite the components of $\mathbf{F}(\mathbf{U})$ and $\mathbf{G}(\mathbf{U})$ in variables $U_1$, $U_2$, $U_3$ and $U_4$.

To find the Jacobians, from now on we will assume $\gamma$ as constant. The system of equations that has to be solved is given here:

$$\begin{aligned} U_1 &== \gamma\rho \\ U_2 &== (P+\rho)\gamma^2 u \\ U_3 &== (P+\rho)\gamma^2 v \\ U_4 &== (P+\rho)\gamma^2 - P \end{aligned}$$

The solutions to this system of equations can be found using Mathematica.

$$\left\{ P \to \frac{U_4 - \gamma U_1}{\gamma^2 - 1}, \rho \to \frac{U_1}{\gamma}, u \to \frac{\left(\gamma^2 - 1\right) U_2}{\gamma(\gamma U_4 - U_1)}, v \to \frac{\left(\gamma^2 - 1\right) U_3}{\gamma(\gamma U_4 - U_1)} \right\}$$

That means the function $\mathbf{F(U)}$ can be rewritten in terms of $U_1$, $U_2$, $U_3$ and $U_4$.

$$\mathbf{F(U)} = \begin{pmatrix} \rho\gamma u \\ (P+\rho)\gamma^2 u^2 + P \\ (P+\rho)\gamma^2 uv \\ u \cdot (E+P) \end{pmatrix} = \begin{pmatrix} \frac{U_1 U_2 (\gamma^2-1)}{\gamma(\gamma U_4 - U_1)} \\ \frac{(\gamma^2-1)^2 U_2^2 \left(\frac{U_4-\gamma U_1}{\gamma^2-1} + \frac{U_1}{\gamma}\right)}{(\gamma U_4 - U_1)^2} + \frac{U_4 - \gamma U_1}{\gamma^2 - 1} \\ \frac{(\gamma^2-1)^2 U_2 U_3 \left(\frac{U_4-\gamma U_1}{\gamma^2-1} + \frac{U_1}{\gamma}\right)}{(\gamma U_4 - U_1)^2} + \frac{U_4 - \gamma U_1}{\gamma^2 - 1} \\ U_2 \end{pmatrix}$$

Now, the derivatives of these functions and thus the Jacobians can be computed.

$$\mathbf{J}_F = \begin{pmatrix} \frac{(\gamma^2-1) U_2 U_4}{(U_1 - \gamma U_4)^2} & \frac{(\gamma^2-1) U_1}{\gamma(\gamma U_4 - U_1)} & 0 & -\frac{(\gamma^2-1) U_1 U_2}{(U_1 - \gamma U_4)^2} \\ \frac{(\gamma^2-1)^2 U_2^2}{(\gamma^2-1)\gamma(U_1 - \gamma U_4)^2} - \frac{\gamma}{\gamma^2-1} & \frac{2(\gamma^2-1) U_2}{\gamma(\gamma U_4 - U_1)} & 0 & \frac{1}{\gamma^2-1} - \frac{(\gamma^2-1)^2 U_2^2}{(\gamma^2-1)(U_1 - \gamma U_4)^2} \\ \frac{(\gamma^2-1) U_2 U_3}{\gamma(U_1 - \gamma U_4)^2} & \frac{(\gamma^2-1) U_3}{\gamma(\gamma U_4 - U_1)} & \frac{(\gamma^2-1) U_2}{\gamma(\gamma U_4 - U_1)} & -\frac{(\gamma^2-1) U_2 U_3}{(U_1 - \gamma U_4)^2} \\ 0 & 1 & 0 & 0 \end{pmatrix}$$

With this Jacobian it is now easy to find the eigenvalues in terms of $U_1$, $U_2$, $U_3$ and $U_4$.

$$\begin{aligned} \lambda_{F,1} &= \frac{\left(\gamma^2 - 1\right) U_2}{\gamma(\gamma U_4 - U_1)} \\ \lambda_{F,2} &= \frac{\left(\gamma^2 - 1\right) U_2}{\gamma(\gamma U_4 - U_1)} \\ \lambda_{F,3} &= \frac{2\gamma^5 U_2 U_4 - \gamma^4 U_1 U_2 - 4\gamma^3 U_2 U_4 + 2\gamma^2 U_1 U_2 + 2\gamma U_2 U_4 - U_1 U_2 - \sqrt{D}}{2\gamma\left(\gamma^2 - 1\right)(U_1 - \gamma U_4)^2} \\ \lambda_{F,4} &= \frac{2\gamma^5 U_2 U_4 - \gamma^4 U_1 U_2 - 4\gamma^3 U_2 U_4 + 2\gamma^2 U_1 U_2 + 2\gamma U_2 U_4 - U_1 U_2 + \sqrt{D}}{2\gamma\left(\gamma^2 - 1\right)(U_1 - \gamma U_4)^2} \end{aligned}$$

The last two eigenvalues have the same terms in the square root.

$$
\begin{aligned}
D &= \left(\gamma^2-1\right)^4 U_2^2(U_1-2\gamma U_4)^2 - 4\gamma^2\left(\gamma^2-1\right)(U_1-\gamma U_4)^2 \\
&\quad \left(\gamma^4 U_2^2+\gamma^3 U_1 U_4-\gamma^2\left(U_1^2+2U_2^2+U_4^2\right)+\gamma U_1 U_4+U_2^2\right)
\end{aligned}
$$

The eigenvalues $\lambda_{F,3}$ and $\lambda_{F,4}$ are real, as long as $D$ is bigger than or equal to zero. To check this, the quantities $\rho$, $P$, $u$ and $v$ have to be inserted back into the equation.

$$
\begin{aligned}
D &= \gamma^2(\gamma^2-1)^4((\rho-2(-P+\gamma^2(P+\rho)))^2(P+\gamma^2\rho u)^2 \\
&\quad -4\gamma^2(\gamma^2-1)(P+\rho)^2(-(-1+\gamma^2)P^2+\gamma^4\rho^2u^2+\gamma^2P\rho(-1+2u))) \\
\underbrace{\geq}_{?} &\ 0
\end{aligned}
$$

It is safe to assume, that $\gamma \geq 1$. That means the term $\gamma^2(\gamma^2-1)^4$ is naturally bigger than or equal to zero. Assuming from now on $\gamma > 1$, we can safely divide $D$ by this term.

$$
\begin{aligned}
\frac{D}{\gamma^2(\gamma^2-1)^4} &= (\rho-2(-P+\gamma^2(P+\rho)))^2(P+\gamma^2\rho u)^2 \\
&\quad -4\gamma^2(\gamma^2-1)(P+\rho)^2(-(-1+\gamma^2)P^2+\gamma^4\rho^2u^2+\gamma^2P\rho(-1+2u))
\end{aligned}
$$

The density $\rho$ is bigger than or equal to zero as well, because a negative density has no physical meaning. Because of the relationship between the pressure and the density, the pressure fulfills $P \geq 0$, too. Therefore, the behaviour of the last term with respect to $u$ has to be checked. This term is of the form of a quadratic equation.

$$A_1 + A_2 u + A_3 u^2$$

with

$$
\begin{aligned}
A_1 &= P(4(\gamma^2-1)^2(\gamma^2+1)P^3+4(1-\gamma^2-3\gamma^4+3\gamma^6)P^2\rho+(1-12\gamma^4+12\gamma^6)P\rho^2+4\gamma^4(\gamma^2-1)\rho^3) \\
A_2 &= 2\gamma^2P\rho(-4(\gamma^2-1)P^2-4(\gamma^2-1)P\rho+\rho^2) \\
A_3 &= \gamma^4\rho^2(-4(\gamma^2-1)P^2-4(\gamma^2-1)P\rho+\rho^2)
\end{aligned}
$$

The two roots of this last equation are easy to compute.

$$
\begin{aligned}
A_1 + A_2 u + A_3 u^2 &= 0 \\
\Rightarrow u_0 &= \frac{-A_2 \pm \sqrt{A_2^2 - 4A_3A_1}}{2A_3}
\end{aligned}
$$

$$
\begin{aligned}
u_{0,1} &= \frac{-4\gamma^4P^2\rho(P+\rho)+\gamma^2P\rho(2P+\rho)^2}{\gamma^4\rho^2\left(4\left(\gamma^2-1\right)P^2+4\left(\gamma^2-1\right)P\rho-\rho^2\right)} \\
&\quad -\frac{2\sqrt{\gamma^8\left(\gamma^2-1\right)P\rho^2(P+\rho)^3\left(4\left(\gamma^2-1\right)P^2+4\left(\gamma^2-1\right)P\rho-\rho^2\right)}}{\gamma^4\rho^2\left(4\left(\gamma^2-1\right)P^2+4\left(\gamma^2-1\right)P\rho-\rho^2\right)} \\
&= -\frac{P}{\gamma^2\rho}-2\sqrt{\frac{\left(\gamma^2-1\right)P(P+\rho)^3}{\rho^2\left(4\left(\gamma^2-1\right)P^2+4\left(\gamma^2-1\right)P\rho-\rho^2\right)}} \\
u_{0,2} &= \frac{-4\gamma^4P^2\rho(P+\rho)+\gamma^2P\rho(2P+\rho)^2}{\gamma^4\rho^2\left(4\left(\gamma^2-1\right)P^2+4\left(\gamma^2-1\right)P\rho-\rho^2\right)} \\
&\quad +\frac{2\sqrt{\gamma^8\left(\gamma^2-1\right)P\rho^2(P+\rho)^3\left(4\left(\gamma^2-1\right)P^2+4\left(\gamma^2-1\right)P\rho-\rho^2\right)}}{\gamma^4\rho^2\left(4\left(\gamma^2-1\right)P^2+4\left(\gamma^2-1\right)P\rho-\rho^2\right)} \\
&= -\frac{P}{\gamma^2\rho}+2\sqrt{\frac{\left(\gamma^2-1\right)P(P+\rho)^3}{\rho^2\left(4\left(\gamma^2-1\right)P^2+4\left(\gamma^2-1\right)P\rho-\rho^2\right)}}
\end{aligned}
$$

To find the behaviour of the function, around the roots, the extrema have to be found, too.

$$
\begin{aligned}
\frac{\partial}{\partial u}(A_1+A_2u+A_3u^2) &= 0 \\
A_2+2A_3u &= 0 \\
\Rightarrow u_e = -\frac{A_2}{2A_3} &= -\frac{P}{\gamma^2\rho}
\end{aligned}
$$

$$
\frac{\partial}{\partial u}(A_2+2A_3u) = 2A_3 = 2\gamma^4\rho^2(-4(\gamma^2-1)P^2-4(\gamma^2-1)P\rho+\rho^2)
$$

Now that we know in which cases the eigenvalues of this matrix are real, the next step for the proof of hyperbolicity is to show that both Jacobians are diagonalizable.

A matrix $\mathbf{A}$ is diagonalizable, if there exist a diagonal matrix $\mathbf{D}$ and an invertible matrix $\mathbf{P}$ such that

$$
\mathbf{AP} = \mathbf{PD}.
$$

In other words, $\mathbf{A}$ needs to have linearly independent eigenvectors, such that the eigenvectors form a basis of $\mathbf{A}$. With respect to the eigenvalues, that means, that their geometric multiplicity has to be equal to their algebraic multiplicity, such that the dimensions of the eigenspaces coincides with the algebraic multiplicity of the corresponding eigenvalue.

Let us shortly recap the eigenvalues to find out their algebraic multiplicity.

$$
\begin{aligned}
\lambda_{F,1} &= \lambda_{F,2} = \frac{\left(\gamma^2-1\right)U_2}{\gamma(\gamma U_4 - U_1)} \Rightarrow \text{algebraic multiplicity 2} \\
\lambda_{F,3} &= \frac{2\gamma^5 U_2U_4 - \gamma^4 U_1U_2 - 4\gamma^3 U_2U_4 + 2\gamma^2 U_1U_2 + 2\gamma U_2U_4 - U_1U_2 - \sqrt{D}}{2\gamma\left(\gamma^2-1\right)\left(U_1-\gamma U_4\right)^2} \\
\lambda_{F,4} &= \frac{2\gamma^5 U_2U_4 - \gamma^4 U_1U_2 - 4\gamma^3 U_2U_4 + 2\gamma^2 U_1U_2 + 2\gamma U_2U_4 - U_1U_2 + \sqrt{D}}{2\gamma\left(\gamma^2-1\right)\left(U_1-\gamma U_4\right)^2}
\end{aligned}
$$

There is an eigenvalue with algebraic multiplicity two. Depending on the value of the discriminant $D$ there are either two other eigenvalues with algebraic multiplicity one or there is just one other eigenvalue with algebraic multiplicity two. The first case being if $D \neq 0$ and the second case if $D = 0$.

With the help of Mathematica the eigenvectors of the matrix can be found. Fortunately Mathematicas output is automatically a set of linearly independent vectors.

$$
\begin{aligned}
e_{F,1} &= \left\{\frac{1}{\gamma}, \frac{\gamma^2\rho u + P}{\gamma^2(P+\rho)}, 0, 1\right\} \\
e_{F,2} &= \{0,0,1,0\} \\
e_{F,3} &= \left\{\frac{\rho N_1}{D_1}, \frac{N_2}{D_2}, \frac{N_1 v}{\hat{D}_1}, 1\right\} \\
e_{F,4} &= \left\{\frac{\rho \hat{N}_1}{\hat{D}_1}, \frac{\hat{N}_2}{D_2}, -\frac{\hat{N}_1 v}{D_1}, 1\right\}
\end{aligned}
$$

$$
\begin{aligned}
S &= 4\left(\gamma^2-1\right)^2\left(\gamma^2+1\right)P^4 + 4\left(\gamma^2-1\right)\rho\left(3\gamma^4 - 2u\gamma^2 - 1\right)P^3 \\
&\quad + \rho^2\left(-4\left(u^2-3\right)\gamma^6 + 4\left(u^2-2u-3\right)\gamma^4 + 8u\gamma^2 + 1\right)P^2 \\
&\quad + 2\gamma^2\rho^3\left(-2\left(u^2-1\right)\gamma^4 + 2\left(u^2-1\right)\gamma^2 + u\right)P + \gamma^4\rho^4u^2 \\
N_1 &= 2\rho^3\gamma^6 - 2\rho^3u^2\gamma^6 - 2\rho^3\gamma^4 + \rho^3u^2\gamma^4 + \rho u\sqrt{S}\gamma^2 + 2\left(\gamma^2-1\right)^2\left(\gamma^2+1\right)P^3 \\
&\quad + P^2\rho\left(6\gamma^6 - 2(2u+3)\gamma^4 + (4u-2)\gamma^2 + 1\right) \\
&\quad + P\left(-2\rho^2\left(u^2-3\right)\gamma^6 + 2\rho^2\left(u^2-2u-3\right)\gamma^4 + 2\rho^2u\gamma^2 + \sqrt{S}\right) \\
\hat{N}_1 &= -2\rho^3\gamma^6 + 2\rho^3u^2\gamma^6 + 2\rho^3\gamma^4 - \rho^3u^2\gamma^4 + \rho u\sqrt{S}\gamma^2 - 2\left(\gamma^2-1\right)^2\left(\gamma^2+1\right)P^3 \\
&\quad - P^2\rho\left(6\gamma^6 - 2(2u+3)\gamma^4 + (4u-2)\gamma^2 + 1\right) \\
&\quad + P\left(2\rho^2\left(u^2-3\right)\gamma^6 - 2\rho^2\left(u^2-2u-3\right)\gamma^4 - 2\rho^2u\gamma^2 + \sqrt{S}\right) \\
D_1 &= 2\gamma\left(\gamma^2-1\right)(P+\rho)^2\left(-\rho^2\left(u^2-1\right)\gamma^4 + 2P\rho\left(\gamma^2-u\right)\gamma^2 + \left(\gamma^4-1\right)P^2\right) \\
\hat{D}_1 &= 2\gamma\left(\gamma^2-1\right)(P+\rho)^2\left(\rho^2\left(u^2-1\right)\gamma^4 + 2P\rho\left(u-\gamma^2\right)\gamma^2 - \left(\gamma^4-1\right)P^2\right) \\
N_2 &= 2\rho^2u\gamma^4 - \rho^2u\gamma^2 + 2\left(\gamma^2-1\right)P^2 + P\rho\left(2u\gamma^4 - 2(u-1)\gamma^2 - 1\right) - \sqrt{S} \\
\hat{N}_2 &= 2\rho^2u\gamma^4 - \rho^2u\gamma^2 + 2\left(\gamma^2-1\right)P^2 + P\rho\left(2u\gamma^4 - 2(u-1)\gamma^2 - 1\right) + \sqrt{S} \\
D_2 &= 2\gamma^2\left(\gamma^2-1\right)(P+\rho)^2
\end{aligned}
$$

There are four linearly independent eigenvectors for the four-dimensional system of equations. That means, that the Jacobian $\mathbf{J}_F$ is diagonalizable.

All of these calculations can also be done for the flux function $\mathbf{G(U)}$.

$$\mathbf{G(U)} = \begin{pmatrix} \rho\gamma v \\ (P+\rho)\gamma^2 uv \\ (P+\rho)\gamma^2 v^2 + P \\ v\cdot(E+P) \end{pmatrix} = \begin{pmatrix} \frac{U_1 U_3(\gamma^2-1)}{\gamma(\gamma U_4 - U_1)} \\ \frac{(\gamma^2-1)^2 U_2 U_3 \left(\frac{U_4-\gamma U_1}{\gamma^2-1}+\frac{U_1}{\gamma}\right)}{(\gamma U_4-U_1)^2} + \frac{U_4-\gamma U_1}{\gamma^2-1} \\ \frac{(\gamma^2-1)^2 U_3^2 \left(\frac{U_4-\gamma U_1}{\gamma^2-1}+\frac{U_1}{\gamma}\right)}{(\gamma U_4-U_1)^2} + \frac{U_4-\gamma U_1}{\gamma^2-1} \\ U_3 \end{pmatrix}$$

The Jacobian $\mathbf{J}_G$ of this flux function and its eigenvalues can be found using Mathematica, too.

$$\mathbf{J}_G = \begin{pmatrix} \frac{(\gamma^2-1)U_3U_4}{(U_1-\gamma U_4)^2} & 0 & \frac{(\gamma^2-1)U_1}{\gamma(\gamma U_4-U_1)} & -\frac{(\gamma^2-1)U_1U_3}{(U_1-\gamma U_4)^2} \\ \frac{(\gamma^2-1)U_2U_3}{\gamma(U_1-\gamma U_4)^2} & \frac{(\gamma^2-1)U_3}{\gamma(\gamma U_4-U_1)} & \frac{(\gamma^2-1)U_2}{\gamma(\gamma U_4-U_1)} & -\frac{(\gamma^2-1)U_2U_3}{(U_1-\gamma U_4)^2} \\ \frac{(\gamma^2-1)^2U_3^2}{(\gamma^2-1)\gamma(U_1-\gamma U_4)^2} - \frac{\gamma}{\gamma^2-1} & 0 & \frac{2(\gamma^2-1)U_3}{\gamma(\gamma U_4-U_1)} & \frac{1}{\gamma^2-1} - \frac{(\gamma^2-1)^2U_3^2}{(\gamma^2-1)(U_1-\gamma U_4)^2} \\ 0 & 0 & 1 & 0 \end{pmatrix}.$$

$$\begin{aligned}
\lambda_{G,1} &= \frac{\left(\gamma^2-1\right)U_3}{\gamma(\gamma U_4 - U_1)} \\
\lambda_{G,2} &= \frac{\left(\gamma^2-1\right)U_3}{\gamma(\gamma U_4 - U_1)} \\
\lambda_{G,3} &= \frac{2U_3U_4\gamma^5 - 4U_3U_4\gamma^3 + 2U_3U_4\gamma - \left(\gamma^2-1\right)^2 U_1U_3 - \sqrt{D}}{2\gamma\left(\gamma^2-1\right)(U_1-\gamma U_4)^2} \\
\lambda_{G,4} &= \frac{2U_3U_4\gamma^5 - 4U_3U_4\gamma^3 + 2U_3U_4\gamma - \left(\gamma^2-1\right)^2 U_1U_3 + \sqrt{D}}{2\gamma\left(\gamma^2-1\right)(U_1-\gamma U_4)^2}
\end{aligned}$$

As it was before, there is a term in the square root, that defines if the eigenvalues are real or not. To find out under which conditions this term becomes imaginary, the term has to be investigated in detail.

$$\begin{aligned}
D &= \left(\gamma^2-1\right)\Big(-U_1^2\left(U_1-2\gamma U_4\right) - 4\gamma^2\left(U_1-\gamma U_4\right)^2 \\
&\quad \left(U_2^2 + \gamma^4 U_2^2 + \gamma U_1 U_4 + \gamma^3 U_1 U_4 - \gamma^2\left(U_1^2 + 2U_2^2 + U_4^2\right)\right)\Big) \\
&= -\gamma^6\left(\gamma^2-1\right)^4(P+\rho)^2\left(-\rho^2v^2 + 4\left(\gamma^2-1\right)P^2\left(v^2-1\right) + 4\left(\gamma^2-1\right)P\rho\left(v^2-1\right)\right) \\
\underbrace{\geq}_{?} & \; 0
\end{aligned}$$

Since $\gamma^6\left(\gamma^2-1\right)^4(P+\rho)^2 > 0$ for $\gamma > 1$ and $\rho > 0$, it is sufficient to check wether $\frac{D}{\gamma^6(\gamma^2-1)^4(P+\rho)^2} \geq 0$.

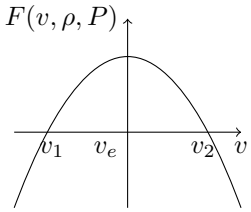


Figure 2: Sketch of the function $F(v,\rho,P)$ showing the two roots with respect to velocity $v$.

$$\begin{aligned}\frac{D}{\gamma^6\left(\gamma^2-1\right)^4(P+\rho)^2} &= \rho^2v^2-4\left(\gamma^2-1\right)P^2\left(v^2-1\right)-4\left(\gamma^2-1\right)P\rho\left(v^2-1\right)\\ &= \left(\rho^2-4\left(\gamma^2-1\right)\left(P^2+P\rho\right)\right)v^2+4\left(\gamma^2-1\right)\left(P^2+P\rho\right)\end{aligned}$$

$$\begin{aligned}&(\rho^2-4P(\gamma^2-1)(P+\rho))v^2+4P(\gamma^2-1)(P+\rho)=0\\ v_{1,2} &= \pm\sqrt{\frac{4P(\gamma^2-1)(P+\rho)}{4P(\gamma^2-1)(P+\rho)-\rho^2}}\end{aligned}$$

Furtheremore,

$$\begin{aligned}&\frac{\partial}{\partial v}((\rho^2-4P(\gamma^2-1)(P+\rho))v^2+4P(\gamma^2-1)(P+\rho))=2(\rho^2-4P(\gamma^2-1)(P+\rho))v_e=0\\ &\Rightarrow v=0\\ &\frac{\partial}{\partial v}(2(\rho^2-4P(\gamma^2-1)(P+\rho))v)=2(\rho^2-4P(\gamma^2-1)(P+\rho))\leq 0\end{aligned}$$

That means the function

$$F(v,\rho,P)=(\rho^2-4P(\gamma^2-1)(P+\rho))v^2+4P(\gamma^2-1)(P+\rho)$$

has two roots and a maximum at $v=0$. Here you can see a sketch of this function.

That means the eigenvalue is only real for certain values of $v$.

$$(\lambda_{G,3},\,\lambda_{G,4})\in\mathbb{R}\,\text{iff}-\sqrt{\frac{4P(\gamma^2-1)(P+\rho)}{4P(\gamma^2-1)(P+\rho)-\rho^2}}\leq v\leq\sqrt{\frac{4P(\gamma^2-1)(P+\rho)}{4P(\gamma^2-1)(P+\rho)-\rho^2}}$$

Mathematica computes the following linearly independent eigenvectors corresponding to these eigenvectors

$$
\begin{aligned}
e_{G,1} &= \{\frac{1}{\gamma}, 0, v, 1\} \\
e_{G,2} &= \{0, 1, 0, 0\} \\
e_{G,3} &= \left\{ \frac{\rho N_1}{D_1}, \frac{\left(\gamma^2 \rho u + P\right) N_1}{\gamma D_1}, \frac{\gamma(v^2-1)(P+\rho)N_2}{D_1}, 1 \right\} \\
e_{G,4} &= \left\{ \frac{\rho \hat{N}_1}{D_1}, \frac{\left(\gamma^2 \rho u + P\right) \hat{N}_1}{\gamma D_1}, \frac{\hat{N}_2}{D_1}, 1 \right\}
\end{aligned}
$$

$$
\begin{aligned}
S &= \sqrt{-\gamma^4 \left(4\left(\gamma^2-1\right)P^2\left(v^2-1\right) + 4\left(\gamma^2-1\right)P\rho\left(v^2-1\right) - \rho^2 v^2\right)} \\
N_1 &= 2\gamma^4\left(v^2-1\right)(P+\rho) + \gamma^2\left(-2P\left(v^2-1\right) - \rho\left(v^2-2\right)\right) - vS \\
\hat{N}_1 &= 2\gamma^4\left(v^2-1\right)(P+\rho) + \gamma^2\left(-2P\left(v^2-1\right) - \rho\left(v^2-2\right)\right) + vS \\
D_1 &= 2\gamma^3\left(\gamma^2-1\right)\left(v^2-1\right)(P+\rho)^2 \\
N_2 &= 2\gamma^4 v(P+\rho) - \gamma^2 v(2P+\rho) - S \\
\hat{N}_2 &= 2\gamma^4 v(P+\rho) - \gamma^2 v(2P+\rho) + S
\end{aligned}
$$

Here, there are also four linearly independent eigenvectors for the four-dimensional system of equations. That means, that the Jacobian $\mathbf{J}_G$ is diagonalizable, too.

In conclusion, we found that both Jacobians $\mathbf{J}_F$ and $\mathbf{J}_G$ are diagonalizable. On top of that, they have real eigenvalues under certain conditions. As long as the velocities $u$ and $v$ fulfill these conditions, that means as long as the eigenvalues are real, we can call the system of equations hyperbolic. The moment one or both of the concerning eigenvalues become complex, the system is a mix of a hyperbolic and an elliptic set of equations. This case won't be the focus of interest in this work. It has to be kept in mind that the case of non-hyperbolicity can occur. The condition of hyperbolicity should be checked, while solving the equations.

## 5.3 Hyperbolicity in time

In section 5.1 we already showed, that the function $\mathbf{F(U)}$ fulfills the following equation, which describes the rotational invariance.

$$\mathbf{T}^{-1}\mathbf{F(TU)} = \mathbf{F(U)}\cos\theta + \mathbf{G(U)}\sin\theta.$$

Analogously to the procedure described in Toros book [17] this can be used to prove, that the system of equations is hyperbolic in time. First the above equation will be differentiated, since not the function, but its jacobian is at interest here.

$$
\begin{aligned}
\mathbf{T}^{-1}\mathbf{F(TU)} &= \mathbf{F(U)}\cos\theta + \mathbf{G(U)}\sin\theta \\
\mathbf{T}^{-1}\frac{\partial \mathbf{F(TU)}}{\partial U}\underbrace{\mathbf{T}}_{\text{inner derivation}} &= \frac{\partial \mathbf{F(U)}}{\partial U}\cos\theta + \frac{\partial \mathbf{G(U)}}{\partial U}\sin\theta \\
\mathbf{T}^{-1}\mathbf{J}_F(\mathbf{TU})\mathbf{T} &= \mathbf{J}_F\cos\theta + \mathbf{J}_G\sin\theta
\end{aligned}
$$

We already proofed in section 4.2, that the Jacobian $\mathbf{J}_F$ is diagonalizable, that means we can replace it by

$$\mathbf{J}_F = \mathbf{P}\mathbf{D}\mathbf{P}^{-1}$$

with $\mathbf{P}$ being a matrix consisting of the eigenvectors of the matrix and $\mathbf{D}$ being a diagonal matrix consisting of the eigenvalues of the matrix.

$$\begin{aligned}
\mathbf{T}^{-1}\mathbf{J}_F(\mathbf{T}\mathbf{U})\mathbf{T} &= \mathbf{T}^{-1}\left(\mathbf{P}\mathbf{D}\mathbf{P}^{-1}\right)\mathbf{T} \\
&= \left(\mathbf{T}^{-1}\mathbf{P}\right)\mathbf{D}\left(\mathbf{P}^{-1}\mathbf{T}\right) \\
&= \left(\mathbf{T}^{-1}\mathbf{P}\right)\mathbf{D}\left(\mathbf{T}^{-1}\mathbf{P}\right)^{-1} \\
&= \tilde{\mathbf{T}}\mathbf{D}\tilde{\mathbf{T}}^{-1}
\end{aligned}$$

Since $\mathbf{D}$ is a diagonal matrix and the matrix $\tilde{\mathbf{T}}$ can be seen as transformation matrix, this last line proofs the diagonalizability. Therefore, we know that the system of equations is hyperbolic in time.

# 6 Rotating frame of reference

The system we want to discuss with this Ansatz is the cyclotron. A cyclotron is a particle accelerator, where particles are accelerated by electric fields while a magnetic field leads them on a curved trajectory. The simplest form of a cyclotron consists of two semicircular magnets, the so-called D's, and an accelerating gap between them. The particles will be accelerated in the gap, then they follow a circular trajectory through the magnetic field and after that they will be accelerated again. That means in the end, the particles will spiral from the middle of the cyclotron outside.

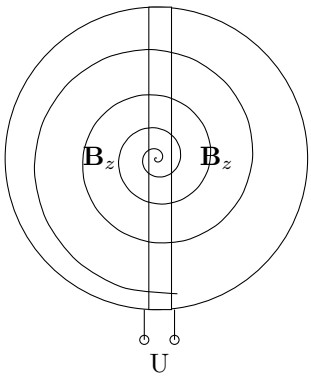


Figure 3: Sketch of a classical cyclotron with the path of an ion circling outside.

The cyclotron that can be seen in Figure 3 is the classic form of a cyclotron. It has a constant magnetic field and a constant RF (radio frequency) for the accelerating gap between the two D's. Relativistic effects can destroy the synchronization of this setup, that means the particle doesn't hit the rf field in the accelerating gap perfectly any more. The output energy of this kind of cyclotron is thus limited. Improvements to this cyclotron model are the Azimuthally-Varying-Field (AVF) Cyclotron and the Separated Sector Cyclotron, which is a special case of the AVF Cyclotron. In this form of a cyclotron, the bending magnet is split into several sectors. This varies the magnetic field and adds an extra horizontal field component and thus leads to vertical focusing.

Because of this setup, the best corresponding coordinate system is a curvilinear one: the cylindrical coordinate system. This coordinate system will be described in the next sections. The center of mass of the particle beam is rotating around the center of the cyclotron, that means if we want to simulate it, ficticious forces have to be considered, too. This will be done in section 6.3 and it will be applied to our equations in section 6.4.

## 6.1 General transformation to curvilinear coordinates

Coordinates $(q_1, q_2, q_3)$ with unit vectors $\{\mathbf{e}_1, \mathbf{e}_2, \mathbf{e}_3\}$ that are orthogonal, thus satisfying $\mathbf{e}_i \mathbf{e}_j = \delta_{ij}$, lead to a line element

$$ds^2 = h_1^2 dq_1^2 + h_2^2 dq_2^2 + h_3^2 dq_3^2$$

The connection to cartesian coordinates is given by

$$h_i^2 = \left(\frac{\partial x}{\partial q_i}\right)^2 + \left(\frac{\partial y}{\partial q_i}\right)^2 + \left(\frac{\partial z}{\partial q_i}\right)^2$$

In this formulation the derivatives can be rewritten as follows

$$\begin{aligned}
\nabla\phi &= \left(\frac{1}{h_1}\partial_1\phi\right)\mathbf{e}_1 + \left(\frac{1}{h_2}\partial_2\phi\right)\mathbf{e}_2 + \left(\frac{1}{h_3}\partial_3\phi\right)\mathbf{e}_3 \\
\nabla\mathbf{A} &= \frac{1}{h_1h_2h_3}\left(\partial_1(\mathbf{A}_1h_2h_3) + \partial_2\left(\mathbf{A}_2h_3h_1\right) + \partial_3\left(\mathbf{A}_3h_1h_2\right)\right)
\end{aligned}$$

## 6.2 Cylindrical Coordinates

The relation between the Euclidean and the cylindrical coordinate system is given as

$$\begin{aligned}
x = r\cos\theta,\ y = r\sin\theta,\ z = z \\
\theta = \tan^{-1}(y/x),\ r = \sqrt{x^2+y^2}
\end{aligned}$$

and

$$\begin{aligned}
dr = \cos\theta dx + \sin\theta dy \\
d\theta = -\frac{1}{r}\sin\theta dx + \frac{1}{r}\cos\theta dy
\end{aligned}$$

The unit basis vectors in this system are

$$\mathbf{e}_r = \begin{pmatrix}\cos\theta\\ \sin\theta\\ 0\end{pmatrix},\ \mathbf{e}_\theta = \begin{pmatrix}-\sin\theta\\ \cos\theta\\ 0\end{pmatrix},\ \mathbf{e}_z = \begin{pmatrix}0\\ 0\\ 1\end{pmatrix}$$

A coordinate transformation between the two systems can be made by applying the transformation matrix $S$:

$$dx^i = S^i_j dx^j$$

$$\begin{aligned}
S &= \begin{pmatrix}\cos\theta & \sin\theta & 0\\ -\frac{1}{r}\sin\theta & \frac{1}{r}\cos\theta & 0\\ 0 & 0 & 1\end{pmatrix} \\
S^{-1} &= \begin{pmatrix}\cos\theta & -r\sin\theta & 0\\ \sin\theta & r\cos\theta & 0\\ 0 & 0 & 1\end{pmatrix}
\end{aligned}$$

The metric tensor for the cylindrical geometry takes the form

$$g_{ij} = \begin{pmatrix}1 & 0 & 0\\ 0 & r^2 & 0\\ 0 & 0 & 1\end{pmatrix},\ g^{ij} = \begin{pmatrix}1 & 0 & 0\\ 0 & 1/r^2 & 0\\ 0 & 0 & 1\end{pmatrix},$$

The resulting derivatives are

$$\nabla\phi = \frac{\partial\phi}{\partial r}\mathbf{e}_r + \frac{1}{r}\frac{\partial\phi}{\partial\theta}\mathbf{e}_\theta + \frac{\partial\phi}{\partial z}\mathbf{e}_z$$

$$\nabla\mathbf{A} = \frac{1}{r}\frac{\partial\left(rA_r\right)}{\partial r} + \frac{1}{r}\frac{\partial A_\theta}{\partial\theta} + \frac{\partial A_z}{\partial z}$$

$$\nabla\times\mathbf{A}\begin{pmatrix} \frac{1}{r}\frac{\partial A_z}{\partial\theta} - \frac{\partial A_\theta}{\partial z} \\ \frac{\partial A_r}{\partial z} - \frac{\partial A_z}{\partial r} \\ \frac{1}{r}\left(\frac{\partial(rA_\theta)}{\partial r} - \frac{\partial A_r}{\partial\theta}\right) \end{pmatrix}$$

$$\Delta\phi = \frac{1}{r}\frac{\partial}{\partial r}\left(r\frac{\partial\phi}{\partial r}\right) + \frac{1}{r^2}\frac{\partial^2\phi}{\partial\theta^2} + \frac{\partial^2\phi}{\partial z^2}$$

$$\begin{aligned}\nabla P = &\left[\partial_r P_{rr} + \frac{1}{r}(\partial_{\theta r}P_{\theta r} + P_{rr} - P_{\theta\theta}) + \partial_z P_{zr}\right]\mathbf{e}_r \\ &+ \left[\partial_r P_{r\theta} + \frac{1}{r}(\partial_\theta P_{\theta\theta} + P_{r\theta} + P_{\theta r}) + \partial_z P_{z\theta}\right]\mathbf{e}_\theta \\ &+ \left[\partial_r P_{rz} + \frac{1}{r}(\partial_\theta P_{\theta z} + P_{rz}) + \partial_z P_{zz}\right]\mathbf{e}_z\end{aligned}$$

(Scalar field $\phi$, Vektor field $A$, Tensor $P$)

## 6.3 Coordinate system rotating with angular velocity $\boldsymbol{\omega}$

Here, we consider a coordinate system rotating with angular velocity $\boldsymbol{\omega}$ relative to a stationary (inertial) system. For a rotation about the z axis of the inertial system, both systems are related by the following equations [vii]:

$$\begin{aligned} x &= x_{rot}\cos(\omega t) - y_{rot}\sin(\omega t) \\ y &= x_{rot}\sin(\omega t) + y_{rot}\cos(\omega t) \end{aligned}$$

$$\begin{aligned} x_{rot} &= x\cos(-\omega t) - y\sin(-\omega t) \\ y_{rot} &= x\sin(-\omega t) - y\cos(-\omega t) \end{aligned}$$

The basis vectors of the rotational system are also rotating with $\boldsymbol{\omega}$:

$$\mathbf{e}_x = \begin{pmatrix}\cos\omega t \\ \sin\omega t \\ 0\end{pmatrix},\ \mathbf{e}_x = \begin{pmatrix}-\sin\omega t \\ \cos\omega t \\ 0\end{pmatrix},\ \mathbf{e}_x = \begin{pmatrix}0 \\ 0 \\ 1\end{pmatrix}$$

$$\frac{d\mathbf{e}_i}{dt} = \boldsymbol{\omega}\times\mathbf{e}_i$$

In the rotating frame fictitious forces occur:

$$\begin{aligned} \mathbf{v}_{inertial} &= \mathbf{v}_{rot} + \boldsymbol{\omega}\times\mathbf{r} \\ \mathbf{a}_{inertial} &= \mathbf{a}_{rot} + 2\boldsymbol{\omega}\times\mathbf{v}_{rot} + \boldsymbol{\omega}\times(\boldsymbol{\omega}\times\mathbf{r}) + \frac{d\boldsymbol{\omega}}{dt}\times\mathbf{r} \\ \mathbf{a}_{rot} &= \mathbf{a}_{inertial} - 2\boldsymbol{\omega}\times\mathbf{v}_{rot} - \boldsymbol{\omega}\times(\boldsymbol{\omega}\times\mathbf{r}) - \frac{d\boldsymbol{\omega}}{dt}\times\mathbf{r} \end{aligned}$$

[vii] Quantities denoted by $_{rot}$ are defined in the rotational frame

The terms in the last equations correspond to the following fictitious forces:

- $2\rho\boldsymbol{\omega} \times \mathbf{v}_{rot}$ Coriolis Force, $\rho = mn$
- $\rho\boldsymbol{\omega} \times (\boldsymbol{\omega} \times \mathbf{r})$ Centrifugal Force
- $\rho\frac{d\boldsymbol{\omega}}{dt} \times \mathbf{r}$ Euler Force (from radial acceleration)

When including these terms into the fluid equations of motion the centrifugal term can be included as part of the radial pressure [18]. However, it is important to consider the coriolis term. To understand the influence of the Coriolis Force we can for now consider the angular velocity to point into $z$ direction, $\boldsymbol{\omega} = \omega\hat{z}$. Now, splitting the motion of the fluid into a radial part, an angular part and a part that goes into z direction, we can deduce the influence of the force to the different parts of the velocity.

$$\begin{aligned}
\boldsymbol{\omega} \times \mathbf{v}_z &= 0 \\
\boldsymbol{\omega} \times \mathbf{v}_r &= v_r\omega\mathbf{e}_\theta \\
\boldsymbol{\omega} \times \mathbf{v}_\theta &= -v_\theta\omega\mathbf{e}_r
\end{aligned}$$

That means Coriolis effects only occur for the radial and angular parts of the fluid velocity.

## 6.4 Transforming the Fluid Equations

The Relativistic Fluid equations (6), (7) and (8) can now be transformed into the cylindrical coordinate system $(t', r', \theta', z')$ and then into the rotating frame $(t'', r'', \theta'', z'')$ using these coordinate relations:

$$\begin{aligned}
t'' &= t' \\
r'' &= r' \\
\theta'' &= \theta' - \omega t' \\
z'' &= z'
\end{aligned}$$

The velocity coordinate also changes with the rotation:

$$\begin{aligned}
v_r'' &= v_r' \\
v_\theta'' &= v_\theta' + r'\omega
\end{aligned}$$

The momentum equation then transforms in the following way[viii]:

$$\partial_t((P + \rho c^2)\gamma^2\frac{\mathbf{v}}{c}) + \nabla((P + \rho c^2)\gamma^2\frac{\mathbf{v}\mathbf{v}}{c^2}) + \nabla P = qn\gamma(\mathbf{E} + \frac{1}{c}\mathbf{v} \times \mathbf{B})$$
$$\partial_t((P' + \rho' c^2)\gamma^2\frac{\mathbf{v}'}{c}) + \nabla'((P' + \rho' c^2)\gamma^2\frac{\mathbf{v}'\mathbf{v}'}{c^2}) + \nabla' P' = qn'\gamma(\mathbf{E}' + \frac{1}{c}\mathbf{v}' \times \mathbf{B})$$

[viii] From now on the ˜ will be omitted.

here the primed derivatives $\nabla'$ correspond to the cylindrical coordinate system (26) and the primed quantities correspond to the quantities from the euclidean coordinate system expressed in the cylindrical coordinate system. Moreover, on the left hand side the additional fictitious forces discussed in section (6.3) have to be added.

$$\begin{aligned}\partial_t((P'+\rho'c^2)\gamma^2\frac{\mathbf{v}'}{c})+\nabla'((P'+\rho'c^2)\gamma^2\frac{\mathbf{v}'\mathbf{v}'}{c^2})+\nabla' P' &= qn'\gamma(\mathbf{E}'+\frac{1}{c}\mathbf{v}'\times\mathbf{B})\\ \partial_t''((P''+\rho''c^2)\gamma^2\frac{\mathbf{v}''}{c})+\nabla''((P''+\rho''c^2)\gamma^2\frac{\mathbf{v}''\mathbf{v}''}{c^2})+\nabla'' P'' &\\ = qn''\gamma(\mathbf{E}''+\frac{1}{c}\mathbf{v}''\times\mathbf{B})+2mn''\boldsymbol{\omega}\times\mathbf{v}''+mn''\boldsymbol{\omega}\times(\boldsymbol{\omega}\times\mathbf{r})+mn''\frac{d\boldsymbol{\omega}}{dt}\times\mathbf{r}&\end{aligned}$$

with $\mathbf{v}_{rot}\equiv\mathbf{v}''$ and

$$\nabla''\mathbf{A}=\frac{1}{r''}\frac{\partial\left(r''A_r''\right)}{\partial r''}+\frac{1}{r''}\frac{\partial A_\theta''}{\partial\theta''}+\frac{\partial A_z''}{\partial z''}$$

Plugging in $\omega=\frac{q\mathbf{B}}{\gamma mc}$

$$\begin{aligned}\partial_t''((P''+\rho''c^2)\gamma^2\frac{\mathbf{v}''}{c})+\nabla''((P''+\rho''c^2)\gamma^2\frac{\mathbf{v}''\mathbf{v}''}{c^2})+\nabla'' P''&\\ = qn''\gamma(\mathbf{E}''+\frac{1}{c}\mathbf{v}''\times\mathbf{B})+2qn''\gamma\mathbf{B}\times\frac{\mathbf{v}''}{c}+mn''\boldsymbol{\omega}\times(\boldsymbol{\omega}\times\mathbf{r}'')+mn''\frac{d\boldsymbol{\omega}}{dt''}\times\mathbf{r}''&\end{aligned}$$

So, omitting the $''$ from now on

$$\begin{aligned}\partial_t((P+\rho c^2)\gamma^2\frac{\mathbf{v}}{c})+\nabla((P+\rho c^2)\gamma^2\frac{\mathbf{v}\mathbf{v}}{c^2})+\nabla P&\\ = qn\gamma(\mathbf{E}-\frac{1}{c}\mathbf{v}\times\mathbf{B})+\rho\boldsymbol{\omega}\times(\boldsymbol{\omega}\times\mathbf{r})+\rho\frac{d\boldsymbol{\omega}}{dt}\times\mathbf{r}&\end{aligned}$$

Now, as discussed in section (6.3) the centrifugal term can be included into the pressure.

$$\begin{aligned}\partial_t((P+\rho c^2)\gamma^2\frac{\mathbf{v}}{c})+\nabla((P+\rho c^2)\gamma^2\frac{\mathbf{v}\mathbf{v}}{c^2})+\nabla P&\\ = qn\gamma(\mathbf{E}-\frac{1}{c}\mathbf{v}\times\mathbf{B})+\rho\frac{d\boldsymbol{\omega}}{dt}\times\mathbf{r}&\end{aligned}$$

If we assume that the angular velocity isn't accelerating the final fluid equation in the rotating frame become

$$\partial_t((P+\rho c^2)\gamma^2\frac{\mathbf{v}}{c})+\nabla((P+\rho c^2)\gamma^2\frac{\mathbf{v}\mathbf{v}}{c^2})+\nabla P=qn\gamma(\mathbf{E}-\frac{1}{c}\mathbf{v}\times\mathbf{B})\qquad(26)$$

# 7 Transformation of the Lorentz force in the momentum equation

In a relativistic framework the electric and magnetic fields have to be transformed to, that means the Lorentz force on the right hand side of the momentum equation (26) has to be transformed correctly.

$$\begin{aligned} \text{RHS (right hand side), lab} &= qn\gamma\left(\mathbf{E}+\mathbf{v}\times\mathbf{B}\right) \\ \text{RHS, moving} &= qn\gamma\left(\mathbf{E}'-\mathbf{v}\times\mathbf{B}'\right)+\rho\boldsymbol{\omega}\times(\boldsymbol{\omega}\times\mathbf{r})+\rho\frac{d\boldsymbol{\omega}}{dt}\times\mathbf{r} \end{aligned}$$

The transformation of the electromagnetic field between the labframe and the moving reference frame is given by [12]

$$\mathbf{E}' = \gamma\left(\mathbf{E}+\mathbf{v}\times\mathbf{B}\right)-\frac{\gamma^2}{\gamma+1}\frac{1}{c^2}\mathbf{v}\left(\mathbf{vE}\right) \tag{27}$$

$$\mathbf{B}' = \gamma\left(\mathbf{B}-\frac{1}{c^2}\mathbf{v}\times\mathbf{E}\right)-\frac{\gamma^2}{\gamma+1}\frac{1}{c^2}\mathbf{v}\left(\mathbf{vB}\right) \tag{28}$$

Let us consider the system being boosted only in y direction, assuming that the motion in the x and z direction is nonrelativistic. We assume to have an external magnetic field defined in the lab frame and a self-electric field created by the charge of the plasma, which can be assumed to fulfill the electrostatic approximation in the moving reference frame. This setup is sketched in Fig 4.

$$E' = \frac{1}{4\pi\epsilon_0}\int_V dV\frac{\rho\hat{\mathbf{r}}}{r_x^2+r_y^2+r_z^2}$$

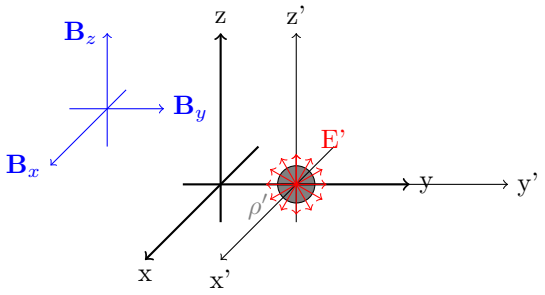


Figure 4: Sketch of the Coordinate systems. The lab system in blue, where the magnetic field is defined and the moving system of the particle beam denoted by primed quantities with the electric field created by the beam.

That means we start with the following two fields, one defined in the lab frame and the other one calculated in the moving frame(primed quantities):

$$\mathbf{B} = \begin{pmatrix} B_x \\ B_y \\ B_z \end{pmatrix} \text{ and } \mathbf{E'} = \begin{pmatrix} E'_x \\ E'_y \\ E'_z \end{pmatrix}$$

The transformations (27) and (28) for a boost in y direction can be rewritten, with $\gamma = \frac{1}{\sqrt{1-v^2/c^2}}$

$$\begin{aligned} E'_x &= \gamma\,(E_x + vB_z) & E_x &= \gamma\,(E'_x - vB'_z) \\ E'_y &= E_y & E_y &= E'_y \\ E'_z &= \gamma\,(E_z - vB_x) & E_z &= \gamma\,(E'_z + vB'_x) \end{aligned}$$

$$\begin{aligned} B'_x &= \gamma\left(B_x - \frac{1}{c^2}vE_z\right) & B_x &= \gamma\left(B'_x + \frac{1}{c^2}vE'_z\right) \\ B'_y &= B_y & B_y &= B'_y \\ B'_z &= \gamma\left(B_z + \frac{1}{c^2}vE_x\right) & B_z &= \gamma\left(B'_z - \frac{1}{c^2}vE'_x\right) \end{aligned}$$

The right hand side can now be given in the lab or in the moving system. Let us start with the lab system.

$$\begin{aligned} \mathrm{RHS}_{lab} &= qn\gamma(\mathbf{E} + \mathbf{u} \times \mathbf{B}) \\ &= qn\gamma\left(\begin{pmatrix}\gamma(E'_x - vB'_z)\\ E'_y \\ \gamma(E'_z + vB'_x)\end{pmatrix} + \begin{pmatrix}u_x\\u_y\\u_z\end{pmatrix} \times \begin{pmatrix}B_x\\B_y\\B_z\end{pmatrix}\right) \end{aligned}$$

The only unknown quantities here are $B'_x$ and $B'_z$. We can replace them using the above transformation relations.

$$\begin{aligned} B_x &= \gamma\left(B'_x + \frac{1}{c^2}vE'_z\right) \\ B'_x &= \frac{1}{\gamma}B_x - \frac{1}{c^2}vE'_z \\ B_z &= \gamma\left(B'_z - \frac{1}{c}vE'_x\right) \\ B'_z &= \frac{1}{\gamma}B_z + \frac{1}{c^2}vE'_x \end{aligned}$$

and it follows

$$\begin{aligned} \mathrm{RHS}_{lab} &= qn\gamma\left(\begin{pmatrix}\gamma(E'_x - v(\frac{1}{\gamma}B_z + \frac{1}{c}vE'_x))\\ E'_y \\ \gamma(E'_z + v(\frac{1}{\gamma}B_x - \frac{1}{c}vE'_z))\end{pmatrix} + \begin{pmatrix}u_yB_z - u_zB_y\\u_zB_x - u_xB_z\\u_xB_y - u_yB_x\end{pmatrix}\right) \\ &= qn\gamma\begin{pmatrix}\gamma(E'_x - v(\frac{1}{\gamma}B_z + \frac{1}{c}vE'_x)) + u_yB_z - u_zB_y\\ E'_y + u_zB_x - u_xB_z \\ \gamma(E'_z + v(\frac{1}{\gamma}B_x - \frac{1}{c}vE'_z)) + u_xB_y - u_yB_x\end{pmatrix} \end{aligned} \tag{29}$$

and in the moving reference system the right hand side is given as

$$
\begin{aligned}
\mathrm{RHS}_{moving} &= qn\gamma\left(\mathbf{E}' - \mathbf{u}\times\mathbf{B}'\right) + \rho\boldsymbol{\omega}\times(\boldsymbol{\omega}\times\mathbf{r}) + \rho\frac{d\boldsymbol{\omega}}{dt}\times\mathbf{r} \\
&= qn\gamma\left(\begin{pmatrix}E'_x\\E'_y\\E'_z\end{pmatrix} - \begin{pmatrix}u_x\\u_y\\u_z\end{pmatrix}\times\begin{pmatrix}\gamma(B_x - \frac{1}{c^2}vE_z)\\B_y\\\gamma(B_z + \frac{1}{c^2}vE_x)\end{pmatrix}\right) \\
&\quad +\rho\omega^2\begin{pmatrix}r_x\\-r_y\\0\end{pmatrix} + \rho\frac{d\omega}{dt}\begin{pmatrix}-r_y\\r_x\\0\end{pmatrix} \\
&= qn\gamma\begin{pmatrix}E'_x - u_y\gamma(B_z + \frac{1}{c^2}vE_x) + u_zB_y\\E'_y - u_z\gamma(B_x - \frac{1}{c^2}vE_z) + u_x\gamma(B_z + \frac{1}{c^2}vE_x)\\E'_z - u_xB_y + u_y\gamma(B_x - \frac{1}{c^2}vE_z)\end{pmatrix} \\
&\quad +\rho\omega^2\begin{pmatrix}r_x\\-r_y\\0\end{pmatrix} + \rho\frac{d\omega}{dt}\begin{pmatrix}-r_y\\r_x\\0\end{pmatrix}
\end{aligned}
$$

The only unknown quantities here are $E_x$ and $E_z$. We can replace them using the above transformation relations.

$$
\begin{aligned}
E'_x &= \gamma\left(E_x + vB_z\right) \\
E_x &= \frac{1}{\gamma}E'_x - vB_z \\
E'_z &= \gamma\left(E_z - vB_x\right) \\
E_z &= \frac{1}{\gamma}E'_z + vB_x
\end{aligned}
$$

So the components can be transformed

$$
\begin{aligned}
E'_x &- u_y\gamma(B_z + \frac{1}{c^2}v(\frac{1}{\gamma}E'_x - vB_z)) + u_zB_y \\
&= E'_x - u_y\gamma B_z + \frac{u_y\gamma v}{c^2}(\frac{1}{\gamma}E'_x - vB_z) + u_zB_y \\
&= E'_x - u_y\gamma B_z + \frac{u_yv}{c^2}E'_x - \frac{u_y\gamma v^2}{c^2}B_z + u_zB_y
\end{aligned}
$$

$$
\begin{aligned}
E'_y &- u_z\gamma(B_x - \frac{1}{c^2}vE_z) + u_x\gamma(B_z + \frac{1}{c^2}vE_x) \\
&= E'_y - u_z\gamma B_x - \frac{u_z\gamma v}{c^2}(\frac{1}{\gamma}E'_z + vB_x) + u_x\gamma B_z + \frac{u_x\gamma v}{c^2}(\frac{1}{\gamma}E'_x - vB_z) \\
&= E'_y - u_z\gamma B_x - \frac{u_zv}{c^2}E'_z - \frac{u_z\gamma v^2}{c^2}B_x + u_x\gamma B_z + \frac{u_xv}{c^2}E'_x - \frac{u_x\gamma v^2}{c^2}B_z
\end{aligned}
$$

$$
\begin{aligned}
E'_z &- u_xB_y + u_y\gamma(B_x - \frac{1}{c^2}v(\frac{1}{\gamma}E'_z + vB_x)) \\
&= E'_z - u_xB_y + u_y\gamma B_x - \frac{u_y\gamma v}{c^2}(\frac{1}{\gamma}E'_z + vB_x) \\
&= E'_z - u_xB_y + u_y\gamma B_x - \frac{u_yv}{c^2}E'_z - \frac{u_y\gamma v^2}{c^2}B_x
\end{aligned}
$$

$$\begin{aligned}\mathrm{RHS}_{moving} &= qn\gamma \begin{pmatrix} E'_x - u_y\gamma B_z + \frac{u_y v}{c^2}E'_x - \frac{u_y\gamma v^2}{c^2}B_z + u_z B_y \\ E'_y - u_z\gamma B_x - \frac{u_z v}{c^2}E'_z - \frac{u_z\gamma v^2}{c^2}B_x + u_x\gamma B_z + \frac{u_x v}{c^2}E'_x - \frac{u_x\gamma v^2}{c^2}B_z \\ E'_z - u_x B_y + u_y\gamma B_x - \frac{u_y v}{c^2}E'_z - \frac{u_y\gamma v^2}{c^2}B_x \end{pmatrix} \\ &\quad +\rho\omega^2 \begin{pmatrix} r_x \\ -r_y \\ 0 \end{pmatrix} + \rho\frac{d\omega}{dt}\begin{pmatrix} -r_y \\ r_x \\ 0 \end{pmatrix} \end{aligned} \tag{30}$$

Let us for now look at a special case. Let us assume the problem to be two-dimensional and let the external magnetic field be given only in z direction, $B_z = B$, that means $B_x = 0$ and $B_y = 0$. Then the two terms become simpler.

$$\mathrm{RHS}_{lab} = qn\gamma \begin{pmatrix} \gamma E'_x - vB + \frac{\gamma}{c}vE'_x + u_y B \\ E'_y - u_x B \end{pmatrix}$$

$$\begin{aligned}\mathrm{RHS}_{moving} &= qn\gamma \begin{pmatrix} E'_x - u_y\gamma B + \frac{u_y v}{c^2}E'_x - \frac{u_y\gamma v^2}{c^2}B \\ E'_y + u_x\gamma B + \frac{u_x v}{c^2}E'_x - \frac{u_x\gamma v^2}{c^2}B \end{pmatrix} \\ &\quad +\rho\omega^2 \begin{pmatrix} r_x \\ -r_y \\ 0 \end{pmatrix} + \rho\frac{d\omega}{dt}\begin{pmatrix} -r_y \\ r_x \\ 0 \end{pmatrix} \end{aligned}$$

# 8 Implementation of the Lorentz Force

## 8.1 Space Charge

The most fundamental collective effect in the particle beam is certainly the electric potential created by the charged particles repelling each other due to the Coulomb force. This effect is also called the space charge. The effect of space charge is proportional to the intensity of the particle beam. That means space charge is a defocusing effect. For a round beam with Radius $R$ there is a defocusing electric field, but also a focusing magnetic field.

$$\begin{aligned}\mathbf{E}_r &= \begin{cases}\frac{\rho}{2\epsilon_0} r, & r \leq R \\ \frac{\rho}{2\epsilon_0}\frac{R^2}{r}, & r \geq R\end{cases} \\ \mathbf{B}_\phi &= \begin{cases}\frac{v\rho}{2\epsilon_0 c^2} r, & r \leq R \\ \frac{v\rho}{2\epsilon_0 c^2}\frac{R^2}{r}, & r \geq R\end{cases}\end{aligned}$$

These two fields are related through

$$\mathbf{B}_\phi = \frac{v}{c^2}\mathbf{E}_r = \frac{\beta}{c}\mathbf{E}_r.$$

The Lorentz Force resulting from the space charge has only a radial component. It is given as

$$\begin{aligned}\mathbf{F}_r &= e\left(\mathbf{E}_r - \beta c \mathbf{B}_\phi\right) \\ &= e\left(1-\beta^2\right)\mathbf{E}_r \\ &= \frac{e}{\gamma^2}\mathbf{E}_r\end{aligned}$$

At high energies, that means for high values of $\gamma$, this force becomes neglectable. The reason for this is, that the focusing magnetic field tends to compensate the defocusing effect of the electric field.

## 8.2 Poissons Equation

The electric field of the charge density distribution can be found by first determining the scalar electrostatic potential and then deducing the electric field components using

$$\mathbf{E} = -\nabla\phi$$

To find the electrostatic potential as a function of space the Poisson equation has to be solved. For simplicity we can assume the electrostatic approximation in the co-moving frame of reference. Then the Poissons equation is given as

$$\Delta\phi = -\frac{\rho}{\epsilon_0}.$$

To solve this equation numerically on the grid it first has to be rewritten in the form $\mathbf{A}\cdot x = b$. This can be done with the help of finite differences.

## 8.3 Finite Differences

The method of finite differences is a numerical method to solve partial differential equations. It helps defining the discretized version of the partial differences on a given grid. These differences are approximated by so-called difference quotients, which can be approximated to an order of choice. In finite differences the forward, backward and central difference scheme can be distinguished. For illustration, the one dimensional first order approximation of the partial derivative is being done here.

| Scheme | First order approximation (1D) |
|---|---|
| Forward | $\partial_x f_i = \frac{f_{i+1}-f_i}{dx}$ |
| Backward | $\partial_x f_i = \frac{f_i-f_{i-1}}{dx}$ |
| Central | $\partial_x f_i = \frac{f_{i+1}-f_{i-1}}{2dx}$ |

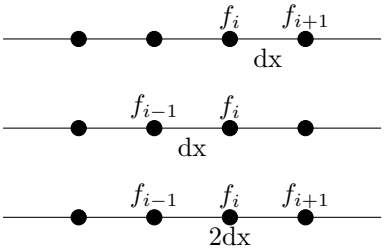


The forward and backward scheme in first order approximation are correct to an order of $O(dx)$, with $dx$ being the spacing between two neighbouring gridpoints. The central differences scheme, however, is correct to an order of $O(dx^2)$, which is why, in the following, this scheme will be used for the numerical calculation of the partial differences. Second derivatives can be approximated by finite difference schemes in the same way.

$$\partial_x^2 f_i \quad = \quad \frac{f_{i+1} - 2f_i + f_{i-1}}{dx^2}$$

Of course, this can also be done in more dimensions and up to higher order.

## 8.4 The $\Delta$ Operator in two dimensions

The Laplacian operator of the Poisson equation consists of second order derivatives and can thus be discretized as it was discussed before. Let $i$ denote the index of the x coordinate of the quantity on the grid and $j$ denote the corresponding y coordinate. The Laplacian of this quantity can than be written as a sum of the right neighbouring grid cells.

$$\Delta\phi = \frac{1}{dx^2}(\phi_{i+1,j} + \phi_{i-1,j} + \phi_{i,j+1} + \phi_{i,j-1} - 4\phi_{i,j}) \tag{31}$$

This discretization of the second derivative can also be written in matrix form and the result is called the Laplacian matrix.

$$\Delta = \frac{1}{dx^2}\begin{pmatrix} -4 & 1 & \cdots & 1 & 0 & \cdots & 0 & 0 \\ 1 & -4 & \cdots & 0 & 1 & \cdots & 0 & 0 \\ & & \ddots & & & \ddots & & \\ 1 & 0 & \cdots & -4 & 1 & \cdots & 1 & 0 \\ 0 & 1 & \cdots & 1 & -4 & \cdots & 0 & 1 \\ & & \ddots & & & \ddots & & \\ 0 & 0 & \cdots & 1 & 0 & \cdots & -4 & 1 \\ 0 & 0 & \cdots & 0 & 1 & \cdots & 1 & -4 \end{pmatrix}$$

In a programming language like Matlab a matrix like this is easily computed.

Listing 1: Implementation for the Laplacian

```
% Laplacian in central differences
        I = speye(N,N);
        E = sparse(2:N,1:N-1,1,N,N);
        D = E+E'-2*I;
        L = kron(D,I)+kron(I,D);
```

And the Poisson equation can be solved using the mldivide function which is build into Matlab. It is a parallelized program and therefore the result can be obtained fast.

Listing 2: Solution of the poissons equation

```
% Solve L*phi = rho/epsilon_0
        phi = L\(rho/epsilon);
```

Another possibility to solve the Poisson equation would be to do a FFT (Fast Fourier Transform).

## 8.5 Boundary conditions

Now that we have a general way to solve the Poisson equation, the boundary conditions have to be included into the problem. There are several possible types of different boundary conditions, the two most famous and mainly used are the Dirichlet and the Neumann problem.

> The Dirichlet boundary condition defines the value of the resulting function on the border of the computational regime to be some constant value or some function. Physically, that refers to fixing the value of the potential at the border of the problem.
>
> The Neumann boundary conditions define the normal derivative of the resulting function on the border of the problem. Physically that corresponds to a given flux on the border of the computational regime.

Here, the Dirichlet boundary condition will be used, that means that the values at the border will be set to a constant value. To avoid unnecessary

jumps in the system the value of the boarder cells will be set to the value of the neighbouring cells. The values corresponding to the boarder in the laplacian matrix will be set to zero.

## 8.6 Implementation of the Lorentz Force

The total force on the particle distribution is the electromagnetic force, the Lorentz force.

$$\mathbf{F}_L = \frac{q}{m} (\mathbf{E} + \mathbf{v} \times \mathbf{B})$$

That means, for the computation, the electric and magnetic field as a function of space are needed. The Poisson solver to compute the electric part of that force has already been described. That means for the implementation, this only has to be combined with the magnetic field to yield the Lorentz force.

# 9 Benchmarking of the Lorentz Force Implementation

## 9.1 Test Cases for the Poisson solver

### 9.1.1 Point Charge

A point charge at the center of the computational domain will create an electric field of the form

$$\mathbf{E} = \frac{q}{\epsilon_0 \mathbf{r}^2}$$

and a potential of the form

$$\phi = -\frac{q}{\epsilon_0 |\mathbf{r}|}$$

The Simulation compared to the exact result can be seen in Fig. 5 and Fig. 6.

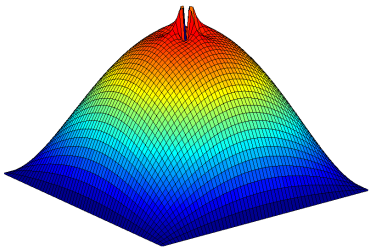

Figure 5: Sketch of the potential of the point charge.

### 9.1.2 Constant Continuous Charge distribution

In this case we look at a constant continuous charge distribution with a total charge $Q$ inside a circle of radius R. For radii that are bigger than R the electric field corresponds to that from a point charge $Q$ situated at R=0.

$$\mathbf{E} = \frac{Q}{\epsilon_0 \mathbf{r}^2}, \; r => R$$

Inside the circle the electric field is given by

$$\mathbf{E} = \frac{Qr}{\pi \epsilon_0 \mathbf{R}^3}, \; r < R$$

The Simulation compared to the exact result can be seen in Fig. 7 and Fig. 8.

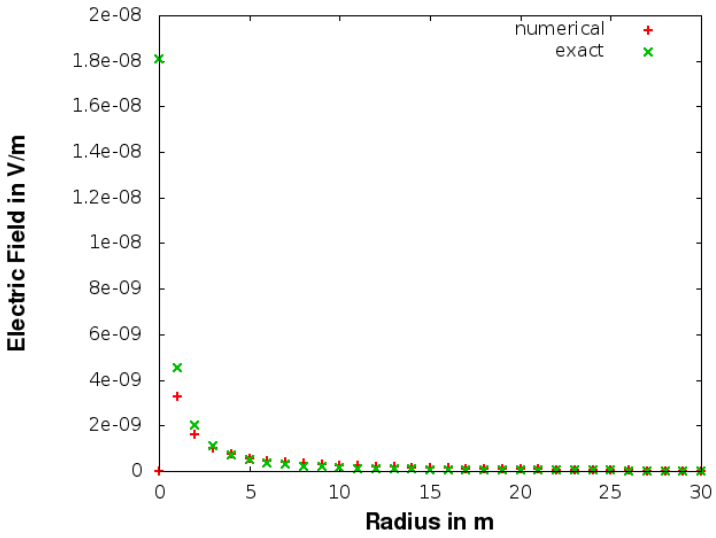


Figure 6: Electric Field of the point charge. Comparison of the numerical calculation with the theoretical value.

### 9.1.3 Continuous Gaussian Charge distribution

Now let us look at a charge distribution of the form

$$\rho(x,y) = \rho_0 \cdot e^{-\left(\frac{x}{\sigma_x}\right)^2} \cdot e^{-\left(\frac{y}{\sigma_y}\right)^2}$$

The electric field of a general continuous charge distribution is given as

$$\mathbf{E} = \frac{1}{\epsilon_0} \int\int dxdy\, \rho(x,y) \frac{1}{r^3}\mathbf{r} = \frac{1}{\epsilon_0} \int\int dxdy\, \rho(x,y) \frac{1}{r^2}\hat{\mathbf{r}}$$

with the position vector $\mathbf{r} = \begin{pmatrix} x \\ y \end{pmatrix}$, its absolute value $|\mathbf{r}| = r$ and its unit vector $\hat{\mathbf{r}} = \frac{\mathbf{r}}{r}$. To get the Electric field inside the Gaussian density distribution the density has to be plugged in here and the integral has to be computed.

$$\mathbf{E} = \frac{\rho_0}{\epsilon_0} \int\int dxdy\, e^{-\left(\frac{x}{\sigma_x}\right)^2} e^{-\left(\frac{y}{\sigma_y}\right)^2} \frac{1}{(x^2+y^2)^{3/2}} \begin{pmatrix} x \\ y \end{pmatrix}$$

For simplicity let us assume a symmetric distribution $\sigma_x = \sigma_y$. Now polar coordinates can be used to be able to integrate the equation analytically

$$\begin{aligned} \mathbf{E} &= = \frac{\rho_0}{\epsilon_0} \int\int dxdy\, e^{-\frac{x^2+y^2}{\sigma^2}} \frac{1}{(x^2+y^2)^{3/2}} \begin{pmatrix} x \\ y \end{pmatrix} \\ &= \frac{\rho_0}{\epsilon_0} \int\int r dr d\phi\, e^{-\frac{r^2}{\sigma^2}} \frac{1}{r^3} \begin{pmatrix} r\cos\phi \\ r\sin\phi \end{pmatrix} \\ &= \frac{\rho_0}{\epsilon_0} \int\int dr d\phi\, e^{-\frac{r^2}{\sigma^2}} \frac{1}{r} \begin{pmatrix} \cos\phi \\ \sin\phi \end{pmatrix} \end{aligned}$$

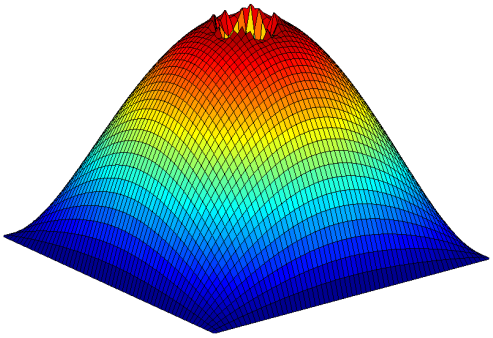

Figure 7: sketch of the potential of a continuous constant charge distribution inside the circle with a Radius of 5 units.

The Simulation compared to the exact result can be seen in Fig. 9 and Fig. 10.

### 9.1.4 Error Analysis

Here, a table of the maximum absolute error will be given (Table 1) for all three test cases above. In the following, you can see how this errors is calculated.

$$\sigma_{\text{absolute error}} = x_{\text{numerical}} - x_{\text{exact}}$$

$$\sigma_{\text{maximum absolute error}} = max\left(x_{\text{numerical}} - x_{\text{exact}}\right)$$

| Test Case | Maximum absolute error |
|---|---|
| Point Charge | $1.1737 \cdot 10^{-10}$ |
| Constant charge distribution | $7.0075 \cdot 10^{-9}$ |
| Gaussian Charge distribution | $2.3642 \cdot 10^{-9}$ |

Table 1: Table of maximum absolute errors for the three Poisson test cases.

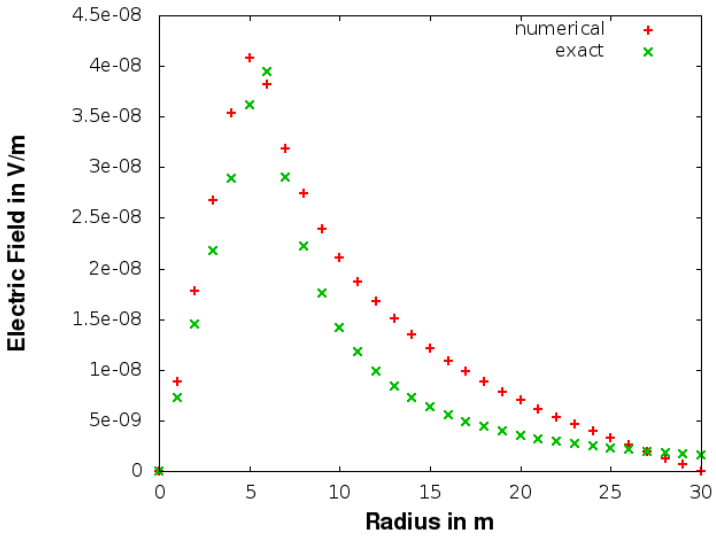


Figure 8: Comparison of the numerical and theoretical electric field for the continuous constant charge.

## 9.2 Test cases for the implementation of the Lorentz Force

To test if the computation of the right hand side of the momentum equation is correct, it will be applied to several test problems of particles in electromagnetic fields. The only non-zero component of the magnetic field vector will be the z component in all of the following cases. Furtheremore the magnetic field is taken to be static.

### 9.2.1 One particle in a magnetic field

The first test will be with only one proton in a magnetic field. The expected path described by the proton in time should be a circle of radius $R$.

$$\begin{aligned} \frac{mv^2}{R} &= qvB \\ \frac{v}{R} &= \frac{qB}{m} = \omega \end{aligned}$$

The initial conditions of the problem are

| | |
|---|---|
| Magnetic field | $B = 0.3T$ |
| Time step | $dt = 1 \cdot 10^{-10} s$ |
| Initial position | $x = -0.002m$ |
| | $y = 0$ |
| Initial velocity | $v_x = 0$ |
| | $v_y = 7.5685 \cdot 10^4 m/s$ |

The result can be seen in Fig. 11. As expected the path of the proton in time describes a circle with Radius $R = 0.002m$.

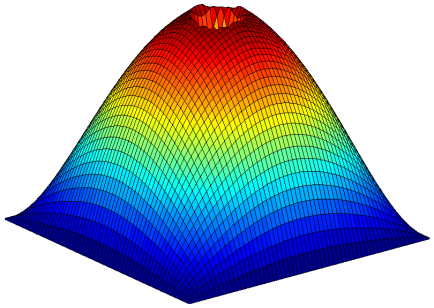

Figure 9: Sketch of the potential of a Gaussian charge distribution.

### 9.2.2 Two particles with no magnetic field

The next test will be with two protons but with the magnetic field turned off. Now we expect both particles to repell each other and thus go in the opposite direction of each other. Because there is no magnetic field, no deviation from a straight path should occur. The initial conditions of the problem are

| | | |
|---|---|---|
| Magnetic field | $B = 0T$ | |
| Time step | $dt = 1 \cdot 10^{-7}s$ | |
| Initial positions | $x_1 = -0.002m$ | $x_2 = 0.002m$ |
| | $y_1 = 0$ | $y_2 = 0$ |
| Initial velocity | $v_{1,x} = 0$ | $v_{2,x} = 0$ |
| | $v_{1,y} = 7.5685 \cdot 10^4 m/s$ | $v_{2,y} = -7.5685 \cdot 10^4 m/s$ |

The result can be seen in Fig. 12.

### 9.2.3 Two particles with magnetic field and no electric interaction

Here two protons in a magnetic field will be simulated. The electric interaction will be turned off for now. We expect both particles to describe circles in time but not influence each other in any way. The initial conditions of the problem are

| | | |
|---|---|---|
| Magnetic field | $B = 0.3T$ | |
| Time step | $dt = 1 \cdot 10^{-9}s$ | |
| Initial positions | $x_1 = -0.002m$ | $x_2 = 0.002m$ |
| | $y_1 = 0$ | $y_2 = 0$ |
| Initial velocity | $v_{1,x} = 0$ | $v_{2,x} = 0$ |
| | $v_{1,y} = 7.5685 \cdot 10^4 m/s$ | $v_{2,y} = -7.5685 \cdot 10^4 m/s$ |

The result can be seen in Fig. 13. As expected the path of both protons are circles like the single proton simulation in the first section.

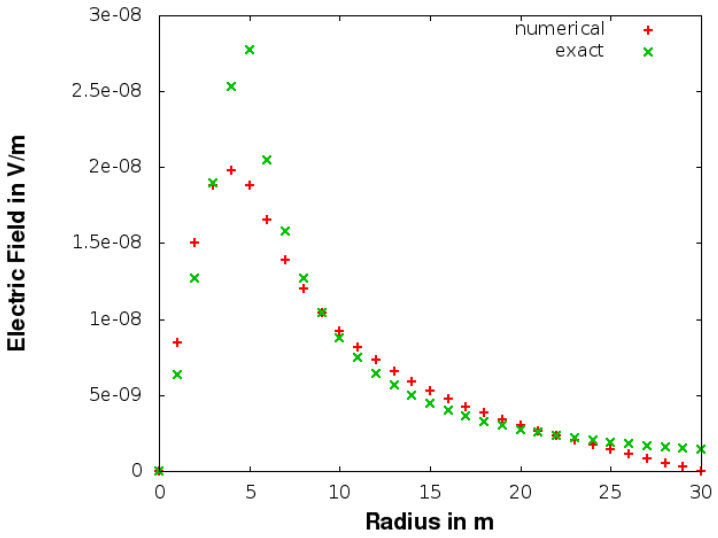


Figure 10: Comparison of the numerical and theoretical electric field for the Gaussian charge distribution.

### 9.2.4 Two particles in a magnetic field with electric interaction

Here two protons in a magnetic field with electric interaction will be simulated. We expect both particles to describe circles in time while repelling each other at the same time. The initial conditions of the problem are

| | | |
|---|---|---|
| Magnetic field | $B = 0.3T$ | |
| Time step | $dt = 1 \cdot 10^{-9} s$ | |
| Initial positions | $x_1 = -0.002m$ | $x_2 = 0.002m$ |
| | $y_1 = 0$ | $y_2 = 0$ |
| Initial velocity | $v_{1,x} = 0$ | $v_{2,x} = 0$ |
| | $v_{1,y} = 7.5685 \cdot 10^4 m/s$ | $v_{2,y} = -7.5685 \cdot 10^4 m/s$ |

The result can be seen in Fig. 14.

There seems to be no difference to the plot in the section before, where the electric interaction was turned off. The reason for this is, that the acceleration due to the electric force is much smaller than the acceleration due to the magnetic force. At time t = 0 the two accelerations are

$$\begin{aligned} a_{el} &= \frac{q^2}{m\epsilon_0 r^2} = 1.47522 \cdot 10^5 \\ a_{mag} &= \frac{qvB}{m} = 2.89817 \cdot 10^{12} \end{aligned}$$

To test the influence of the electric field, the charge and mass of the particles can be increased by a factor $\alpha$. This way the magnetic acceleration will not change, while the electric acceleration will change by the factor $\alpha$.

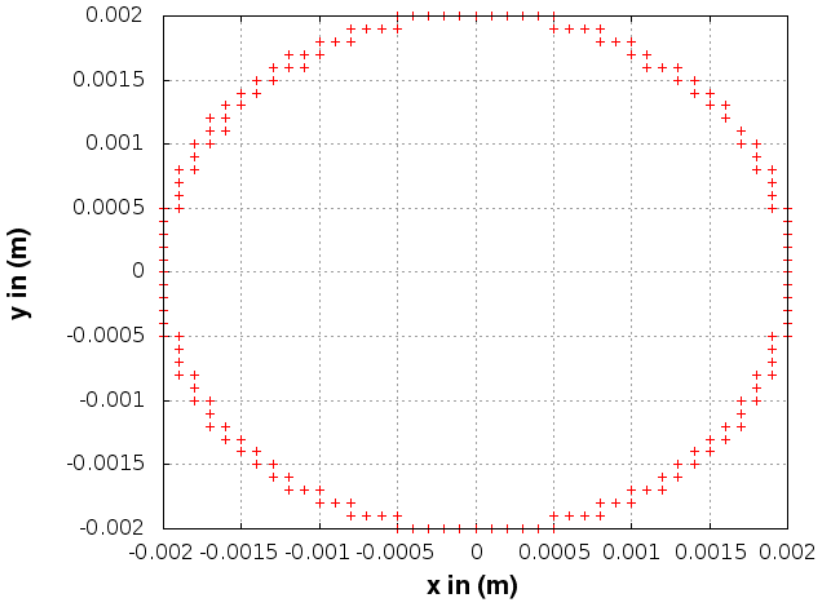


Figure 11: One proton in a magnetic field of strength $B = 0.3T$. Initial position of the particle: $(-0.002m, 0)$, initial velocity of the particle: $(0, 7.5684 \cdot 10^4 m/s)$, Time: $T = 2 \cdot 10^{-7} s$

$$q \to \alpha q, \qquad m \to \alpha m$$

$$\begin{aligned} a_{el}(\alpha) &= \frac{(\alpha q)^2}{(\alpha m)\epsilon_0 r^2} = \frac{\alpha q^2}{m\epsilon_0 r^2} \\ &= \alpha \cdot 1.47522 \cdot 10^5 \\ a_{mag}(\alpha) &= \frac{(\alpha q)vB}{\alpha m} = \frac{qvB}{m} \\ &= 2.89817 \cdot 10^{12} \end{aligned}$$

The simulation with $\alpha = 10^6$ can be seen in Fig. 15.

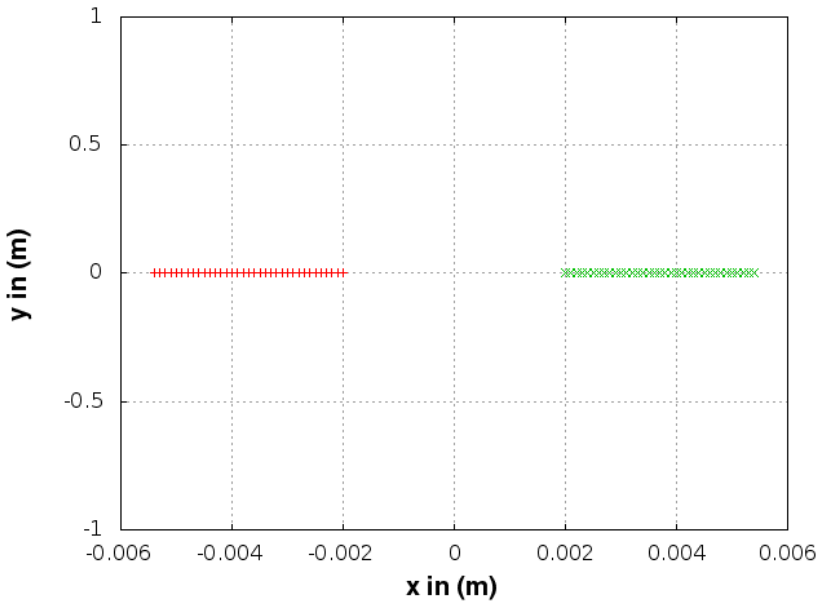


Figure 12: Two protons repelling each other due to Coulomb force. Initial position of the particles: $(-0.002m, 0)$(red) and $(0.002m, 0)$(green), initial velocities of the particles: $(0, 0)$, Time: $T = 2 \cdot 10^{-4}s$

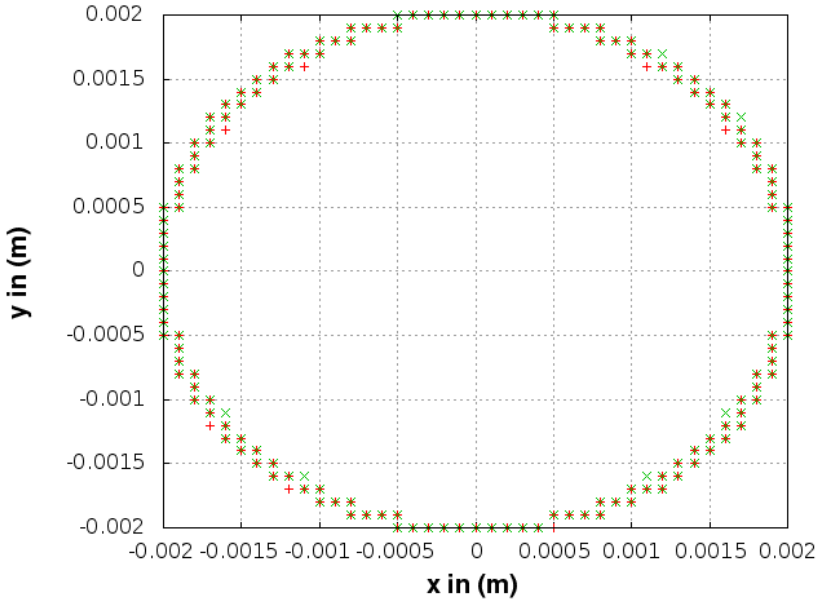


Figure 13: Two protons in a magnetic field of strength $B = 0.3T$ with electric interaction turned off. Initial position of the particles: $(-0.002m, 0)$(red) and $(0.002m, 0)$(green), initial velocities of the particles: $(0, 7.5684 \cdot 10^4 m/s)$ and $(0, -7.5684 \cdot 10^4 m/s)$, Time: $T = 2 \cdot 10^{-7}s$

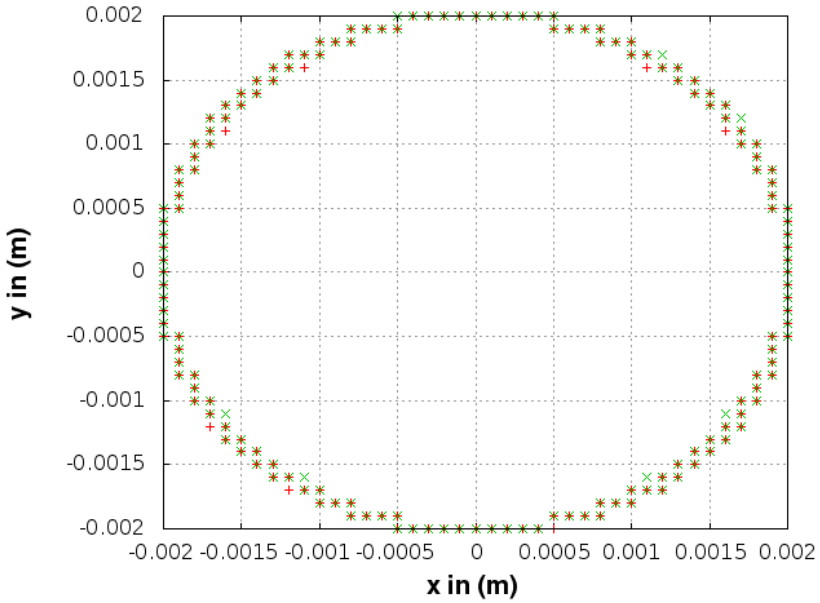


Figure 14: Two protons in a magnetic field of strength $B = 0.3T$ with electric interaction. Initial position of the particles: $(-0.002m, 0)$(red) and $(0.002m, 0)$(green), initial velocities of the particles: $(0, 7.5684 \cdot 10^4 m/s)$ and $(0, -7.5684 \cdot 10^4 m/s)$, Time: $T = 2 \cdot 10^{-7} s$

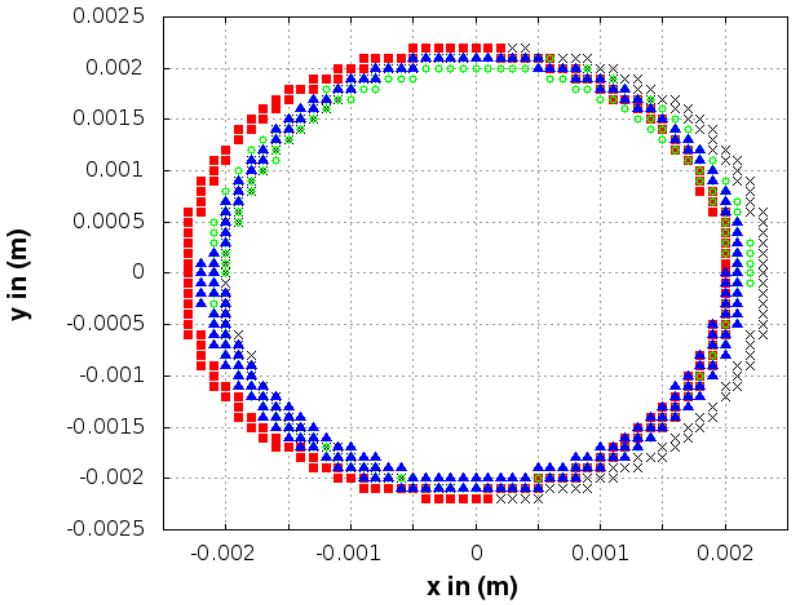


Figure 15: Two particles of charge $Q = 10^6 e$, with $e$ being the elementary charge, in a magnetic field of strength $B = 0.3T$. Initial position of the particles: $(-0.002m, 0)$ and $(0.002m, 0)$, initial velocities of the particles: $(0, 7.5684 \cdot 10^4 m/s)$ and $(0, -7.5684 \cdot 10^4 m/s)$, Time: $T = 2 \cdot 10^{-7} s$. Comparison between electric interaction turned off ((particle 1: green, circle) and (particle 2: blue, triangle)) and electric interaction turned on ((particle 1: black, cross) and (particle 2: red, square))

# 10 Numerical Solution Schemes

Let us quickly recall the main equations that govern the dynamics of our system. First of all there is the equation describing the number conservation, the continuity equation.

$$\partial_t(\rho\gamma) + \nabla(\rho\gamma\mathbf{v}) = 0$$

The next equation is describing the energy in the system.

$$\partial_t\left(\left(P+\rho c^2\right)\gamma^2 - P\right) + \nabla\left(\left(P+\rho c^2\right)\gamma^2\frac{\mathbf{v}}{c}\right) = -\frac{q}{m}\rho\frac{\mathbf{v}}{c}\mathbf{E}$$

The last equation is describing the momentum components of the system.

$$\partial_t((P+\rho c^2)\gamma^2\frac{\mathbf{v}}{c}) + \nabla((P+\rho c^2)\gamma^2\frac{\mathbf{v}\mathbf{v}}{c^2}) + \nabla P = \text{RHS}$$

Let us take a look at the two-dimensional version of this problem and write the set of equations in another form, the so-called two dimensional conservation form. In the following we will use the notation $\mathbf{v} = (u, v)$ for the x and y velocity. It is important to keep in mind that the term containing $\mathbf{v}^2$ will lead to mixed term expressions, because for any vectors $\mathbf{a}$ and $\mathbf{b}$ the following identity holds.[ix]

$$\nabla(\mathbf{ab}) = (\mathbf{a}\nabla)\,\mathbf{b} + (\mathbf{b}\nabla)\,\mathbf{a} + \mathbf{a}\times(\nabla\times\mathbf{b}) + \mathbf{b}\times(\nabla\times\mathbf{a})$$

So in two dimensions the system of equation can be written as

$$\frac{\partial}{\partial t}\begin{pmatrix}\rho\gamma\\ \left(P+\rho c^2\right)\gamma^2\\ (P+\rho c^2)\gamma^2\frac{u}{c}\\ (P+\rho c^2)\gamma^2\frac{v}{c}\end{pmatrix} + \frac{\partial}{\partial x}\begin{pmatrix}\rho\gamma u\\ \left(P+\rho c^2\right)\gamma^2\frac{u}{c}\\ (P+\rho c^2)\gamma^2\frac{u^2}{c^2}\\ (P+\rho c^2)\gamma^2\frac{uv}{c^2}\end{pmatrix} + \frac{\partial}{\partial y}\begin{pmatrix}\rho\gamma v\\ \left(P+\rho c^2\right)\gamma^2\frac{v}{c}\\ (P+\rho c^2)\gamma^2\frac{uv}{c^2}\\ (P+\rho c^2)\gamma^2\frac{v^2}{c^2}\end{pmatrix} = \begin{pmatrix}0\\ \partial_t P - \frac{q}{m}\rho\frac{\mathbf{v}}{c}\mathbf{E}\\ \text{RHS}_x - \partial_x P\\ \text{RHS}_y - \partial_y P\end{pmatrix}$$

.

It can be easily seen, that these equations are of the form

$$\partial_t\mathbf{Q} + \partial_x\mathbf{F}(\mathbf{Q}) + \partial_y\mathbf{G}(\mathbf{Q}) \quad = \quad \text{RHS}$$

## 10.1 Motivation for the application of numerical schemes for the simulations

There are several ways to resolve and simulate this kind of system of equations. In this case, the so-called numerical schemes were chosen to simulate the set of equations. These methods are widely used in the context of computational Magneto-Hydro-Dynamics (MHD). Most of the time, MHD is discussed in an astrophysical context. The simulation of neutron star or galaxy dynamics, for instance, are describe using the concepts of MHD. If we think a bit about the

[ix] Proof in the Appendix

problems discussed in MHD, this is not that far from what we want to simulate here. The simulations always concern a magnetic field. Also, electric fields are involved in the problems, which aim to simulate the dynamics of a system of individual elements. Furtheremore, most of the time, the problems even have relativistic forms. Because of these accordances, I made the decision of using the same methods simulating this set of fluid equations.

There is a huge variety of schemes available, some of which are so-called mixed schemes. Here, some of the most basic ones will be discussed and implemented. In the following sections 10.3 to 10.6 you can find the FTCS (Forward Time Central Space) Scheme, the Lax-Friedrichs Scheme, the Lax-Wendroff Scheme and the FORCE Scheme. Before that, the criterium to check for numerical stability has to be established. This is the so-called CFL (Courant-Friedrichs-Levy) condition.

## 10.2 Courant-Friedrichs-Levy Condition

The stability of the methods is given by the Courant-Friedrichs-Levy (CFL) condition. This condition is a stability criterion, that is derived from comparing the analytical domain of dependence with the numerical one. Here the physical domain of dependence can be seen in blue and the numerical domain of dependence is in red.

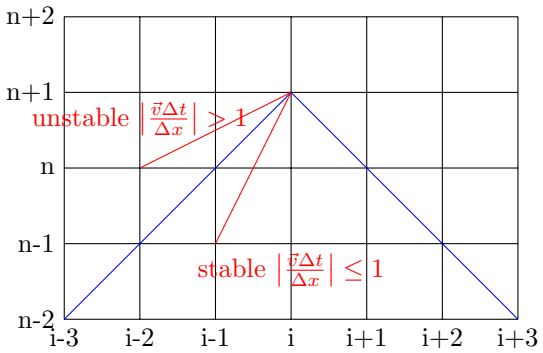


The resulting CFL Criteria is

$$\left|\frac{\vec{v}\Delta t}{\Delta x}\right| \leq C_{max}$$

If the solver is explicit the quantity on the right hand side is given as

$$C_{max} = 1.$$

## 10.3 Forward Time Central Space (FTCS) Scheme

While trying to solve a hyperbolic conservation or balance law the simplest scheme that comes to mind is the Forward Time Central Space (FTCS) Scheme. It consists of a straightforward implementation of the finite differences.

**One dimensional form:**

$$\begin{aligned} \partial_t \mathbf{Q} + \partial_x \mathbf{F}(\mathbf{Q}) &= \text{RHS} \\ \frac{Q^{n+1}_{i,k} - Q^n_{i,k}}{\Delta t} + \frac{F^n_{i+1,k} - F^n_{i-1,k}}{2\Delta x} &= \text{RHS}_{i,k} \end{aligned}$$

**Two dimensional form:**

$$\begin{aligned} \partial_t \mathbf{Q} + \partial_x \mathbf{F}(\mathbf{Q}) + \partial_y \mathbf{G}(\mathbf{Q}) &= \text{RHS} \\ \frac{Q^{n+1}_{i,j,k} - Q^n_{i,j,k}}{\Delta t} + \frac{F^n_{i+1,j,k} - F^n_{i-1,j,k}}{2\Delta x} + \frac{G^n_{i,j+1,k} - G^n_{i,j-1,k}}{2\Delta y} &= \text{RHS}_{i,j,k} \end{aligned}$$

This scheme is first-order and explicit in time and it is also unstable when applied to hyperbolic partial differential equations like the equation above. This unstable behaviour can be avoided by including artificial viscosity, as it is done in the Lax-Friedrichs scheme.

## 10.4 Lax-Friedrichs scheme

The Lax-Friedrichs method of solving hyperbolic conservation laws or balance equations proposed by Peter Lax and Kurt O. Friedrichs is a finite difference method that uses central differences in space and a forward time difference [16]. The Scheme is explicit and approximates the spatial derivatives to first order. The accuracy in time depends on the time integration scheme that is used. Here a simple time integration will be used, but, as can be seen in section 10.6, a higher order time integration can be easily implemented, to increase the accuracy of the scheme. The Lax-Friedrichs method avoids solving the Riemann problem by adding a term that is known as artificial viscosity. In our case the main interest lies in solving the balance equation.

One dimensional balance law: $\partial_t \mathbf{Q} + \partial_x \mathbf{F}(\mathbf{Q}) = \text{RHS}$
Two dimensional balance law: $\partial_t \mathbf{Q} + \partial_x \mathbf{F}(\mathbf{Q}) + \partial_y \mathbf{G}(\mathbf{Q}) = \text{RHS}$

The variables $\mathbf{Q}$, $\mathbf{F(Q)}$ and $\mathbf{G(Q)}$ are vectors and the system of equation contains the continuity equation, the momentum equations and the energy equation of our problem. Let us define $k$ to be the $k$th component of the equation and $(i, j)$ to be grid points on the computational regime. Then the conserved vector $\mathbf{Q}$ at timestep $t + dt$ can be computed as:

**One dimensional form:**

$$\mathbf{Q}^{n+1}_{i,k} = \frac{1}{2}(\mathbf{Q}^n_{i+1,k} + \mathbf{Q}^n_{i-1,k}) - \frac{\Delta t}{2\Delta x}(\mathbf{F}^n_{i+1,k} - \mathbf{F}^n_{i-1,k})$$

**Two dimensional form:**

$$\begin{aligned} \mathbf{Q}^{n+1}_{i,j,k} = \; & \frac{1}{4}(\mathbf{Q}^n_{i+1,j,k} + \mathbf{Q}^n_{i,j+1,k} + \mathbf{Q}^n_{i-1,j,k} + \mathbf{Q}^n_{i,j-1,k}) \\ & - \frac{\Delta t}{2\Delta x}(\mathbf{F}^n_{i+1,j,k} - \mathbf{F}^n_{i-1,j,k}) - \frac{\Delta t}{2\Delta y}(\mathbf{G}^n_{i,j+1,k} - \mathbf{G}^n_{i,j-1,k}) \end{aligned}$$

The Lax-Friedrich scheme is straightforward to implement, while still being numerically stable as long as the CFL condition is met. Unfortunately, this scheme is only first order accurate in space and hence very dissipative.

Since the indices go from $i-1$ and $j-1$ to $i+1$ and $j+1$, the implementation of this scheme has to include a first step, where a layer of so-called ghost cells are created around the components of the conserved vector $\mathbf{Q}$. That means the quantities on a $Nx \times Ny$ grid are being expanded to an $(Nx+2) \times (Ny+2)$ grid.

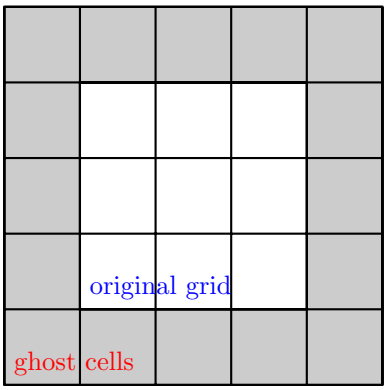


The values of the ghost cells differ with respect to the chosen boundary conditions. Here the value of a ghostcell will be set to its neighbouring normal cell to avoid jumps.

## 10.5 Lax-Wendroff Scheme

The Lax-Wendroff method, proposed by P.D. Lax and B. Wendroff in 1960 [14] is a higher order scheme than Lax-Friedrich, since it is second-order accurate in space and time. This scheme is also explicit and conservative. For nonlinear systems, this is also called the Richtmyer two step Lax Wendroff scheme. The scheme consists of several computation steps, since it involves a half-time step computation to increase the accuracy. For simplicity we omit the index $k$ for the component from now on.

**One dimensional form:**

i) Determine $\mathbf{Q}$ at half-timestep $t + dt/2$

$$\mathbf{Q}_i^{n+1/2} = \frac{1}{4}(\mathbf{Q}_{i+1}^n + 2\mathbf{Q}_i^n + \mathbf{Q}_{i-1}^n) - \frac{\Delta t}{2\Delta x}(F_{i+1}^n - F_{i-1}^n)$$

ii) Compute $F_i^{n+1/2} = F(\mathbf{Q}_i^{n+1/2})$

iii) Leapfrog to find $\mathbf{Q}^{n+1}$

$$\mathbf{Q}_i^{n+1} = \mathbf{Q}_i^n - \frac{\Delta t}{2\Delta x}(F_{i+1}^{n+1/2} - F_{i-1}^{n+1/2})$$

**Two dimensional form:**

i) Determine $\mathbf{Q}$ at half-timestep $t + dt/2$

$$\begin{aligned}\mathbf{Q}_{i,j}^{n+1/2} &= \frac{1}{4}(\mathbf{Q}_{i+1,j}^{n} + \mathbf{Q}_{i,j+1}^{n} + \mathbf{Q}_{i-1,j}^{n} + \mathbf{Q}_{i,j-1}^{n}) \\ &\quad -\frac{\Delta t}{2\Delta x}(F_{i+1,j}^{n} - F_{i-1,j}^{n}) - \frac{\Delta t}{2\Delta y}(G_{i,j+1}^{n} - G_{i,j-1}^{n})\end{aligned}$$

ii) Compute $F_{i,j}^{n+1/2} = F(\mathbf{Q}_{i,j}^{n+1/2})$ and $G_{i,j}^{n+1/2} = G(\mathbf{Q}_{i,j}^{n+1/2})$.

iii) Leapfrog to find $\mathbf{Q}^{n+1}$

$$\mathbf{Q}_{i,j}^{n+1} = \mathbf{Q}_{i,j}^{n} - \frac{\Delta t}{2\Delta x}(F_{i+1,j}^{n+1/2} - F_{i-1,j}^{n+1/2}) - \frac{\Delta t}{2\Delta y}(G_{i,j+1}^{n+1/2} - G_{i,j-1}^{n+1/2})$$

Schematically in one dimension this algorithm takes the following form

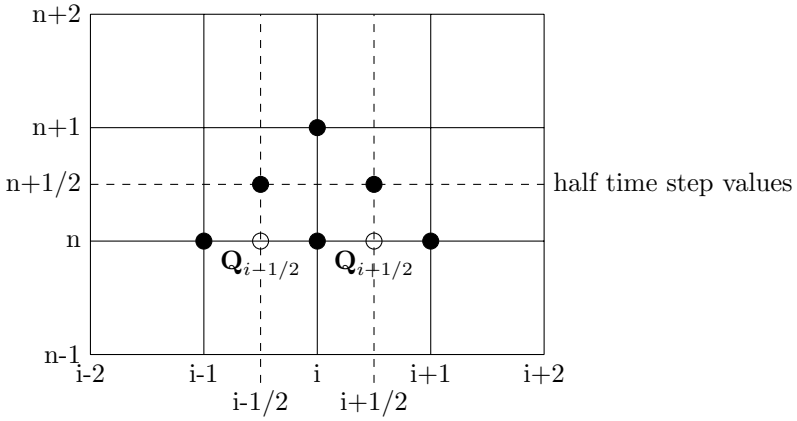


## 10.6 First Order Centered Scheme (FORCE)

The first-order centered scheme (FORCE) was developed by Toro [17] for compressible Euler equations. It is a combination of the Lax Friedrichs Scheme and the Richtmyer/two-step Lax-Wendroff Scheme.

**One dimensional form:**

i) Determine $\mathbf{Q}$ at half-timestep $t + dt/2$

$$\mathbf{Q}_{i}^{n+1/2} = \frac{1}{2}(\mathbf{Q}_{i}^{n} + \mathbf{Q}_{i}^{n}) + \frac{\Delta t}{2\Delta x}(F_{i}^{n} - F_{i+1}^{n})$$

ii) Compute $F_{i}^{n+1/2} = F(\mathbf{Q}_{i}^{n+1/2})$

iii) $F_{i}^{force} = \frac{1}{2}(F_{i}^{n+1/2} + \frac{1}{2}(F_{i}^{n} + F_{i+1}^{n})) + \frac{\Delta x}{4\Delta t}(\mathbf{Q}_{i}^{n} - \mathbf{Q}_{i+1}^{n})$

iv) $\mathbf{Q}_{i}^{n+1} = \mathbf{Q}_{i}^{n} + \frac{\Delta t}{\Delta x}(F_{i-1}^{force} - F_{i}^{force})$

**Two dimensional form:**

i) Compute Lax-Friedrichs and Lax-Wendroff fluxes

$$
\begin{aligned}
F^{LF}_{i+1/2,j} &= \frac{1}{2}(F_{i-1,j} + F_{i+1,j}) + \frac{1}{2}\frac{\Delta x}{\Delta t}(\mathbf{Q}_{i-1,j} - \mathbf{Q}_{i+1,j}) \\
F^{LW}_{i+1/2,j} &= \frac{1}{2}(\mathbf{Q}_{i-1,j} + \mathbf{Q}(i+1,j)) + \frac{1}{2}\frac{\Delta t}{\Delta x}(F_{i-1,j} - F_{i+1,j}) \\
G^{LF}_{i,j+1/2} &= \frac{1}{2}(G_{i,j-1} + G_{i,j+1}) + \frac{1}{2}\frac{\Delta y}{\Delta t}(\mathbf{Q}_{i,j-1} - \mathbf{Q}_{i,j+1}) \\
G^{LW}_{i,j+1/2} &= \frac{1}{2}(\mathbf{Q}_{i,j-1} + \mathbf{Q}(i,j+1)) + \frac{1}{2}\frac{\Delta t}{\Delta y}(G_{i,j-1} - G_{i,j+1})
\end{aligned}
$$

ii) Compute the FORCE flux

$$
\begin{aligned}
F^{force}_{i+1/2,j} &= \frac{1}{2}(F^{LF}_{i+1/2,j} + F^{LW}_{i+1/2,j}) \\
G^{force}_{i,j+1/2} &= \frac{1}{2}(G^{LF}_{i,j+1/2} + G^{LW}_{i,j+1/2})
\end{aligned}
$$

iii) $\mathbf{Q}^{n+1}_{i,j} = \mathbf{Q}^{n}_{i,j} - \frac{\Delta t}{\Delta x}(F^{force}_{i+1/2,j} - F^{force}_{i-1/2,j}) - \frac{\Delta t}{\Delta y}(G^{force}_{i,j+1/2} - G^{force}_{i,j-1/2})$

## 10.7 Higher order time integration

The numerical order of the scheme can be easily improved using a higher order time integration scheme like Leapfrog or a Runge-Kutta scheme.

Leapfrog

$$
\begin{aligned}
Q^{(1)} &= Q^n + \tfrac{\Delta t}{2} \cdot \mathrm{Flux}(Q^n) \\
Q^{n+1} &= Q^{(1)} + \tfrac{\Delta t}{2} \cdot \mathrm{Flux}(Q^{(1)})
\end{aligned}
$$

Runge-Kutta 2nd order

$$
\begin{aligned}
Q^{(1)} &= Q^n + \Delta t \cdot \mathrm{Flux}(Q^n) \\
Q^{n+1} &= \tfrac{1}{2}Q^n + \tfrac{1}{2}Q^{(1)} + \tfrac{1}{2}\Delta t \cdot \mathrm{Flux}(Q^{(1)})
\end{aligned}
$$

Runge-Kutta 3rd order

$$
\begin{aligned}
Q^{(1)} &= Q^n + \Delta t \cdot \mathrm{Flux}(Q^n) \\
Q^{(2)} &= \tfrac{3}{4}Q^n + \tfrac{1}{4}Q^{(1)} + \tfrac{1}{4}\Delta t \cdot \mathrm{Flux}(Q^{(1)}) \\
Q^{n+1} &= \tfrac{1}{3}Q^n + \tfrac{2}{3}Q^{(2)} + \tfrac{2}{3}\Delta t \cdot \mathrm{Flux}(Q^{(2)})
\end{aligned}
$$

# 11 Benchmarking of the CFD Schemes

## 11.1 One dimensional Test Problems - Inviscid Burgers equation

For velocity $u$, the general one dimensional Burgers equation is given as [3]

$$\partial_t u + u \cdot \partial_x u = \nu \partial_x^2 u.$$

This is called the advection form of the equation. Burgers equation can also be written in conservative form

$$\partial_t u + \partial_x \left( \frac{1}{2} u^2 \right) = \nu \partial_x^2 u.$$

For $\nu \neq 0$ the equation is called viscous and for $\nu = 0$ Burgers equation is called inviscid. Here the inviscid Burgers equation is used for benchmarking the code. For the comparison of the numerical solution of the schemes with the exact solution, the exact solution to this equation has to be found first. This will be done with the method of characteristics. Characteristics are defined as the lines on which u is constant, that means

$$\frac{D}{Dt} u = (\partial_t + u\nabla) u = 0.$$

For an equation of the form

$$a \frac{\partial u}{\partial x} + b \frac{\partial u}{\partial y} = 0$$

the characteristics are defined as

$$\frac{Dy}{Dx} = \frac{b}{a}.$$

That means here

$$\begin{aligned} \frac{Dx}{Dt} &= u \\ \frac{Du}{Dt} &= 0 \end{aligned}$$

and therefore the solution is

$$\begin{aligned} x &= ut + C_1 \\ u &= C_2 = C_2(C_1) \end{aligned}$$

To benchmark the one dimensional form of the implemented schemes, two different simulations regarding the inviscid Burgers equation were done. One of them was the Single Shock problem, where a shockwave travels from the left to the right of the system and the other one is the Sine-Problem, where the initial condition is given as a sine distribution. Both problems have exact solutions, that's why they are suitable test problems for the schemes.

### 11.1.1 Single Shock Problem

In this case an initial shock on the left side of the system travels to the right. Thus, the initial distribution is a step function.

$$\text{Initial condition:} \quad u(x,0) = \begin{cases} 1.0, & \text{for } x < 0.1 \\ 0.0, & \text{otherwise} \end{cases}$$

$$\text{Exact solution at time } t\text{:} \quad u(x,t) = \begin{cases} 1.0, & \text{for } x < 0.1 + 0.5t \\ 0.0, & \text{otherwise} \end{cases}$$

The simulation result compared to the exact values can be seen in Fig. 16.

The maximum deviation from the exact solution and the standard deviation over all gridpoints and timesteps are given in the following table.

| Scheme | Lax-Friedrichs | Lax-Wendroff | FORCE |
|---|---|---|---|
| maximum Error | 0.0393 | 0.0405 | 0.0358 |
| standard deviation | 0.0316 | 0.0293 | 0.0254 |

All three schemes seem to be in the same range of accuracy, looking at the maximum deviation from the exact solution. Looking at the plots, it can be seen that Lax-Wendroff has the biggest error at the edge of the shock. The standard deviation is getting better going from Lax-Friedrichs to Lax-Wendroff and FORCE.

### 11.1.2 Sine function

Here an initial sine like distribution in the velocity is developing according to the inviscid form of Burgers equation.

$$\text{Initial condition:} \quad u(x,0) = \sin(\pi x)$$
$$\text{Exact solution at time } t\text{:} \quad u(x,t) = \sin(\pi(x - ut))$$

The simulation result compared to the exact values can be seen in Fig. 17.

The maximum deviation from the exact solution and the standard deviation over all gridpoints and timesteps are given in the following table.

| Scheme | Lax-Friedrichs | Lax-Wendroff | FORCE |
|---|---|---|---|
| maximum Error | 0.0451 | 0.0417 | 0.0447 |
| standard deviation | 0.0243 | 0.0223 | 0.0238 |

Looking at the errors, it becomes clear, that there is no significant difference to be found between the schemes. All of them solve the problem with high accuracy.

## 11.2 Two dimensional Test problem - Inviscid 2D Burgers equation

The two dimensional form of the inviscid Burgers equation is given as

$$\begin{aligned} \partial_t u + u\partial_x u + v\partial_y u &= 0 \\ \partial_t v + u\partial_x v + v\partial_y v &= 0. \end{aligned}$$

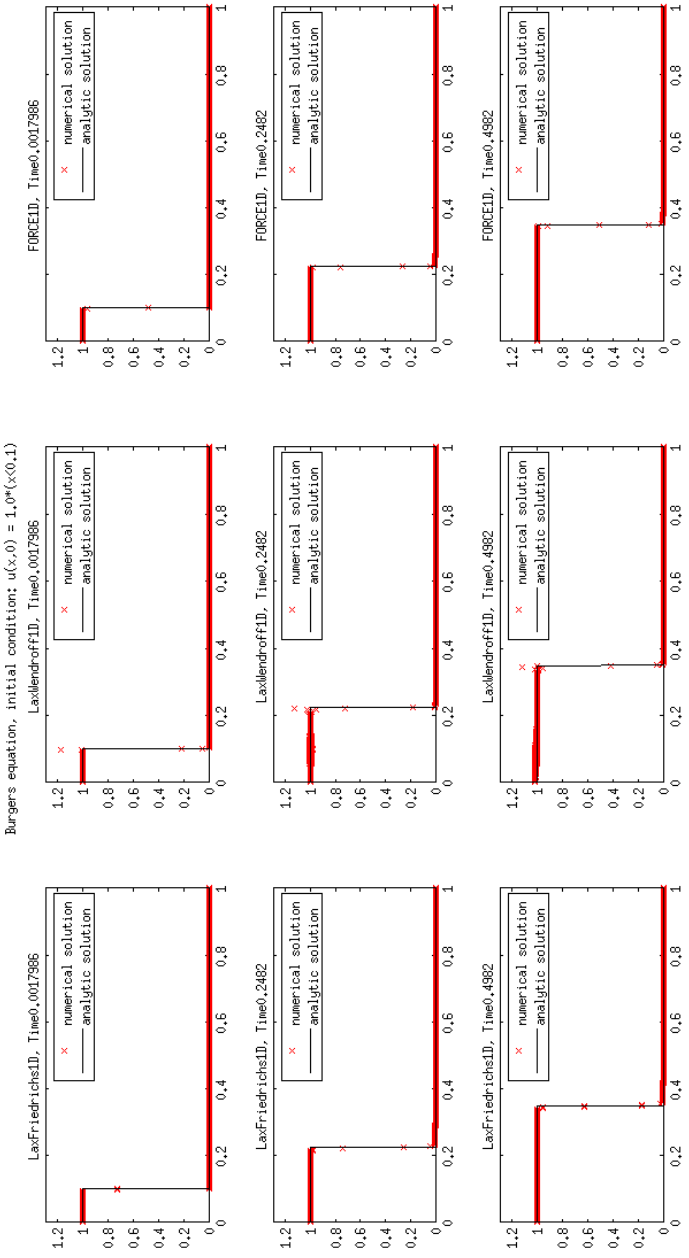


Figure 16: Simulation of the one dimensional Burgers equation with an initial single shock on the left side of the system. Comparison of the schemes Lax-Friedrichs, Lax Wendroff and FORCE. Simulated values in red and exact solution in black.

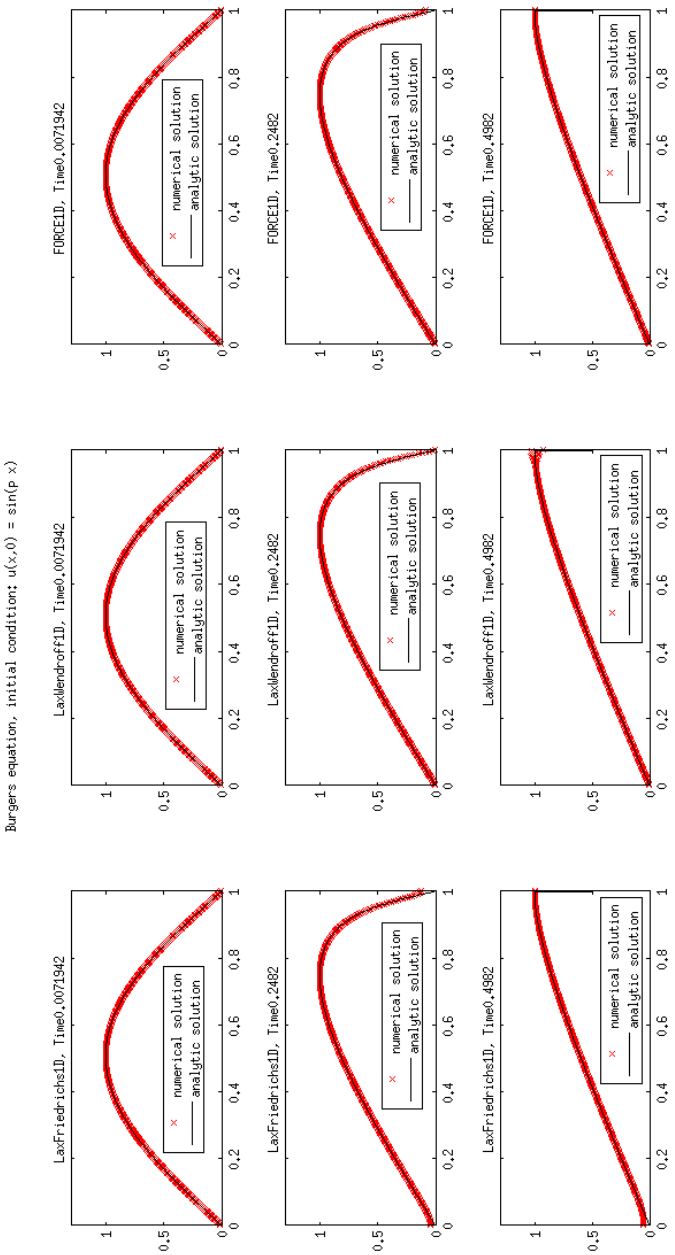


Figure 17: Simulation of the one dimensional Burgers equation with an initial sine function. Comparison of the schemes Lax-Friedrichs, Lax Wendroff and FORCE. Simulated values in red and exact solution in black.

Here the quantities $u$ and $v$ describe the velocity in x and y direction.

### 11.2.1 Comparison with the results from *Burgers_equation_2D.m* from mathworks.com

The numerical solution to the two dimensional Burgers equation from the matlab webpage mathworks.com was compared to the solution given by the Lax-Friedrichs and Lax-Wendroff scheme. The equation in the matlab file was changed to be inviscid, by setting the viscosity factor $\nu = 0$.

Initial conditions:

$$u(x,y) = \begin{cases} 0 & \text{for } 0.5 \leq y \leq 1 \text{ and } 0.5 \leq x \leq 1 \\ 1 & \text{otherwise} \end{cases}$$

$$v(x,y) = \begin{cases} 1 & \text{for } 0.5 \leq y \leq 1 \text{ and } 0.5 \leq x \leq 1 \\ 0 & \text{otherwise} \end{cases}$$

Boundary conditions:

$$\begin{aligned} u(1,:) &= 0; & v(1,:) &= 0; \\ u(nx,:) &= 0; & v(nx,:) &= 0; \\ u(:,1) &= 0; & v(:,1) &= 0; \\ u(:,ny) &= 0; & v(:,ny) &= 0; \end{aligned}$$

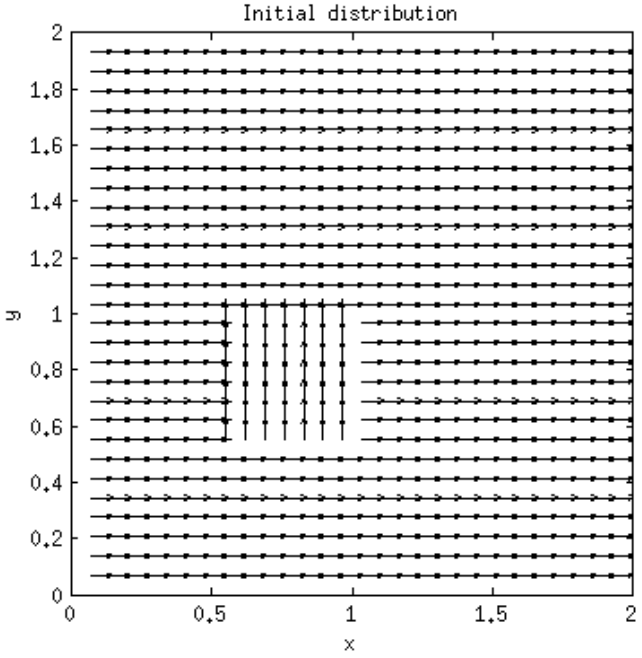

The comparison between the reference code and the two implementations of Lax-Friedrichs and Lax-Wendroff scheme can be seen in the two tables Table 2 and Table 3. These tables show the distributions after 0.25s and 0.50s.

Quantitative comparison (standard deviation compared to the reference values from the mathworks code):

$$\sigma = \sqrt{\frac{1}{N}\sum \left(x_{i,\text{Scheme}} - x_{i,\text{reference}}\right)^2}$$

| Time | $\sigma_{\text{LaxFriedrichs}}$ | $\sigma_{\text{LaxWendroff}}$ |
|---|---|---|
| 0.25s | 0.01 | 0.0091 |
| 0.50s | 0.0124 | 0.0117 |

Reference

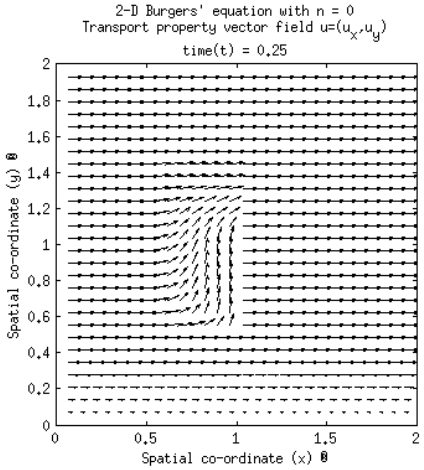


Lax-Friedrichs

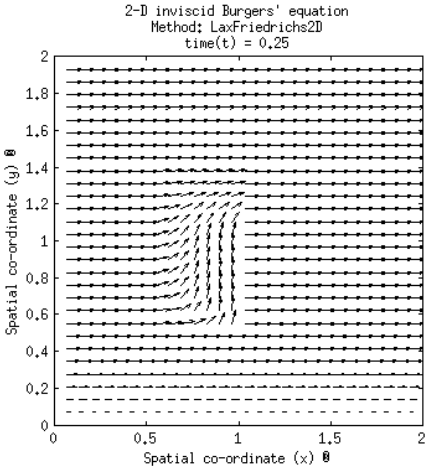


Lax-Wendroff

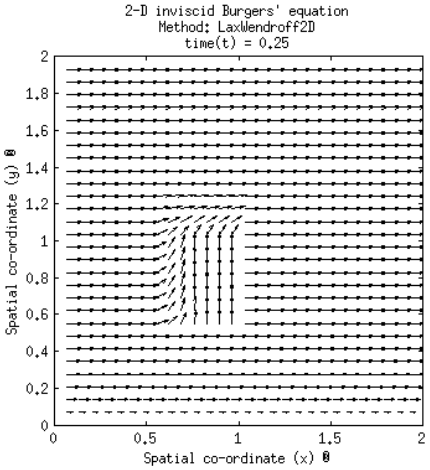


Table 2: Comparison of the three distributions after 0.25s.

Reference

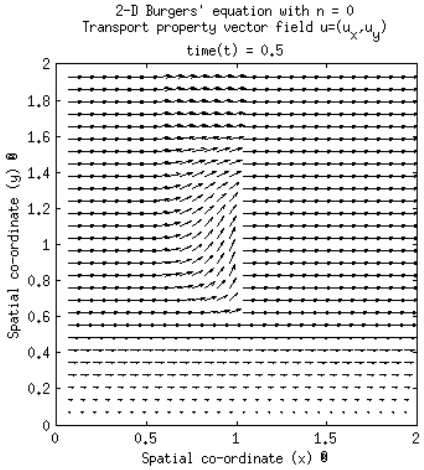


Lax-Friedrichs

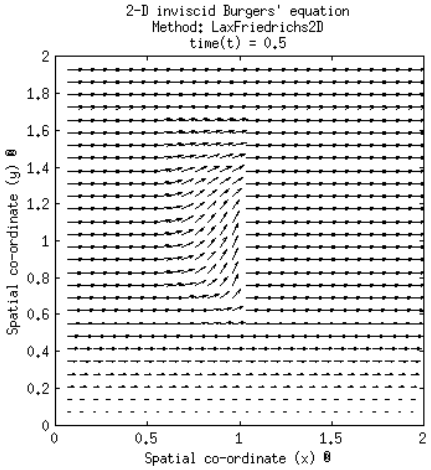


Lax-Wendroff

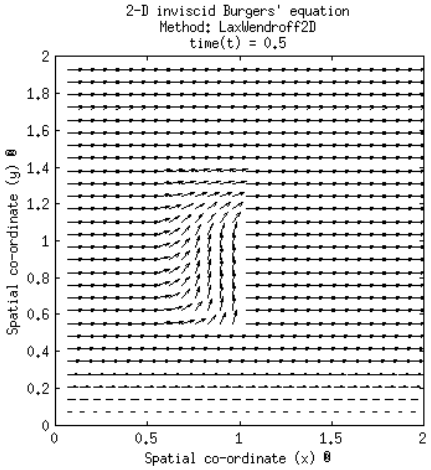


Table 3: Comparison of the three distributions after 0.50s.

# 12 Simulation of the Fluid Model

## 12.1 Simulation of a drifting sphere of charge

A drifting sphere with a uniform initial distribution of charge will be simulated. The initial distribution of the charge in the sphere can be see in Fig 18.

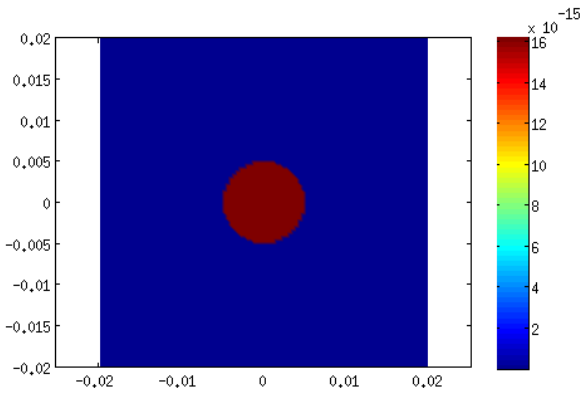


Figure 18: Initial charge distribution in the radial longitudinal plane of the drifting sphere of charge. The total charge corresponds to the charge of $10^9$ protons. The radius of the initial distribution was set to $R_0 = 5 \cdot 10^{-3} m$.

The sphere will be drifting with velocity $v$ in y direction. There will be no external magnetic field affecting it, the only force affecting the beam will be the space charge. The result can be seen in Fig 19.

Qualitatively, the simulation results confirm the model. The sphere expands due to the repulsing Coulomb forces between the protons. In parallel to that effect, the density decreases, due to particle number conservation. A quantitative confirmation can be made by solving the so-called beam envelope equations [1], that describe the behaviour of the distribution in this problem. Since the beam density distribution is uniform and no focusing effects are considered, the equation for the beam envelope can be written in a simple form.

$$
\begin{aligned}
m\gamma\frac{d^2r}{dt^2} &= q\left(\mathbf{E}_{sc} - v\mathbf{B}_{sc}\right) \\
\text{with} \qquad \mathbf{E}_{sc} &= \begin{cases} \frac{I}{2\pi\epsilon_0 v R^2} r,\ r \le R \\ \frac{I}{2\pi\epsilon_0 v r},\ r > R \end{cases} \\
\mathbf{B}_{sc} &= \begin{cases} \mu_0 \frac{I}{2\pi R^2} r,\ r \le R \\ \mu_0 \frac{I}{2\pi r},\ r > R \end{cases} \\
\text{and} \qquad dt &= ds/v \\
\frac{d^2r}{ds^2} &= \frac{qIr}{2\pi\epsilon_0 R^2 m v^3 \gamma^3} = \underbrace{K}_{\text{generalized perveance}} \frac{r}{R^2}
\end{aligned}
$$

For a particle on the envelope this can be written even simpler.

$$\frac{d^2r}{ds^2} = \frac{K}{r}$$

To do that, the radius of the sphere was measured at each timestep of the simulation. Using Mathematica, the envelope equations were solved numerically and could be compared to the results of the simulation, see Fig 20. Clearly both solution coincide well. The Fluid Model simulation (in black) is not as smooth as the solution to the envelope equation, due to the grid spacing. The error between the two solutions can be easily calculated.

$$error = \frac{1}{N-1}\sqrt{\sum (x_{i,FM} - x_{i,ENV})^2} = 1.3799 \cdot 10^{-4}$$

Here, $x_{i,FM}$ is the value of the Fluid Model solution and $x_{i,ENV}$ is the value of the envelope solution.

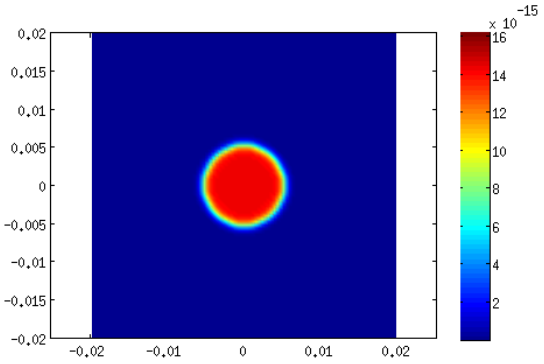


(a) Distribution after 100 timesteps.

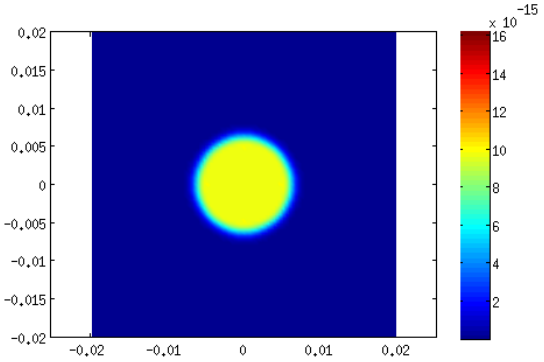


(b) Distribution after 200 timesteps.

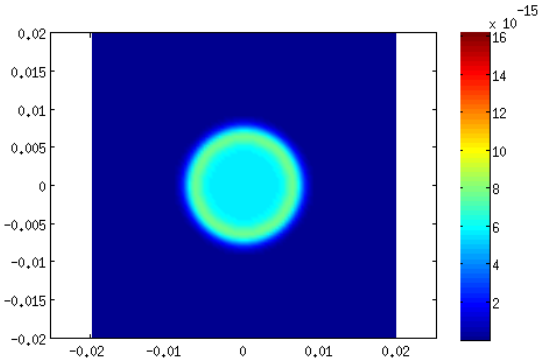


(c) Distribution after 300 timesteps.

Figure 19: Snapshots of the simulation results. The simulation was done with a constant timestep of $10^{-9}s$ and the sphere was drifting with a velocity of $1.2901 \cdot 10^{7}m/s$ corresponding to a kinetic energy per ion of $0.87MeV$.

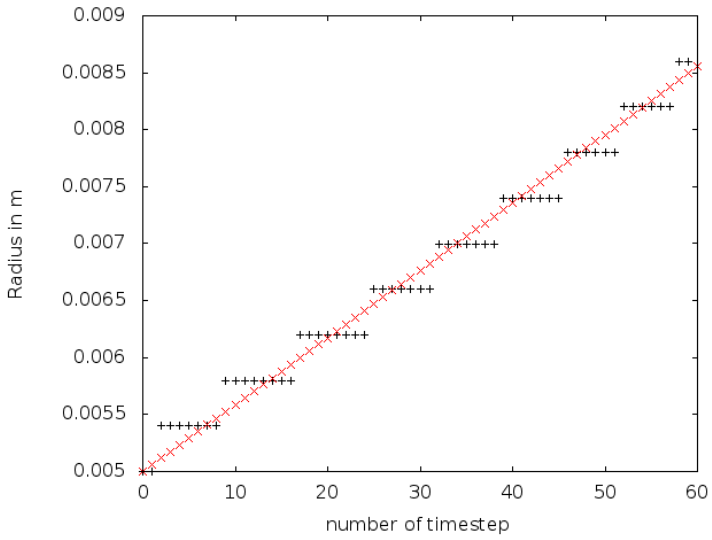


Figure 20: Value of the radius for each timestep. In black, the solution of the Fluid Model simulation, in red as comparison, the solution of the envelope equation.

## 12.2 Simulation of the coasting beam

The radial-longitudinal plane of a cyclotron will be simulated. All of the simulations assume a constant magnetic field in z direction. It will be the simulation of the beam in its co-moving frame of reference on the trajectory in the cyclotron. Initially, the velocities in this frame of reference will be set to zero, but they are allowed to change due to the electromagnetic forces in the source term of the equations.

The simulation of the coasting beam includes two parts. First of all, a simulation of a beam with a round profile and secondly, the simulation of a beam with an elongated or elliptical profile. The density profile will follow a Gaussian distribution.

$$f(x,y) = f_0 \exp\left(-\left(\frac{(x-x_0)^2}{2\sigma_x^2} + \frac{(y-y_0)^2}{2\sigma_y^2}\right)\right)$$

The parameters of the simulations include particle number and strength of the magnetic field. The charge per particle and the grid stays unmodified by the simulation process. The timestep will be given as initial timestep. During the simulation, the timestep can change due to the CFL condition.

A Pseudo-Code of the simulation program (Listing 3) and a description of the functions used in the program are given in the Appendix.

All of the simulations were done with the grid and turn specifications given in Table 4. Tables 5 to 9 show the individual parameters for the different simulations. Simulations A1 and A2 given in tables 5 and 6 describe the simulation of a stationary round beam with different numbers of particles, that means $\rho(t) = \rho = const.$ Simulations B1 to B3 corresponding to the tables 7 to 9 describe the simulation of elongated beams. Here, we expect the development of spiral arms.

| | |
|---|---|
| Grid size | $100 \times 100$ grid points |
| Minimum and maximum values | $x_{min} = -0.02m$, $x_{max} = 0.02m$<br>$y_{min} = -0.02m$, $y_{max} = 0.02m$ |
| Grid spacing | $dx = (x_{max} - x_{min})/100 = 4 \cdot 10^{-4}m$<br>$dy = (y_{max} - y_{min})/100 = 4 \cdot 10^{-4}m$ |
| Number of simulated turns | 20 |
| Start value of the timestep | $dt = 10^{-10}s$ |

Table 4: General specifications for all simulations

The results of simulations A1 and A2 show the same behaviour that [4] already exhibited: a round beam will not develop the spiral arms. Simulation

A1 shows a very stable behaviour over all of the 25 simulated turns, while with more charge, in simulation A2, the beam starts to pulse, that means it expands and contracts over time. This is probably due to mismatched initial conditions.

| | |
|---|---|
| Number of particles | $10^9$ particles |
| Total charge | $Q = 10^9 e = 1.602 \cdot 10^{-10} C$ |
| Strength of magnetic field | $B = 0.3T$ |
| FWHM of gaussian distribution | $\sigma_x = 5 \cdot 10^{-3} m$<br>$\sigma_y = 5 \cdot 10^{-3} m$ |

Table 5: Simulation A1, stationary round beam.

| | |
|---|---|
| Number of particles | $10^{10}$ particles |
| Total charge | $Q = 10^{10} e = 1.602 \cdot 10^{-9} C$ |
| Strength of magnetic field | $B = 0.3T$ |
| FWHM of gaussian distribution | $\sigma_x = 5 \cdot 10^{-3} m$<br>$\sigma_y = 5 \cdot 10^{-3} m$ |

Table 6: Simulation A2, stationary round beam.

Now, that we saw, the round beams don't develop the spiral arms, we expect to see them as soon as the initial density distribution is elongated in one direction. Here, the beam will be longer in direction of propagation, that means it will be longer in y direction.

To sum up, the results of the simulations of different charge configurations with elongated beams show the beginnings of spirals or halos. Unfortunately, they develope rather late. However, it is important to notice that the model and its implementation is able to simulate this effect.

| | |
|---|---|
| Number of particles | $10^{10}$ particles |
| Total charge | $Q = 10^{10}e = 1.602 \cdot 10^{-9}C$ |
| Strength of magnetic field | $B = 0.3T$ |
| FWHM of gaussian distribution | $\sigma_x = 2 \cdot 10^{-3}m$<br>$\sigma_y = 8 \cdot 10^{-3}m$ |

Table 7: Simulation B1

| | |
|---|---|
| Number of particles | $10^{10}$ particles |
| Total charge | $Q = 10^{10}e = 1.602 \cdot 10^{-9}C$ |
| Strength of magnetic field | $B = 0.3T$ |
| FWHM of gaussian distribution | $\sigma_x = 3 \cdot 10^{-3}m$<br>$\sigma_y = 10 \cdot 10^{-3}m$ |

Table 8: Simulation B2

| | |
|---|---|
| Number of particles | $3 \cdot 10^{10}$ particles |
| Total charge | $Q = 3 \cdot 10^{10}e = 4.806 \cdot 10^{-9}C$ |
| Strength of magnetic field | $B = 0.3T$ |
| FWHM of gaussian distribution | $\sigma_x = 4 \cdot 10^{-3}m$<br>$\sigma_y = 10 \cdot 10^{-3}m$ |

Table 9: Simulation B3

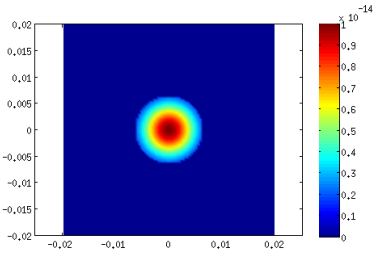

(a) Initial distribution.

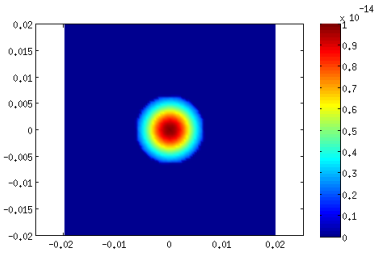

(b) Turn 5

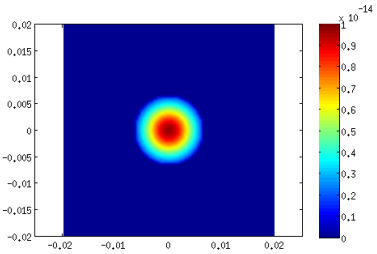

(c) Turn 10

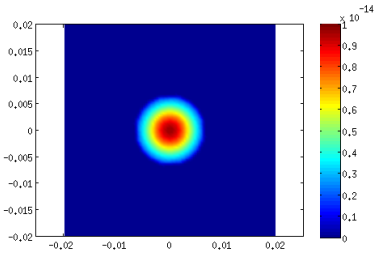

(d) Turn 15

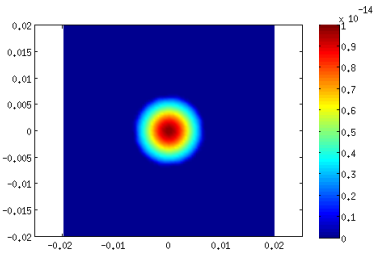

(e) Turn 20

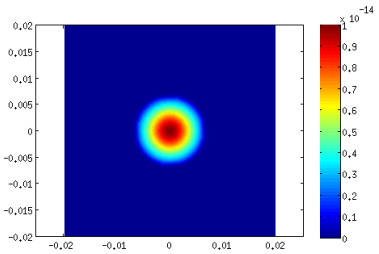

(f) Turn 25

Figure 21: Snapshots of the results of the simulation of Table 5.

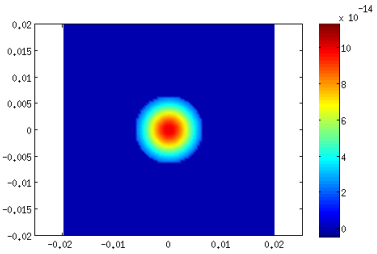

(a) Initial distribution.

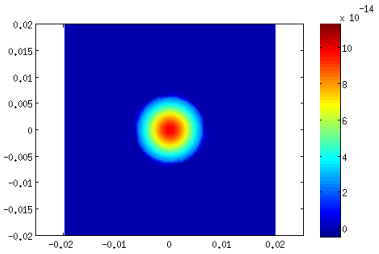

(b) Turn 5

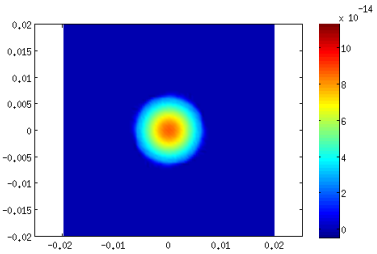

(c) Turn 10

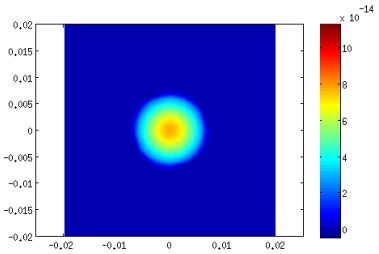

(d) Turn 15

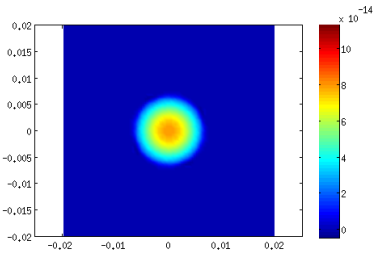

(e) Turn 20

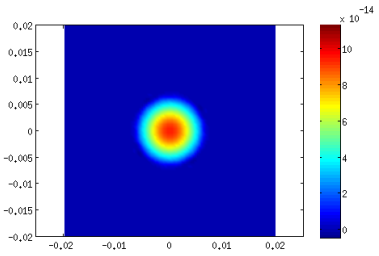

(f) Turn 25

Figure 22: Snapshots of the results of the simulation of Table 6.

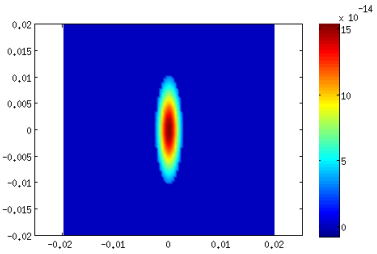

(a) Initial distribution.

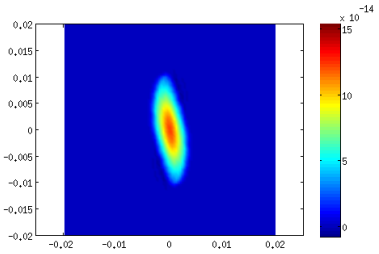

(b) Turn 10

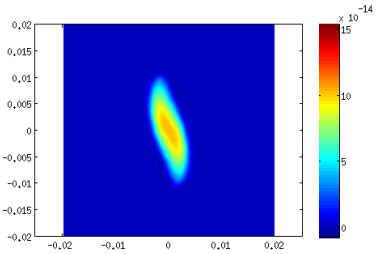

(c) Turn 20

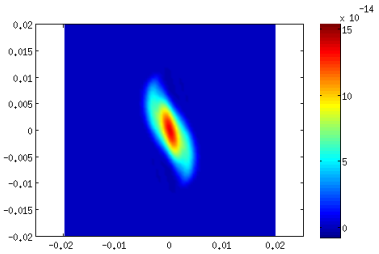

(d) Turn 30

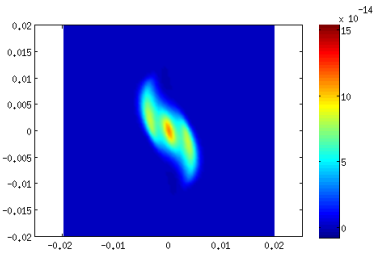

(e) Turn 40

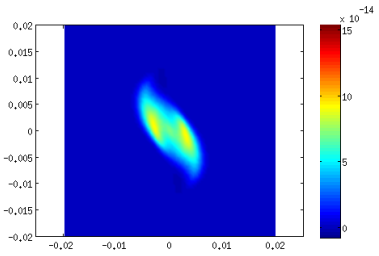

(f) Turn 50

Figure 23: Snapshots of the results of the simulation of Table 7.

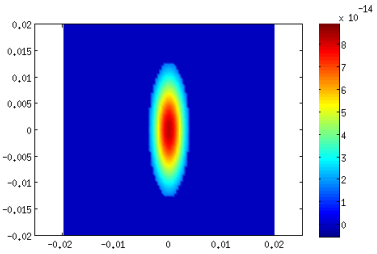

(a) Initial distribution.

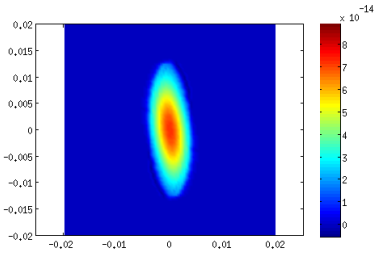

(b) Turn 10

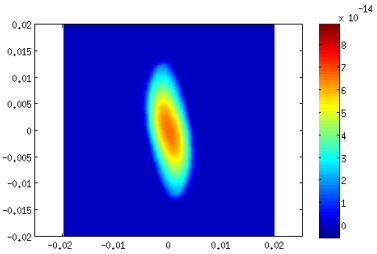

(c) Turn 20

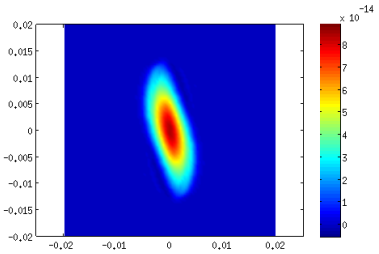

(d) Turn 30

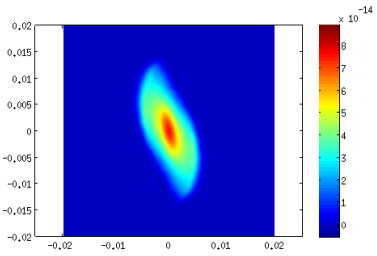

(e) Turn 40

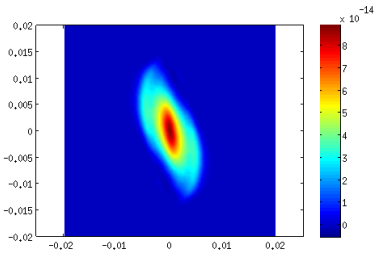

(f) Turn 50

Figure 24: Snapshots of the results of the simulation of Table 8.

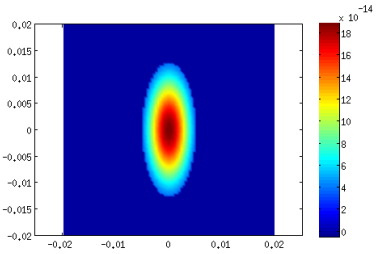

(a) Initial distribution.

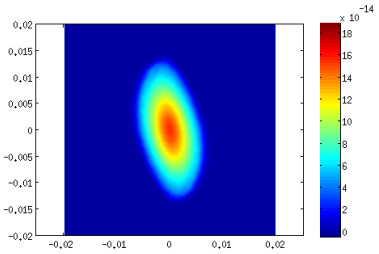

(b) Turn 10

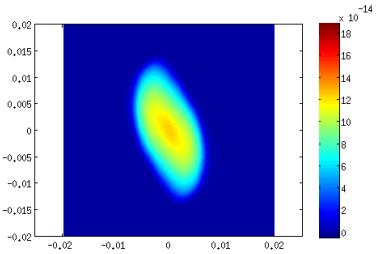

(c) Turn 20

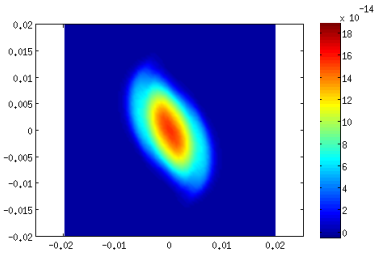

(d) Turn 30

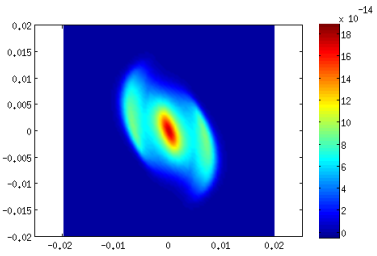

(e) Turn 40

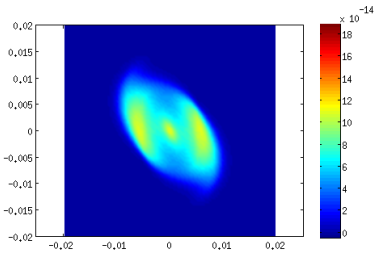

(f) Turn 50

Figure 25: Snapshots of the results of the simulation of Table 9.

## 12.3 Comparison

As a reference to this code, a short comparison to results created with the Matlab code from [4] will be done. The parameters in this code were changed to make it comparable to our results, that means, instead of having dimensionless quantities, the dimensions were considered here and the values of the gaussian distribution were adjusted as well. The changes can be seen in the Appendix.

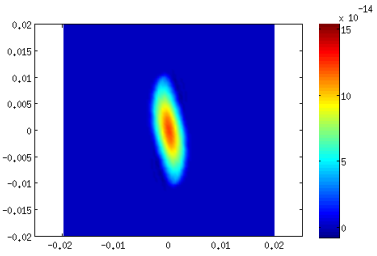

(a) Turn 10

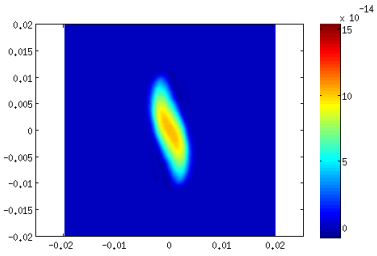

(b) Turn 20

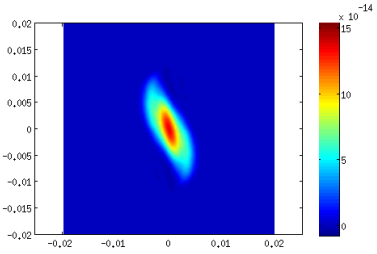

(c) Turn 30

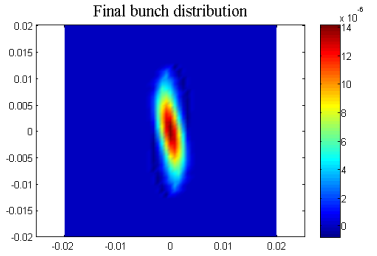


(d) Turn 10

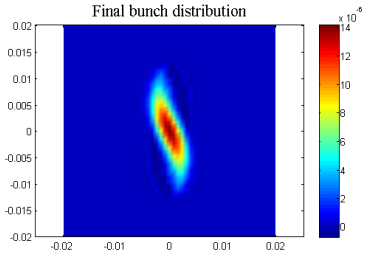


(e) Turn 20

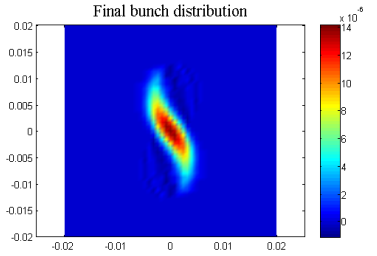


(f) Turn 30

Figure 26: Comparison of the two implementations. Top line is simulation B1, bottom line is the comparable simulation with the code from [4].

Even with the different approach of using numerical schemes for the solution of the equations, the results are qualitatively similar to each other. Both show the same tilting of the beam.

# 13 Conclusion

In this thesis, a relativistic set of fluid equations was derived in order to describe the dynamics of a particle beam in a cyclotron. The basic set of equations derived in the first part of the work allows a full three dimensional relativistic description of the problem. The implementation of a general magnetic field in three dimensions and the addition of acceleration is possible, too. Nevertheless, as it was shown in the validation of the fluid approach, the dimension parallel to the magnetic field has to be treated with care.

To verify the set of equations, a dimensional analysis and a non-relativistic approximation were done. Afterwards, the two dimensional version of the equations was investigated. Considering Chew, Goldberger and Lows work, there should not arise any issues describing the problem using the radial-longitudinal version of the fluid equations. I have been able to show the rotational invariance of the relativistic equations and to derive conditions under which the two-dimensional set of equations is hyperbolic. The proof of hyperbolicity led to restrictions in the velocities. If those conditions are not met, the equations are mixed, that means they contain real and complex eigenvalues.

From then on, hyperbolicity was expected to be fulfilled and the two dimensional, radial-longitudinal form of the equations was explored further with the aim of simulating the system in the context of a cyclotron. For the simulation, a general fluid dynamic approach was chosen, that means fluid dynamical schemes were used, with the Lorentz force acting as a source term. For the verification of the code, the implemented schemes and the implementation of the Lorentz force were tested separately. Burgers equation helped for the benchmarking of the fluid dynamical schemes and simple electrodynamical problems with exact solutions were used for the benchmarking of the Lorentz force. Then, a drifting sphere of charge and a coasting beam were simulated. In the end, the results were compared to the code used in [4].

The simulation showed a development of spiral arms. This effect develops over time and it increases with intensity. Unfortunately, it is still unstable and the implementation seems not to be energy conserving so far. The reason for this could be a bug in the self-magnetic field and/or a problem of the scheme. The Lax-Friedrichs scheme, with its artificial viscosity is sensitive to velocity changes. Nevertheless, the comparison with the results simulated in [4] showed that the approach has the potential to succesfully simulate the system. In the results of the simulations, the same spiral effects as in the particle-in-cell simulations can be observed. However, in order to achieve comparable results, the Fluid Model needs to be modified. A higher order scheme should probably be used and a more realistic version of a cyclotron should be implemented. That means, the model should contain accelerating gaps, a field map and fringe fields.

The implementation of a more general problem than the two-dimensional one would be certainly the next step in this fluid model. This problem would contain a more general magnetic field than the homogeneous static external field. Also fringe field effects should be included in the simulation. Finally, the external electric fields in the accelerating gaps of the cyclotron have to be

implemented as well. Furtheremore, for the realistic description of a cyclotron, effects like mirror charges have to be considered, too. The basic relativistic set of equations derived at the beginning of this work is general enough to do that, because the equations allow acceleration and a general magnetic field. However, while including these effects makes the model more realistic, dealing with them on a numerical level will lead to some difficulties. To be exact, these kind of effects could lead to jumps in some of the values, which leads to the necessity of another scheme than Lax-Friedrichs, since the Lax-Friedrichs method is not able to deal with shock-like problems.

To sum up, there is still some work to do to get comparable results which can show the capabilities of the Fluid Model approach for particle accelerator simulations. Nonetheless, the model already shows some promising results that propose a further investigation of the topic.

# Appendix

## Proof for $u_j F^{\alpha j} = \gamma(\mathbf{E} + \mathbf{u} \times \mathbf{B})$

$$
\begin{aligned}
u_j F^{\alpha j} \quad \underbrace{=}_{\alpha=1,2,3} \quad & \gamma(c, u_x, u_y, u_z) \begin{pmatrix} \frac{E_x}{c} & 0 & -B_z & B_y \\ \frac{E_y}{c} & B_z & 0 & -B_x \\ \frac{E_z}{c} & -B_y & B_x & 0 \end{pmatrix} \\
= \quad & \gamma(\mathbf{E} + u_x \begin{pmatrix} 0 \\ B_z \\ -B_y \end{pmatrix} + u_y \begin{pmatrix} -B_z \\ 0 \\ B_x \end{pmatrix} + u_z \begin{pmatrix} B_y \\ -B_x \\ 0 \end{pmatrix}) \\
= \quad & \gamma(\mathbf{E} + \mathbf{u} \times \mathbf{B})
\end{aligned}
$$

## Proof for $\nabla(\mathbf{ab}) = (\mathbf{a}\nabla)\mathbf{b} + (\mathbf{b}\nabla)\mathbf{a} + \mathbf{a} \times (\nabla \times \mathbf{b}) + \mathbf{b} \times (\nabla \times \mathbf{a})$

$$
\begin{aligned}
\nabla(\mathbf{ab}) &= \begin{pmatrix} \partial_x \\ \partial_y \\ \partial_z \end{pmatrix} (a_x b_x + a_y b_y + a_z b_z) \\
&= \begin{pmatrix} a_x \partial_x b_x + a_y \partial_x b_y + a_z \partial_x b_z + \partial_x(a_x) b_x + \partial_x(a_y) b_y + \partial_x(a_z) b_z \\ \partial_y(a_x) b_x + \partial_y(a_y) b_y + \partial_y(a_z) b_z + a_x \partial_y b_x + a_y \partial_y b_y + a_z \partial_y b_z \\ \partial_z(a_x) b_x + \partial_z(a_y) b_y + \partial_z(a_z) b_z + a_x \partial_z b_x + a_y \partial_z b_y + a_z \partial_z b_z \end{pmatrix} \\
&= (a_x \partial_x + a_y \partial_y + a_z \partial_z) \begin{pmatrix} b_x \\ b_y \\ b_z \end{pmatrix} + \begin{pmatrix} (-a_y \partial_y - a_z \partial_z) b_x \\ (-a_x \partial_x - a_z \partial_z) b_y \\ (-a_x \partial_x - a_y \partial_y) b_z \end{pmatrix} \\
&\quad + (b_x \partial_x + b_y \partial_y + b_z \partial_z) \begin{pmatrix} a_x \\ a_y \\ a_z \end{pmatrix} + \begin{pmatrix} (-b_y \partial_y - b_z \partial_z) a_x \\ (-b_x \partial_x - b_z \partial_z) a_y \\ (-b_x \partial_x - b_y \partial_y) a_z \end{pmatrix} \\
&\quad + \begin{pmatrix} a_y \partial_x b_y + a_z \partial_x b_z + \partial_x(a_y) b_y + \partial_x(a_z) b_z \\ \partial_y(a_x) b_x + \partial_y(a_z) b_z + a_x \partial_y b_x + a_z \partial_y b_z \\ \partial_z(a_x) b_x + \partial_z(a_y) b_y + a_x \partial_z b_x + a_y \partial_z b_y \end{pmatrix} \\
&= (\mathbf{a}\nabla)\mathbf{b} + (\mathbf{b}\nabla)\mathbf{a} \\
&\quad + \begin{pmatrix} -a_y \partial_y b_x - a_z \partial_z b_x - b_y \partial_y a_x - b_z \partial_z a_x \\ -a_x \partial_x b_y - a_z \partial_z b_y - b_x \partial_x a_y - b_z \partial_z a_y \\ -a_x \partial_x b_z - a_y \partial_y b_z - b_x \partial_x a_z - b_y \partial_y a_z \end{pmatrix} \\
&\quad + \begin{pmatrix} a_y \partial_x b_y + a_z \partial_x b_z + b_y \partial_x a_y + b_z \partial_x a_z \\ b_x \partial_y a_x + b_z \partial_y a_z + a_x \partial_y b_x + a_z \partial_y b_z \\ b_x \partial_z a_x + b_y \partial_z a_y + a_x \partial_z b_x + a_y \partial_z b_y \end{pmatrix}
\end{aligned}
$$

$$
\begin{aligned}
\mathbf{a} \times (\nabla \times \mathbf{b}) &= \begin{pmatrix} a_x \\ a_y \\ a_z \end{pmatrix} \times \begin{pmatrix} \partial_y b_z - \partial_z b_y \\ \partial_z b_x - \partial_x b_z \\ \partial_x b_y - \partial_y b_x \end{pmatrix} \\
&= \begin{pmatrix} a_y(\partial_x b_y - \partial_y b_x) - a_z(\partial_z b_x - \partial_x b_z) \\ a_z(\partial_y b_z - \partial_z b_y) - a_x(\partial_x b_y - \partial_y b_x) \\ a_x(\partial_z b_x - \partial_x b_z) - a_y(\partial_y b_z - \partial_z b_y) \end{pmatrix}
\end{aligned}
$$

$$\begin{aligned}
\mathbf{b}\times(\nabla\times\mathbf{a}) &= \begin{pmatrix} b_x \\ b_y \\ b_z \end{pmatrix} \times \begin{pmatrix} \partial_y a_z - \partial_z a_y \\ \partial_z a_x - \partial_x a_z \\ \partial_x a_y - \partial_y a_x \end{pmatrix} \\
&= \begin{pmatrix} b_y(\partial_x a_y - \partial_y a_x) - b_z(\partial_z a_x - \partial_x a_z) \\ b_z(\partial_y a_z - \partial_z a_y) - b_x(\partial_x a_y - \partial_y a_x) \\ b_x(\partial_z a_x - \partial_x a_z) - b_y(\partial_y a_z - \partial_z a_y) \end{pmatrix}
\end{aligned}$$

Therefore

$$\nabla(\mathbf{ab}) = (\mathbf{a}\nabla)\mathbf{b} + (\mathbf{b}\nabla)\mathbf{a} + \mathbf{a}\times(\nabla\times\mathbf{b}) + \mathbf{b}\times(\nabla\times\mathbf{a})$$

## Proof for $\frac{D}{Dt}\mathbf{v}^2 = 2\mathbf{v}\frac{D}{Dt}\mathbf{v}$

$$\begin{aligned}
\frac{D}{Dt}\mathbf{v}^2 &= (\partial_t + (\mathbf{v}\nabla))(v_x^2 + v_y^2 + v_z^2) \\
&= (\partial_t + (v_x\partial_x + v_y\partial_y + v_z\partial_z))(v_x^2 + v_y^2 + v_z^2) \\
&= (2v_x\partial_t v_x + 2v_y\partial_t v_y + 2v_z\partial_t v_z) \\
&\quad +(v_x\partial_x(v_x^2 + v_y^2 + v_z^2) + v_y\partial_y(v_x^2 + v_y^2 + v_z^2) + v_z\partial_z(v_x^2 + v_y^2 + v_z^2)) \\
&= 2\mathbf{v}\partial_t\mathbf{v} + 2v_x(v_x\partial_x v_x + v_y\partial_x v_y + v_z\partial_x v_z) \\
&\quad +2v_y(v_x\partial_y v_x + v_y\partial_y v_y + v_z\partial_y v_z) + v_z(v_x\partial_z v_x + v_y\partial_z v_y + v_z\partial_z v_z) \\
&= 2\mathbf{v}\partial_t\mathbf{v} + 2v_x(v_x\partial_x + v_y\partial_y + v_z\partial_z)v_x \\
&\quad +2v_y(v_x\partial_x + v_y\partial_y + v_z\partial_z)v_y + 2v_z(v_x\partial_x + v_y\partial_y + v_z\partial_z)v_z \\
&= 2\mathbf{v}\partial_t\mathbf{v} + 2\mathbf{v}(\mathbf{v}\nabla)\mathbf{v} \\
&= 2\mathbf{v}\frac{D}{Dt}\mathbf{v}
\end{aligned}$$

## Proof for $\nabla\times(\gamma^2\mathbf{v}) = \gamma^2(\nabla\times\mathbf{v}) + 2\gamma(\mathbf{v}\times\nabla)\gamma$

$$\begin{aligned}
\nabla\times(\gamma^2\mathbf{v}) &= \begin{pmatrix} \partial_y(\gamma^2 v_z) - \partial_z(\gamma^2 v_y) \\ \partial_z(\gamma^2 v_x) - \partial_x(\gamma^2 v_z) \\ \partial_x(\gamma^2 v_y) - \partial_y(\gamma^2 v_x) \end{pmatrix} \\
&= \gamma^2 \begin{pmatrix} \partial_y v_z - \partial_z v_y \\ \partial_z v_x - \partial_x v_z \\ \partial_x v_y - \partial_y v_x \end{pmatrix} + 2\gamma \begin{pmatrix} v_z\partial_y\gamma - v_y\partial_z\gamma \\ v_x\partial_z\gamma - v_z\partial_x\gamma \\ v_y\partial_x\gamma - v_x\partial_y\gamma \end{pmatrix} \\
&= \gamma^2(\nabla\times\mathbf{v}) + 2\gamma(\mathbf{v}\times\nabla)\gamma
\end{aligned}$$

**Proof for** $\partial_i \gamma = \frac{\gamma^3}{c^2}(v_x \partial_i v_x + v_y \partial_y v_y + v_z \partial_i v_z)$

$$\begin{aligned}
\partial_i \gamma &= \partial_i \left( \frac{1}{(1-(\mathbf{v}^2/c^2))^{1/2}} \right) \\
&= \partial_i \left(1-(\mathbf{v}^2/c^2)\right)^{-1/2} \\
&= -\frac{1}{2}\left(1-(\mathbf{v}^2/c^2)\right)^{-3/2} (-\frac{2}{c^2} v_x \partial_i v_x - \frac{2}{c^2} v_y \partial_i v_y - \frac{2}{c^2} v_z \partial_i v_z) \\
&= \frac{\gamma^3}{c^2}(v_x \partial_i v_x + v_y \partial_y v_y + v_z \partial_i v_z)
\end{aligned}$$

## Pseudo Code for the Fluid Model

Functions that are used in the main program

- **grid2D**: Initialize the grid and compute the grid spacing
- **derivatives**: Compute the finite differences matrices
- **righthandside**: Computes the Lorentz term/ Source term
- **CFL**: Check the CFL condition and update the timestep size if necessary
- **LF**: Computation of the Lax-Friedrichs flux

Listing 3: Pseudo-Code Fluid Model

```
% Initialization
        grid2D(xmin,xmax,ymin,ymax,NrGridpoints)
        derivatives(x,y,xx,yy,xmax,xmin,ymax,ymin,dx,dy)
% Initial density, pressure and velocity field
        rho_0, P_0, u_0, v_0
% Computation of the initial self-electric field
        righthandside(rho_0)
% Initialize the conserved vector Q
        Q(rho_0, P_0, u_0, v_0)

% Time evolution
for n = 1:NumberOfTimesteps

        Q1 = Q(n-1) + (dt/2)*LF(Q(n-1));
        Q(n) = Q1 + (dt/2)*LF(Q1);

        from Q(n) compute rho_n, P_n
        using Lorentz force compute u_n, v_n
        compute new self-electric field

end
```

## Changes in the reference code for comparability reasons

The initial density was changed to transform it from a non-dimensional density to a dimension-full density. To do this transformation step it simply had to be multiplied by the following factor:

$$\rho_0 = \frac{N_p q}{A}.$$

Here, $N_p$ is the total number of particles, $q$ is the elementary charge and $A$ is the total area covered by the beam. This leads to a density that has the units of a charge density, namely

$$[\rho] = \frac{C}{mm^2}.$$

Since the density was designed as gaussian density, the units of the variance in x and y, $\sigma_x$ and $\sigma_y$ respectively, have to be changed, too.

$$[\sigma] \rightarrow mm.$$

Lastly, the Poisson equation, which was also used without units in the reference code has to be changed, to account for units. Here the Poisson equation simply has to be divided by the vacuum permetivity $\epsilon_0$.

$$\Delta\Phi = -\rho \qquad \rightarrow \qquad \Delta\Phi = -\frac{\rho}{\epsilon_0}$$

The extract from the reference code that have been changed can be seen in table 10.

| Extracts from original code | Corresponding extracts from changed code |
|---|---|
| | Change the units of the variance to $mm$ |
| $decaylx = 2.52/sqrt(2);$<br>$decayly = 13.4/sqrt(2);$ | $decaylx = 2.52/sqrt(2) * 1e-3;$<br>$decayly = 13.4/sqrt(2) * 1e-3;$ |
| | Change the units of the initial density |
| $A = ...$<br>$exp(-((xx - xcenter)/decaylx).^2)...$<br>$.* exp(-((yy - ycenter)/decayly).^2)...$<br>$.* ((exp(-((xx - xcenter)/decaylx).^2)...$<br>$.* exp(-((yy - ycenter)/decayly).^2))...$<br>$>= 0.1);$ | $A = ...$<br>$exp(-((xx - xcenter)/decaylx).^2)...$<br>$.* exp(-((yy - ycenter)/decayly).^2)...$<br>$.* ((exp(-((xx - xcenter)/decaylx).^2)...$<br>$.* exp(-((yy - ycenter)/decayly).^2))...$<br>$>= 0.1);$ |
| | Find covered area $a$ and multiply by the unit length of a voxel $hx$ and $hy$ respectively to get the unit $mm^2$ |
| | $a = find(A \ = 0);$<br>$a = length(a) * hx * hy;$<br>$rho0 = (NP * q)/a;$ |
| | Initialize the density |
| $Dens(:, 1) = A(:);$ | $Dens(:, 1) = rho0. * A(:);$ |
| | Use the dimension-full version of Poissons equation by dividing by the vacuum permetivity |
| $rhsx = -Dx * Dens(:, k)$<br>$rhsy = -Dy * Dens(:, k)$ | $rhsx = -Dx * Dens(:, k)./eps0;$<br>$rhsy = -Dy * Dens(:, k)./eps0;$ |

Table 10: Comparison between extracts from the original code with the corresponding extracts from the changed code.

# References


[1] Christopher K. Allen and Nicholas D. Pattengale. Theory and technique of beam envelope simulation. *LOS ALAMOS NATIONAL LABORATORY*, LA - UR - 02 - 4979, 2002.

[2] Y. J. Bi, A. Adelmann, R. Dölling, M. Humbel, W. Joho, M. Seidel, and T. J. Zhang. Towards quantitative simulations of high power proton cyclotrons. *Phys. Rev. ST Accel. Beams*, 14:054402, May 2011.

[3] J. M. Burgers. *The Nonlinear Diffusion Equation - Asymptotical Solutions and Statistical Problems.* Institute for Fluid Dynamics and Applied Mathematics, University of Maryland, 1973.

[4] A. J. Cerfon, J. P. Freidberg, F. I. Parra, and T. A. Antaya. Analytic fluid theory of beam spiraling in high-intensity cyclotrons. *Phys. Rev. ST Accel. Beams*, 16:024202, Feb 2013.

[5] Francis F. Chen. *Introduction to Plasma Physics.* Plenum Press, 1974. Chapter 3, Plasmas as Fluids.

[6] G. F. Chew, M. L. Goldberger, and F. E. Low. The boltzmann equation and the one-fluid hydromagnetic equations in the absence of particle collisions. *Proceedings of the Royal Society of London. Series A. Mathematical and Physical Sciences*, 236(1204):112–118, 1956.

[7] Ronald C. Davidson. *Physics Of Nonneutral Plasmas.* World Scientific Pub Co, 2nd Revised edition (Dezember 2001). Chapter 2.

[8] Dennis Dieks. Space, Time and Coordinates in a Rotating World. 2010.

[9] R. D. Hazeltine and S. M. Mahajan. *Relativistic magnetohydrodynamics.* Institute for Fusion Studies, The University of Texas, Austin, Texas 78712, 2000.

[10] M. Rome I. Kotelnikov. Relativistic thermal equilibrium of non-neutral plasmas. *Physics Letters A (2010).*

[11] Stefaan Poedts J. P. Goedbloed, Rony Keppens. *Advanced Magnetohydrodynamics: With Applications to Laboratory and Astrophysical Plasmas.* Cambridge University Press, 2010.

[12] John D. Jackson. *Classical Electrodynamics Third Edition.* Wiley, third edition, 1998.

[13] E.M. Landau, L.D.; Lifshitz. *Fluid Mechanics.* Butterworth-Heinemann, 2nd ed. (1987). pages 3–4.

[14] B. Wendroff P.D. Lax. Systems of conservation laws. *Commun. Pure Appl. Math.*, 13:217–237, 1960.

[15] G. Rizzi and L. Ruggiero. *Relativity in Rotating Frames: Relativistic Physics in Rotating Reference Frames.* Fundamental Theories of Physics. Springer, 2004.

[16] J. W. Thomas. *Numerical Partial Differential Equations: Finite Difference Methods*. Springer-Verlag, 1995.

[17] Eleuterio F. Toro. *Riemann Solvers and Numerical Methods for Fluid Dynamics, A Practical Introduction*. Springer-Verlag, third edition, 2009.

[18] James P. Vanyo. *Rotating Fluids in Engineering and Science*. Courier Dover Publications, 1993. Chapter 7 (p.113).